Solution Behaviors and Reactions of Five-Coordinate Hydridobis(diphosphine)ruthenium(II) Complexes

5配位ヒドリドビス(ジホスフィン)ルテニウム(II)錯体の溶存挙動と反応

Masamichi OGASAWARA

①

Solution Behaviors and Reactions of Five-Coordinate Hydridobis(diphosphine)ruthenium(II) Complexes

5配位ヒドリドビス(ジホスフィン)ルテニウム(II)錯体の溶存挙動と反応

by
Masamichi OGASAWARA

Department of Industrial Chemistry
Faculty of Engineering
The University of Tokyo

February, 1994

Contents

Chapter 1

General Introduction.

Coordinations of species having lone pair, such as NH_3 and PPh_3, or π-bonding electrons, such as C_2H_4 and C_6H_6, to metals are common and well-known in transition metal chemistry. Only recently it has established that σ-bonding electron pairs can also ligate to transition metal center.[1] These σ-bond coordinations are examples of the electron-deficient bonds and their main bonding patterns are explained as so-called "three-center, two-electron bonds". Although electrons of σ-bonding, such as C–H, Si–H, and H–H, have potential to coordinate to transition metals, these electron pairs are fairly weak donors.[1d] Accordingly it is necessary that transition metal fragments, the acceptors of the σ-bonding electron pairs, are powerful Lewis acids. Usually coordinatively unsaturated transition metal complexes, most of them have sixteen valence electrons, exhibit strong Lewis acidity. In these complexes there is a tendency to fill the 18-electron rule, so they have a potential to be coordinated to the σ-bonding electron pairs of C–H and H–H.

What are the Agostic Interactions ?

Carbon-hydrogen bonds, especially those of saturated (sp^3) carbon centers, are considered to be chemically inert. As described above, the C–H group is not thought of as a potential ligand which can have a structural role or play an energetically significant part in ground states or in reaction intermediates, however, recently it was shown that C–H bonds can act as ligands to transition metal centers by formation of three-center, two-electron bonds (3c-2e). The agostic C–H→M bond is similar to the familiar and long-known bridging hydrogen systems which occur in B–H→B, M–H→M, and B–H→M groups.

The term "agostic" was defined in 1983 by Brookhart and Green as covalent interactions between carbon-hydrogen groups and transition metal centers in

organometallic compounds,[1a, 2] in which a hydrogen atom is covalently bonded simultaneously to both a carbon atom and to a transition metal atom.

The activation of carbon-hydrogen bonds is one of the most important target reactions in organometallic chemistry.[3] Therefore, compounds, which include an agostic interaction, are important and have attracted considerable attention, because they represent a plausible intermediate stage on the way to oxidative addition of carbon-hydrogen bonds to a metal complex. Regarding them in this light can give us information about the approach to the transition state for the C–H moiety and metal center reaction.[4] A large number of examples of C–H→M bridges have now been described in a variety of complexes (see Figure 1.1 and 1.2). In each case, the metal fragments, which are coordinated by C–H moieties, would have 16 valence electrons or less, i.e. those fragments are coordinatively unsaturated. The C–H groups coordinations can therefore be seen as a way for the metal to become coordinatively saturated. In the absence of any suitable lone pairs, the C–H bonding pair is donated to the metal in a three-center, two-electron bond.

Historic Background of the Agostic Interactions.

The first discovery of the agostic interaction, of course the term "agostic" had not defined in that days, was accomplished in 1965 by Mason, Ibers, and their co-workers. They observed close approach of the *ortho*-hydrogen atoms of phenyl-phosphine ligands to the metal center in the compounds $[RuCl_2(PPh_3)_3]$ (**1**)[5] and [*trans*-$PdI_2(PMe_2Ph)_2$] (**2**)[6] respectively. Coordinations of *ortho*-hydrogens of phenyl rings are the most well-known types of the agostic interactions,[5–8] which have a close relationship with orthometallation, the most common system of the intramolecular C–H activation.

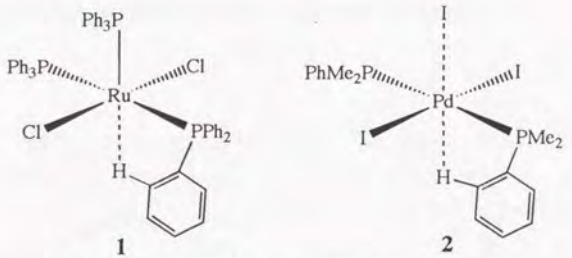

1 2

Fig. 1.1 Early examples of close approeaches of hydrogen atoms to transition metal centers.

In 1967, Trofimenko observed unusual low field shifts of the ethyl hydrogens in the ^{1}H NMR spectrum of Ni[$Et_2B(pz)_2]_2$ (pz = pyrazole, **3**), and suggested that the hydrogens were held close to the nickel center.[9] Maitlis reported the crystal structure of the compound $Pd(PPh_3)_2(CMe{=}CMeCMe{=}CHMe)Br$ (**4**).[10] The Pd–C(HMe) distance of 2.3 Å is less than the expected sum of the van der Waals radii (ca. 3.1 Å) and it was proposed that there was a direct Pd–H–C interaction. This was supported by the observation of spin-spin coupling between the proposed bridging hydrogen and the two equivalent ^{31}P nuclei (J_{PH} = 1.4 Hz).

The first neutron diffraction characterization of an agostic C–H→M system which definitively showed the position of the agostic hydrogen was that of the compound $\{Fe[P(OMe)_3]_3(\eta^3\text{-}C_8H_{13})\}BF_4$ (**5**).[11]

The first example of an agostic interaction to be characterized in a polynuclear system is that in $[Os_3H(CO)_{10}(\mu^2\text{-}CH_3)]$ (**6**).[12] Neutron diffraction studies exhibited, however, that only the μ-CH_2 isomer exists in the solid state. In solution there is an equilibrium mixture of the two isomers. The elegant technique of partial deuteration

was developed by Shapley and collaborators to characterize the agostic interaction by NMR spectroscopy, this NMR technique is called the Shapley effect.

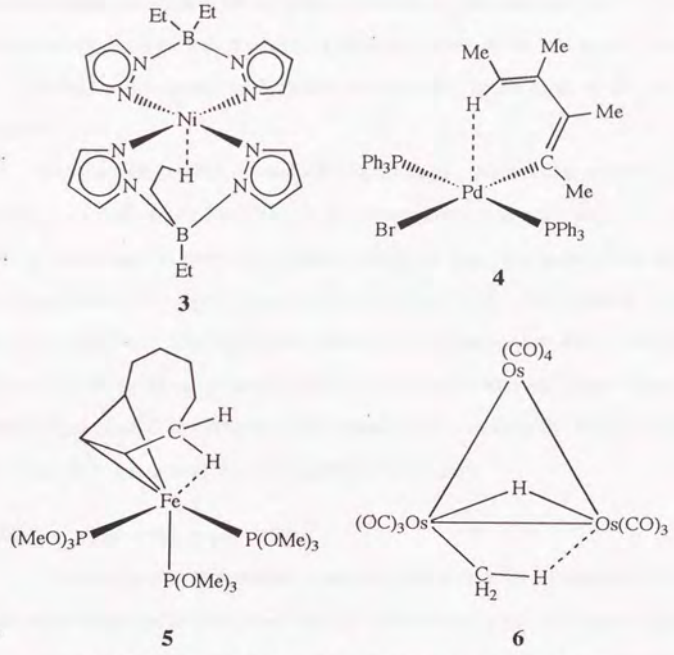

3 **4**

5 **6**

Fig. 1.2 The molecular structures of some agostic complexes.

In very recent years increasing the presence of agostic hydrogens has been shown both by NMR and by crystal structure determinations and this work is described in detail below.

Physical and Chemical Properties of the Agostic System.

a. Structural Determinations Using Some Diffraction Techniques.

The most interesting structural feature of C–H→M bonds is the location of the hydrogen atom and the C–H and M–H bond distances. In several X-ray structure determinations, particularly the early ones, evidence for interaction of the C–H group with metal was inferred from a close M–C distance. Many X-ray structures locate and refine hydrogen atom positions, but such data give only approximate M–H and C–H distances.

For more reliable r(C–H) and r(M–H) distances, neutron or possibly electron diffraction data are required and these have been reported for several compounds.[11a, 13 – 15] By these data it is clear that all agostic bonds are bent. Furthermore, the agostic C–H distance is in the range 1.13 to 1.19 Å and is elongated 5 – 10 % relative to a non-bridging C–H bond. The M–H distances in C–H→M bonds are also substantially longer (10 – 20 %) than expected for a normal terminal M–H bond. These effects can clearly be ascribed to the presence of a three-center, two-electron C–H→M bond with the consequent reduction of the C–H and M–H bond orders.

b. Nuclear Magnetic Resonance Studies.

The most useful spectroscopic technique for detecting the presence of C–H→M systems in complexes is NMR spectroscopy. Where spectra of static agostic systems can be obtained, the ^{1}H and ^{13}C chemical shifts, and in particular J_{CH} values can be used with confidence to assign agostic structures. Many agostic compounds are, however, highly fluxional and undergo rapid exchange of the agostic hydrogen with other hydrogens, normally those attached to the same carbon atom. These fluxional compounds give averaged spectra at around room temperature. Barrier to these hydrogen exchange reactions are frequently of such a magnitude (> 8 kcal mol^{-1}) that

static (slow exchange) spectra can be obtained at low temperatures (e.g., –90 °C). In cases where even at the lowest accessible temperatures static spectra cannot be observed, it is often difficult to distinguish between the agostic formulation and classical structures. Partial deuteration experiments, coupled with careful analysis of the chemical shift and J_{CH} values, are useful in these cases (Shapley effects).

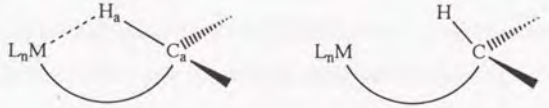

Agostic **Unsaturated**

The most characteristic feature of a C–H→M agostic interaction is the low value of $J_{C_a\text{-}H_a}$ due to the reduced C–H bond order. Typical values for $J_{C_a\text{-}H_a}$ are in the range of 60 to 90 Hz. These value are significantly lower than those expected for normal C(sp^3)–H bonds (120 – 130 Hz) in, for example, the coordinatively unsaturated structure. These low values were first reported by Brookhart and Whitesides for the compound $[Fe(\eta^3\text{-}C_6H_9)(CO)_3]^+$.[16]

The chemical shifts of agostic hydrogens in C–H_a→M systems for d^n (n > 0) metal centers normally occur at high fields and occur in the range typical for normal terminal metal hydride. For d^0 systems, resonances due to the agostic hydrogens normally do not shift to higher fields than 0 ppm.[17]

When a spectrum of the static species cannot be obtained then only averaged values of chemical shifts and J_{CH} can be measured. However, when the fluxional process does not involve scrambling of H_a with other hydrogen atoms in the system, then the averaged values of J_{CH} and the chemical shifts of H_a normally give a clear indication of agostic structures.[18]

An important NMR method for probing agostic interactions in fluxional systems is that involving partial deuteration developed by Calvert and Shapley on the trinuclear osmium system $[Os_3H(CO)_{10}(\mu^2\text{-}CH_3)]$.[12a] They observed that the average ^1H chemical shifts and J_{CH} values are quite sensitive to the extent of deuteration of the methyl group and fall in the order $\delta(CH_3) > \delta(CH_2D) > \delta(CHD_2)$ and $J_{CH}(CH_3) > J_{CH}(CH_2D) > J_{CH}(CHD_2)$. Furthermore, both the chemical shifts and J_{CH} values of the partially deuterated species CH_2D and CHD_2 are strongly temperature dependent. These effects arise because there is a thermodynamic preference for the deuterium atom

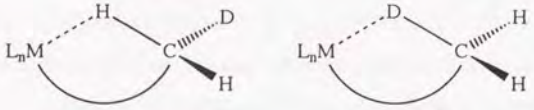

more stable **less stable**

to occupy the terminal positions and hydrogen atoms to occupy the bridging, i.e. agostic site. The fundamental reason for this preference is the smaller zero point energy difference between H and D in the C–H→M and C–D→M bonds relative to the differences in the terminal (no bridging) C–H and C–D bonds and the consequent preference of deuterium to occupy the terminal sites leaving hydrogen to occupy the bridging site. This isotopic perturbation effect has now been widely used.[19]

c. Infrared Spectroscopy.

The stretching frequencies of agostic C–H→M bonds have been reported for relatively few of the large number of agostic compounds. Consequently ν(C-H) data have not often been used as a probe of agostic interactions. In all cases, however, bands assignable to ν(C–H) are found at lower frequencies than for normal sp^3-C–H

bonds and occur in the range 2250 – 2800 cm^{-1}. This lowering may be associated with the observed increase in length of the agostic C–H bonds.[20 – 22]

Molecular Hydrogen Complexes (Dihydrogen Complexes).[23]

In 1984, a new ligand was added in the world of transition metal chemistry. Kubas and collaborators demonstrated the coordination of the molecular hydrogen to a transition metal center in a side-on manner without breaking H–H bonding in $[M(H_2)(CO)(PR_3)_2]$ (M = Mo, W; R = *i*-Pr or Cy).[24] This discovery was one of the most exciting results in inorganic chemistry in the 1980s, and has led to intense activity by several research groups worldwide. At the present time (1993) more than 170 dihydrogen complexes have been reported. The very rapid development of this fields is remarkable. In less than ten years the investigation of molecular hydrogen complexes has become a significant branch of coordination chemistry. Dihydrogen is the simplest molecule with single σ-bonding, and the H–H bond activation is the simplest process of the σ-bond dissociation.

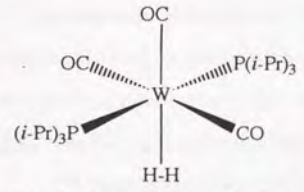

Fig. 1.3 The structure of the first molecular hydrogen complex.

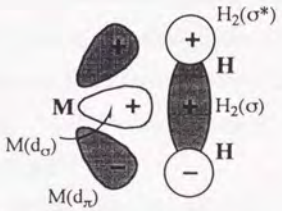

Fig. 1.4 Bonding model in transition metal dihydrogen complex.

The bonding of the dihydrogen ligands to the metal centers is explained as below. The metals involved have both empty d_σ and filled d_π orbitals. Electron donation from the filled $H_2(\sigma)$ orbital to the empty $M(d_\sigma)$ weakens, but does not break, the H–H bond because the resulting three-center, two-electron orbital is bonding over all three atoms. On the other hand, sufficient "back-donation" from filled d_π orbital into the empty $H_2(\sigma^*)$ will tend to break the H–H bond, because $H_2(\sigma^*)$ is H–H antibonding in character.[25] Electron-withdrawing ligands or a net cationic charge tends to reduce the bonding of M to H_2, so some back-bonding is necessary.[26]

Preparation of Dihydrogen Complexes.

a. Reaction with Hydrogen Gas.

Reaction of a coordinatively unsaturated metal fragment with hydrogen gas was employed by Kubas and co-workers in the preparation of the first dihydrogen complexes.[24] The precursor complexes are formally 16-electron coordinatively unsaturated species. In some cases, an agostic interaction between the metal center and a C_γ–H bond of a phosphine ligand in the precursor molecules has been established by X-ray crystallography[27, 28] or NMR spectroscopy.[29] This chemistry can be thought of as ligand exchange of a weakly bound ligand (the agostic C–H bond) by the incoming dihydrogen ligand. A similar strategy was employed by Crabtree and Lavin to prepare the cationic iridium complex $[Ir(PPh_3)_2(bq)(\eta^2\text{-}H_2)H]^+$ by displacement of bound water from the aquo complex $[Ir(PPh_3)_2(bq)(OH_2)H]^+$.[4b]

This methodology was also exploited by Morris, Saburi, and their collaborators in the synthesis of compounds of the general formula, $[MH(\eta^2\text{-}H_2)(L_2)_2]^+$, where M = Fe, Ru, or Os, and L_2 is a variety of chelating diphosphines.[29b, 30, 31]

b. Protonation of Hydride Complexes.

Protonation of a neutral hydride complex to give a cationic dihydrogen complex was firstly reported by Crabtree and Lavin in 1985. $[Ir(PPh_3)_2(bq)(\eta^2\text{-}H_2)H]^+$ initially prepared by displacement of bound water as described above, was shown to react with MeLi to generate $Ir(PPh_3)_2(bq)H_2$. The dihydrogen species can be regenerated quantitatively upon addition of 1 equiv. of $PhCH(SO_2CF_3)_2$.[32] Morris initially employed this particular methodology to prepare $[MH(\eta^2\text{-}H_2)(dppe)_2]^+$ (M = Fe and Ru).[33]

This method have been applied to synthesize a variety of the cationic dihydrogen complexes.[34 – 37]

Characterization of the Dihydrogen Complexes.

a. Diffraction Studies.

In some cases X-ray diffraction has given useful data. The difficulties associated with precise location of hydrogen atoms, particularly on second- and third-row transition metals, limit the usefulness of this method. While neutron diffraction is perhaps the most definitive technique, the requirement for large high-quality single crystals has so far limited this method to a small number (only 5 cases !) of examples. In all cases so far studied by neutron diffraction methods, the H_2 ligand is bound in a side-on fashion with an H–H distance of ca. 0.82 Å.[24a, 38 – 41]

b. Solution NMR Methods.

The proton NMR spectra of dihydrogen complexes generally give a single resonance of highly variable line width to high field of TMS. If other spin active nuclei are present in the molecule, coupling to the bound H_2 is in most cases not resolvable. Although there are many examples of H_2 complexes with phosphine ligands, coupling to ^{31}P has rarely been reported. The first case of resolved coupling between

dihydrogen ligand and adjacent phosphorus nuclei was reported in the ruthenium cations of the form $[CpRu(R_2PCH_2CH_2PR_2)(H_2)]^+$. For R = Me, J_{HP} =3.6 Hz,[36a] for R = Ph, J_{HP} = 2 Hz.[42] These values of J_{HP} are much lower than those observed in comparable hydride complexes.

It has often proven quite difficult in the absence of diffraction data to definitively establish the presence of the intact H_2 ligand. A very useful experiment that was first employed by Kubas is the partial substitution of deuterium in the H_2 ligand, which allows the direct measurement of the coupling between hydrogen and deuterium.[24a] The measurement of J_{HD} values has proven to be a very important characterization tool, with over 65 values reported to date in a wide variety of complexes. While J_{HD} in H–D gas is 43.2 Hz, the range of J_{HD} values of H–D ligands reported up to 1991 was 11 to 34 Hz.

In 1985 Crabtree and Lavin reported that the broadness of the NMR resonances due to bound dihydrogen was largely attributable to rapid dipole-dipole relaxation (short T_1).[32] The rapid relaxation is due to the short H–H distance in the bound H_2 ligand. Since dipole-dipole relaxation is proportional to the inverse sixth power of the internuclear distance, the measurement of T_1 values could in principle allow the definitive detection of dihydrogen complexes by a simple solution NMR method. The observation of short T_1 values is particularly useful in diagnosing the presence of H_2 ligands in fluxional polyhydride complexes, where J_{HD} is generally not observable. Subsequently Crabtree and Hamilton developed a quantitative treatment of the problem which allows the H–H distance in the coordinated dihydrogen ligand to be extracted from T_1 measurements.[43]

As described above, the chemistry of agostic interactions and dihydrogen complexes has appeared in the field of coordination chemistry in this decade. This new chemistry, however, has been attracted considerable attention of many chemists of inorganic and organometallic fields. The studies presented in Chapter 2 describe characterization, behaviors, and reactivity of the agostic complexes, $[RuH(diphosphine)_2]PF_6$. The results presented in Chapter 2 are the first example of the observation of the direct intramolecular hydrogen exchange involving the agostic interaction. I believe and hope that these results will be the important clue to solve the many problems concerning the C–H activation.

In Chapter 3 and 4, the behaviors of the ruthenium hydrido-dihydrogen complexes, $[RuH(\eta^2\text{-}H_2)(diphosphine)_2]PF_6$, are described. It is known that the complexes, where the dihydrogen ligand coexists with the terminal hydride, exhibits the intramolecular hydrogen exchange between the terminal hydride and the molecular hydrogen ligand. These intramolecular hydrogen exchange reactions are considered as the simplest process for the H–H bond activation, and some mechanisms and intermediates of these reactions have been proposed. I focus on this hydrogen exchange, here, and inquire into the mechanistic problems of this process on the ruthenium system $[RuH(\eta^2\text{-}H_2)(diphosphine)_2]PF_6$.

In Chapter 5, the application of the ruthenium five-coordinate complex to homogeneous hydrogenation catalyst and the mechanistic studies on the catalytic hydrogenation process are described.

References and Notes

(1) General reviews: (a) Brookhart, M.; Green, M. L. H. *J. Organomet. Chem.*, **1983**, *250*, 395. (b) Crabtree, R. H. *Chem. Rev.*, **1985**, *85*, 245. (c) Brookhart, M.; Green, M. L. H.; Wong, L.-L. *Prog. Inorg. Chem.*, **1988**, *36*, 1. (d) Crabtree, R. H.; Hamilton, D. G. *Adv. Organomet. Chem.*, **1988**, *28*, 299.

(2) The term "agostic" is derived from the Greek word "αγοστος", which may be translated as to clasp, to draw towards, to hold to oneself.

(3) (a) Parshall, G. W. *Acc. Chem. Res.*, **1975**, *8*, 113. (b) Webster, D. E. *Adv. Organomet. Chem.*, **1977**, *15*, 147. (c) Bruce, M. I. *Angew. Chem. Int. Ed. Engl.*, **1977**, *16*, 73. (d) Halpern, J. *Inorg. Chim. Acta*, **1985**, *100*, 41. (e) Ryabov, A. D. *Chem. Rev.*, **1990**, *90*, 403.

(4) (a) Crabtree, R. H.; Lavin, M. E.; Holt, E. M. *Inorg. Chem.*, **1985**, *24*, 1986. (b) Crabtree, R. H.; Lavin, M. *J. Chem. Soc., Chem. Commun.*, **1985**, 794.

(5) LaPlace, S. J.; Ibers, J. A. *Inorg. Chem.*, **1965**, *4*, 778.

(6) Bailey, N. A.; Jenkins, J. M.; Mason, R.; Shaw, B. L. *J. Chem. Soc., Chem. Commun.*, **1965**, 237.

(7) Yared, Y. W.; Miles, S. L.; Bau, R.; Reed, C. A. *J. Am. Chem. Soc.*, **1977**, *99*, 7076.

(8) Muir, K. W.; Ibers, J. A. *Inorg. Chem.*, **1970**, *9*, 440.

(9) (a) Trofimenko, S. *J. Am. Chem. Soc.*, **1967**, *89*, 6288. (b) Trofimenko, S. *J. Am. Chem. Soc.*, **1968**, *90*, 4754. (c) Trofimenko, S. *Inorg. Chem.*, **1970**, *9*, 2493.

(10) Roe, D. M.; Bailey, P. M.; Mosely, K.; Maitlis, P. M. *J. Chem. Soc., Chem. Commun.*, **1972**, 1273.

(11) (a) Brown, R. K.; Williams, J. M.; Schultz, A. J.; Stucky, G. D.; Ittel, S. D., Harlow, R. L. *J. Am. Chem. Soc.*, **1980**, *102*, 981. (b) Williams, J. M.; Brown, R. K.; Schultz, A. J.; Stucky, G. D.; Ittel, S. D. *J. Am. Chem. Soc.*, **1978**, *100*, 7409. (c) Ittel, S. D.; Van-Catledge, F. A.; Jesson, J. P. *J. Am. Chem. Soc.*, **1979**, *101*, 6905.

(12) (a) Calvert, R. B.; Shapley, J. R. *J. Am. Chem. Soc.*, **1978**, *100*, 7726. (b) Calvert, R. B.; Shapley, J. R. *J. Am. Chem. Soc.*, **1977**, *99*, 5225.

(13) (a) Dawoodi, Z; Green, M. L. H.; Mtetwa, V. S. B.; Prout, K.; Schultz, A. J.; Williams, J. M.; Koetzle, T. F. *J. Chem. Soc., Dalton Trans.*, **1986**, 1629.

(14) Beno, M. A.; Williams, J. M.; Tachikaura, M.; Muetterties, E. L. *J. Am. Chem. Soc.*, **1980**, *102*, 4541.

(15) Schultz, A. J.; Teller, R. G.; Beno, M. A.; William, J. M.; Brookhart, M.; Lamanna, W.; Humphrey, H. B. *Science*, **1983**, *220*, 197.

(16) Brookhart, M.; Whitesides, T. H.; Crockett, J. M. *Inorg. Chem.*, **1976**, *15*, 1550.

(17) (a) Dawoodi, Z.; Green, M. L. H.; Mtetwa, V. S. B.; Pout, K. *J. Chem. Soc., Chem. Commun.*, **1982**, 802. (b) Dawoodi, Z.; Green, M. L. H.; Mtetwa, V. S. B.; Prout, K. *J. Chem. Soc., Chem. Commun.*, **1982**, 1410.

(18) Brookhart, M.; Green, M. L. H.; Pardy, R. B. A. *J. Chem. Soc., Chem. Commun.*, **1983**, 691.

(19) Brookhart, M.; Lamanna, W.; Humphrey, M. B. *J. Am. Chem. Soc.*, **1982**, *104*, 2117.

(20) Berry, A.; Dawoodi, Z.; Derome, A. E.; Dickenson, J. M.; Downs, A. J.; Green, J. C.; Green, M. L. H.; Hare, P. M.; Payne, M. P.; Rankin, D. W. H.; Robertson H. E. *J. Chem. Soc., Chem. Commun.*, **1986**, 520.

(21) Tompson, M. E.; Baxter, S. M.; Bulls, A.; Burger, B. J.; Nolan, M. C.; Santarsiero, B. D.; Shafer, W. P.; Bercaw, J. E. *J. Am. Chem. Soc.*, **1987**, *109*, 203.

(22) Mckean, D. C.; McQuillan, G. P.; Morrison, A. R.; Torto, I. *J. Chem. Soc., Dalton Trans.*, **1985**, 1207.

(23) Recent Reviews: (a) Kubas, G. J. *Acc. Chem. Res.*, **1988**, *21*, 120. (b) Crabtree, R. H. *Acc. Chem. Res.*, **1990**, *23*, 95. (c) Crabtree, R. H.; Luo, X.-L.; Michos, D. *Chemtracts-Inorg. Chem.*, **1991**, *3*, 245. (d) Jessop, P. G.; Morris, R. H. *Coord. Chem. Rev.*, **1992**, *121*, 155. (e) Heinekey, D. M.; Oldham, Jr., W. J. *Chem. Rev.*, **1993**, *93*, 913.

(24) (a) Kubas, G. J.; Ryan, R. R.; Swanson, B. I.; Vergamini, P. J.; Wasserman, H. J. *J. Am. Chem. Soc.*, **1984**, *106*, 451. (b) Kubas, G. J.; Ryan, R. R.; Swanson, B. I.; Vergamini, P. J.; Wasserman, H. J. *J. Am. Chem. Soc.*, **1985**, *106*, 451.

(25) (a) Burdett, J. K.; Phillips, J. R.; Pourian, M. R.; Poliakoff, M.; Turner, J. J.; Upmacis, R. *Inorg. Chem.*, **1987**, *26*, 3054. (b) Saillard, J.-Y.; Hoffman, R. *J. Am. Chem. Soc.*, **1984**, *106*, 2006. (c) Jean, Y.; Eisenstein, O.; Volatron, F.; Maouche, B.; Sefta, F. *J. Am. Chem. Soc.*, **1986**, *108*, 6587. (d) Hay, P. J. *J. Am. Chem. Soc.*, **1987**, *109*, 705.

(26) Morris, R. H.; Earl, K. A.; Luck, R. L.; Lazarowych, N. J.; Sella, A. *Inorg. Chem.*, **1987**, *26*, 2674.

(27) (a) Sato, M.; Tatsumi, T.; Kodama, T.; Hidai, M.; Uchida, T.; Uchida, Y. *J. Am. Chem. Soc.*, **1978**, *100*, 4447. (b) Kubas, G. J.; Ryan, R. R.; Wrobleski, D. A. *J. Am. Chem. Soc.*, **1986**, *108*, 1339.

(28) Wasserman, H. J.; Kubas, G. J.; Ryan, R. R. *J. Am. Chem. Soc.*, **1986**, *108*, 2294.

(29) (a) Ogasawara, M.; Aoyagi, K.; Saburi, M. *Organometallics*, **1993**, *12*, 3393. (b) Saburi, M.; Aoyagi, K.; Takahashi, T.; Uchida, Y. *Chem. Lett.*, **1990**, 601.

(30) Bautista, M.; Earl, K. A.; Morris, R. H.; Sella, A. *J. Am. Chem. Soc.*, **1987**, *109*, 3780.

(31) (a) Tsukahara, T.; Kawano, H.; Ishii, Y.; Takahashi, T.; Saburi, M.; Uchida, Y.; Akutagawa, S. *Chem. Lett.*, **1988**, 2055. (b) Saburi, M.; Aoyagi, K.; Takeuchi, H.; Takahashi, T.; Uchida, Y. *Chem. Lett.*, **1990**, 991. (c) Saburi, M.; Aoyagi, K.; Kodama, T.; Takahashi, T.; Uchida, Y.; Kozawa, K.; Uchida, T. *Chem. Lett.*, **1990**, 1909.

(32) Crabtree, R. H.; Lavin, M. *J. Chem. Soc., Chem. Commun.*, **1985**, 1661.

(33) Morris, R. H.; Sawyer, J. F.; Shiralian, M.; Zubkowski, J. D. *J. Am. Chem. Soc.*, **1985**, *107*, 5581.

(34) Albertin, G.; Antoniutte, S.; Bordignon, E. *J. Am. Chem. Soc.*, **1989**, *111*, 2072.

(35) Conroy-Lewis, F. M.; Simpson, S. J. *J. Chem. Soc., Chem. Commun.*, **1986**, 506.

(36) (a) Chinn, M. S.; Heinekey, D. M. *J. Am. Chem. Soc.*, **1987**, *109*, 5865. (b) Chinn, M. S.; Heinekey, D. M.; Payne, N. G.; Sofield, C. D. *Organometallics*, **1989**, *8*, 1824.

(37) Jia, G.; Morris, R. H. *J. Am. Chem. Soc.*, **1991**, *113*, 875.

(38) Ricci, J. S.; Koetzle, T. F.; Bautista, M. T.; Hofstede, T. M.; Morris, R. H.; Sawyer, J. F. *J. Am. Chem. Soc.*, **1989**, *111*, 8823.

(39) Van der Sluys, L. S.; Eckert, J.; Eisenstein, O.; Hall, J. H.; Huffman, J. C.; Jackson, S. A.; Koetzle, T. F.; Kubas, G. J.; Vergamini, P. J.; Caulton, K. G. *J. Am. Chem. Soc.*, **1990**, *112*, 4831.

(40) Brammer, L.; Howard, A. K.; Johnson, O.; Koetzle, T. f.; Spencer, J. L. *J. Chem. Soc., Chem. Commun.*, **1991**, 241.

(41) Kubas, G. J.; Burns, C. J.; Eckert, J.; Johnson, S. W.; Larson, A. C.; Vergamini, P. J.; Unkefer, C. J.; Khalsa, G. R. K.; Jackson, S. A.; Eisenstein, O. *J. Am. Chem. Soc.*, **1993,** *115*, 569.

(42) Conroy-Lewis, F. M.; Simpson, S. J. *J. Chem. Soc., Chem. Commun.*, **1987**, 1675.

(43) (a) Hamiltion, D. G.; Crabtree, R. H. *J. Am. Chem. Soc.*, **1988**, *110*, 4126.

(b) Luo, X.-L.; Crabtree, R. H. *Inorg. Chem.*, **1990**, *29*, 2788.

Chapter 2

Agostic Interaction and Intramolecular Hydrogen Exchange in Coordinatively Unsaturated Ruthenium Complexes: Effects of Chelate Ring Size on Intramolecular Carbon-Hydrogen Bond Activation of Diphosphine Ligands.

Abstract

The solution properties of formally five-coordinate ruthenium complexes $[RuH(P–P)_2]PF_6$ (P–P = 1,4-bis(diphenylphosphino)butane (dppb); **1a**, 2,3-*O*-isopropylidene-2,3-dihydroxy-1,4-bis(diphenylphosphino)butane (diop); **1b**, 1,3-bis(diphenylphosphino)propane (dppp); **1c**, 1,2-bis(diphenylphosphino)ethane (dppe); **1d**) were examined by various NMR measurements. Variable temperature ^1H NMR measurements suggest that the behaviors of **1a** and **1b** at low temperature differ significantly from those at high temperature. The agostic interaction between an α-methylene CH moiety of the diphosphine ligand and the ruthenium center was detected in **1a** below –30 °C and in **1b** below –60 °C. In **1c** and **1d** no agostic interaction could be detected. The hydrogen exchanges among the terminal hydride, the agostic hydrogen, and a noncoordinating methylene hydrogen of dppb in **1a** were proved on the basis of spin saturation transfer phenomena in the ^1H NMR measurements. The exchange rate between the agostic hydrogen and the terminal hydride was estimated in the temperature range –55 to –90 °C by spin saturation transfer studies, to reveal that $\Delta G^{\ddagger}$ for the hydrogen exchange is about 11 kcal mol^{-1}. At high temperature the hydrogen scrambling between *ortho* hydrogens on the phenyl groups, all the methylene hydrogens, and the terminal hydride in **1a** was proved by employing the partially deuterized ligand $Ph_2P(CD_2)_4PPh_2$. Upon the contact of **1a**, **1c**, and **1d** with D_2 gas in solution, deuterium incorporation takes place at *ortho* and all methylene positions of diphosphines in these complexes. In the case of **1a**, the deuterium content of each site is in the order β-CH_2 > α-CH_2 > *o*-CH. In **1b** and **1c**, the H/D exchange at *o*-CH proceeded in preference to those at α-CH_2 or β-CH_2.

Introduction

The activation of carbon-hydrogen σ bond is one of the most important target reactions in organo-transition metal chemistry.[1] In order to facilitate the cleavage of a chemical bond with a metal complex, the interaction between the bonds and the metal center is necessary either in the transition state or in an intermediate. Organometallic moieties involving the coordination of σ bond to a transition metal center have attracted considerable attention as possible models for the intermediate of σ bond dissociation.[2]

It was proposed that M←H–C bonds, i.e. agostic interactions, are similar in the bonding character to η^2-type coordination of a dihydrogen ligand to a transition metal (three-center two-electron bond).[2c] The facts that some coordinatively unsaturated 16-electron complexes, which are the precursors of molecular hydrogen complexes, involve agostic interactions demonstrate the similarity in bondings between agostic interaction and dihydrogen coordination.[3, 4] Due to that the isolation of such coordinatively unsaturated complexes is often difficult because of their high reactivities, it is required in such occasion to generate them in situ by thermochemical[5] or photochemical[6] ligand dissociation of saturated precursors. Although agostic interactions are regarded as intermediates on the way to oxidative addition of carbon-hydrogen bonds, few cases are known as the examples of actual C–H bond activation, especially of aliphatic C–H groups.[7]

I describe herein the solution behavior of the formally five-coordinate ruthenium complexes $[RuH(P\text{–}P)_2]PF_6$ (P–P = dppb; **1a**,[8] diop; **1b**,[9] dppp; **1c**,[8] and dppe; **1d**[8]). It was disclosed by NMR measurements that, at low temperature, the interaction between an aliphatic C–H moiety of the diphosphine ligand and the ruthenium center is detected clearly for complexes **1a** and **1b**, and that the agostic hydrogen undergoes

exchanges with the terminal hydride (Ru–H) at a considerable rate. Such agostic interaction could not be detected for analogous complexes **1c** and **1d**. The rate and thermodynamic parameters for the exchange between the terminal hydride and the agostic hydrogen in **1a** were determined in the temperature range –55 to –90 °C. At high temperature, however, the agostic interaction in **1a** was no longer observed, and, instead, rapid hydrogen scrambling including the terminal hydride and all the methylene hydrogens and the *ortho* hydrogens on the phenyl groups of the ligands could be proved by employing the partially deuterated ligand $Ph_2P(CD_2)_4PPh_2$. It was demonstrated, further, that facile deuterium incorporation takes place at the diphosphines of the five-coordinate complexes (**1a**, **1c**, and **1d**) in solution under D_2 atmosphere. The mechanism for such H/D exchange, which could be promoted by a deuteride complex as $[RuD(P–P)_2]^+$, is proposed. The difference of the H/D exchange reactivity between complexes **1a**, **1c**, and **1d** is also discussed.

Results and Discussion

Preparation of [RuH(diphosphine)$_2$]PF_6 (1).

The formally five coordinate complexes **1a-d** are prepared from [RuH(cod)(NH_2NMe_2)$_3$]PF_6[11] and two equivalents of respective diphosphines according to the reported method[8a, 9b] with slight modifications.

$$[RuH(cod)(NH_2NMe_2)_3]PF_6 + 2\ P\text{–}P \rightarrow [RuH(P\text{–}P)_2]PF_6 + COD + 3\ NH_2NMe_2 \quad (1)$$

In the previous paper, methanol or ethanol was used as a solvent for the synthesis of **1** (eq. 1).[8a, 12] These complexes are coordinatively unsaturated, and, therefore, tend to react slowly with primary or secondary alcohols to give dihydride complexes (eq. 2). The proton thus formed can react with 1,1-dimethylhydrazine, the salt of which remains in a reaction mixture as a by-product.

$$[RuH(P\text{–}P)_2]^+ + RR'CHOH \rightarrow RuH_2(P\text{–}P)_2 + RR'C{=}O + H^+ \quad (2)$$

It was found that the side reaction with alcoholic solvent can be avoided by employing *tert*-butyl alcohol or acetone as a solvent.

^1H and ^{31}P NMR Characteristics of [RuH(dppb)$_2$]PF_6 (1a) and [RuH(diop)$_2$]PF_6 (1b).

The high field region of the variable temperature ^1H NMR spectra of **1a** is shown in Figure 2.1. Above –10 °C, a single broad peak was observed in the hydride region. As temperature decreased below –10 °C, the broad signal observed above –10 °C decoalesced into two resonances with equal intensities. The intensity of the broad signal above –10 °C corresponds to one hydrogen nucleus, and that of each resonance

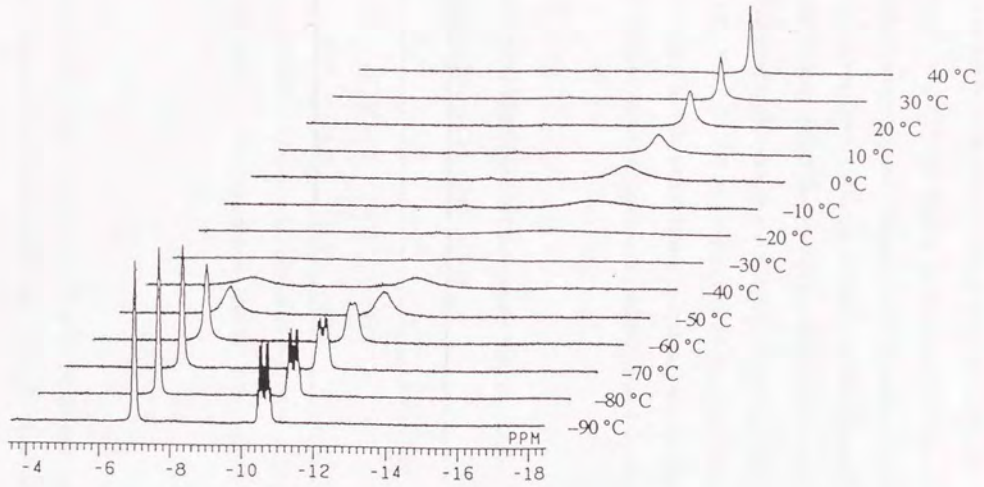

Fig. 2.1 Variable temperature ^1H NMR spectra of $[RuH(dppb)_2]PF_6$ (**1a**) in the high field region at 400 MHz in CD_2Cl_2.

detected below –30 °C also corresponds to one proton, respectively. Below –70 °C, the signal at δ –10.6 turned into a doublet of quartets due to the spin couplings with phosphorus nuclei ($^2J_{HP}$ = 25 and 77 Hz), while another resonance was detected as a broad signal throughout the accessible temperature. The averaged chemical shift of the two resonances at lower temperatures (ca. δ –8.8) considerably shifted to lower field compared to the chemical shift of the broad peak detected above –10 °C (ca. δ –14.7). This observation could suggest that an intrinsic structural change occurs in **1a** between –10 and –30 °C. The $^{31}P\{^1H\}$ NMR spectrum of **1a** at –90 °C (see Figure 2.2) showed the presence of four inequivalent phosphorus nuclei (see Table 2.1).[13] Possibility for the existence of two isomers or the formation of a polynuclear complex

Table 2.1 $^{31}P\{^1H\}$ NMR data for $[RuH(dppb)_2]PF_6$ (**1a**) and $[RuH(diop)_2]PF_6$ (**1b**) in CD_2Cl_2 at –90 °C[a]

Complex	δ_A[b]	δ_B[b]	δ_M[b]	δ_X[b]	$J_{AM} = J_{BM}$[c]	$J_{AX} = J_{BX}$[c]
1a[d]	37.9[e]		–13.4	79.1	30	10
1b[d]	30.4	31.1	–9.5	73.2	20	30

[a] Recorded at 162 MHz. [b] Relative to external 85 % D_3PO_4. [c] Coupling constants in hertz. [d] J_{AB} and J_{MX} were not observed clearly. [e] Observed as an unresolved multiplet.

at low temperature was entirely denied by the $^{31}P\{^1H\}$ NMR spectrum. Below –30 °C, **1a** seems to have two hydride-like nuclei in a molecule. The signal at δ –10.6,

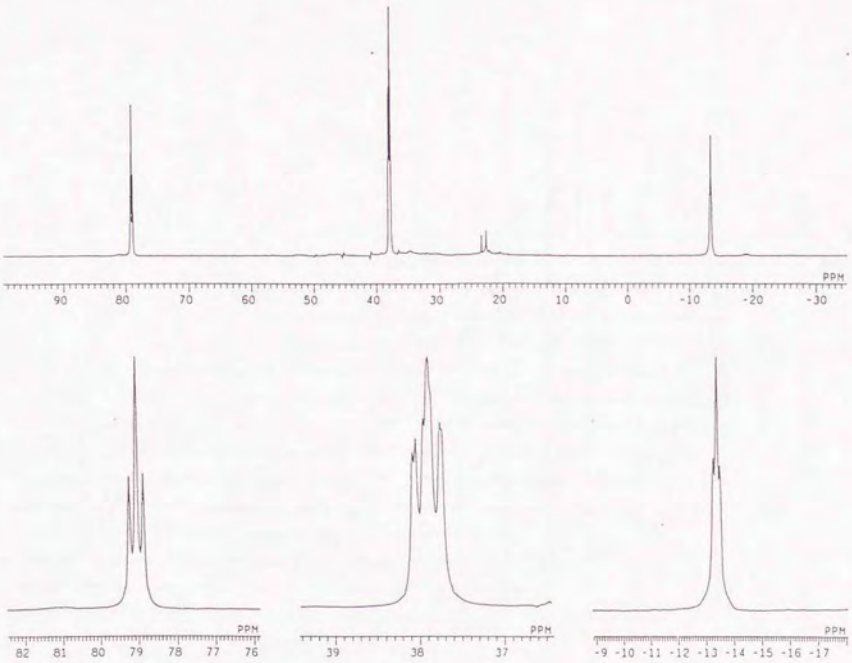

Fig 2.2 ^{31}P NMR spectrum of $[RuH(dppb)_2]PF_6$ (**1a**) at 162 MHz in CD_2Cl_2 at –90 °C.

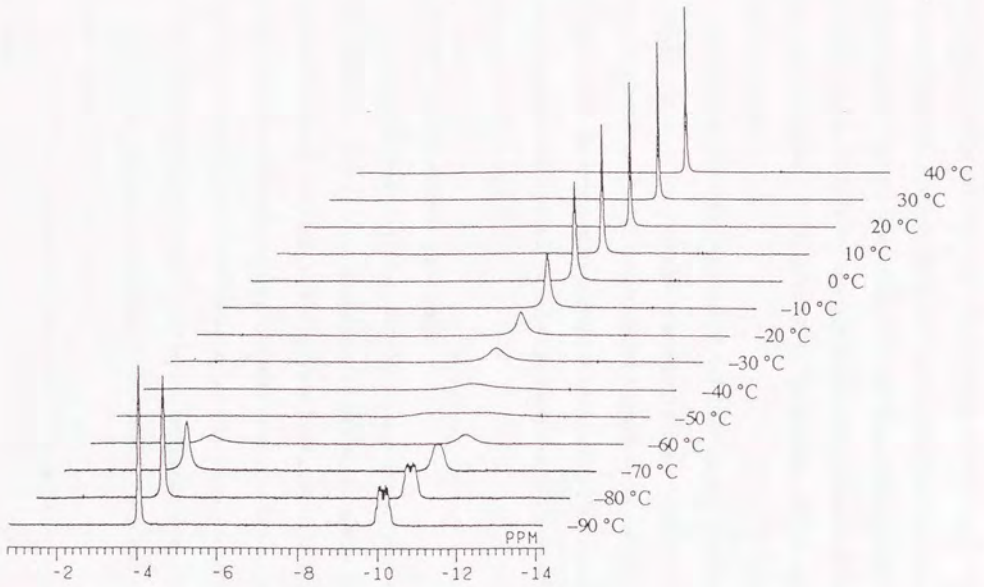

Fig. 2.3 Variable temperature ^1H NMR spectra of $[RuH(diop)_2]PF_6$ (**1b**) in the high field region at 400 MHz in CD_2Cl_2.

which reveals the couplings with phosphorus nuclei at –90 °C is ascribed to the terminal hydride (Ru–H), while the other at δ –7.0, showing no coupling with phosphorus at the same temperature, is assigned to the hydrogen in a C-H moiety interacting with the ruthenium center (agostic interaction).[2a, b] All these NMR characteristics were observed for the tetraphenylborate analogue [RuH(dppb)$_2$]BPh$_4$ (**1a-BPh$_4$**). This fact indicates that the anions, PF_6^- in **1a** and BPh_4^- in **1a-BPh$_4$**, have no interaction with the ruthenium center.

The diop complex **1b** exhibited similar ^{1}H NMR features to those of **1a** (Figure 2.3). In the case of **1b**, two hydriditic resonances, a broad signal (ca. δ –4.1) and a doublet of quartets (ca. δ –10.2), were detected at and below –60 °C. The highest temperature where the agostic interaction can be observed for **1b** is considerably lower than that for **1a**. As we expected, **1b** shows an ABMX pattern in the ^{31}P{^{1}H} NMR spectrum at –90 °C (Table 2.1).

Assignment of the Agostic Hydrogen.

There are two possible C-H moieties for the coordinating diphosphines in **1a** and **1b**, which can interact with the ruthenium center in an agostic fashion; an *o*-hydrogen of the phenyl group and one of methylene hydrogens. It is supposed that the agostic hydrogen would show spin couplings with some other hydrogens, such as *m*-hydrogen in the former case or the neighboring protons of the methylene chain in the latter case. These two possible parts for the agostic interaction in **1a** and **1b** could be distinguished from each other on the basis of the chemical shifts and the number of cross peaks in the ^{1}H-^{1}H COSY spectra.

The ^{1}H-^{1}H COSY spectrum of **1a** at –90 °C (Figure 2.4) revealed three cross peaks between the agostic C–H resonance (δ –7.0) and the methylene signals of

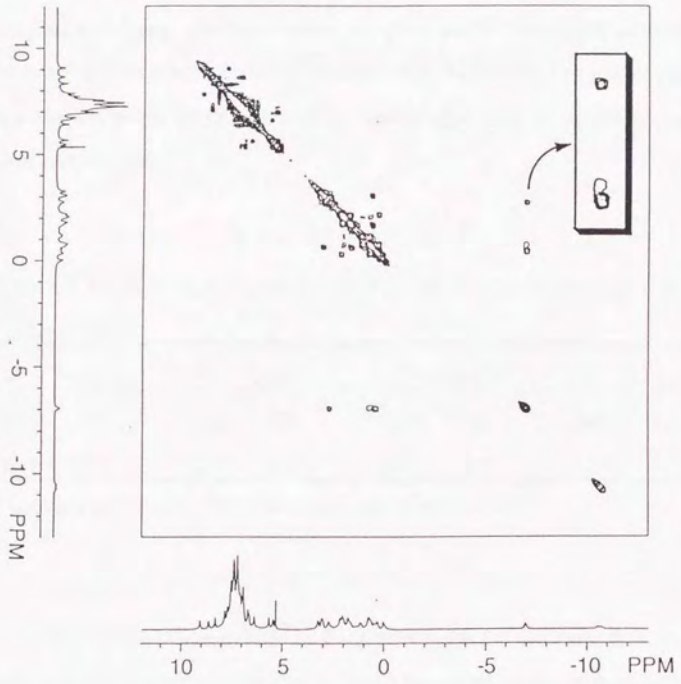

Fig. 2.4 ^{1}H-^{1}H COSY spectrum of $[RuH(dppb)_2]PF_6$ (**1a**) at –90 °C in CD_2Cl_2 at 400 MHz.

coordinating dppb ligand (δ ca. 0.8, 1.2, and 3.1). These facts strongly support that the agostic hydrogen should be ascribed to an α-methylene proton of dppb, which shows spin couplings with a geminal hydrogen and two inequivalent adjacent β-methylene hydrogens. It is demonstrated, therefore, that the complex **1a** involves the coordination of an α-methylene C–H moiety, not an *ortho* phenyl proton, of dppb at the sixth coordination site of the ruthenium center to give rise to the agostic interaction at low temperatures.

Table 2.2 ^{13}C NMR data for $[RuH(dppb)_2]PF_6$ (**1a**) in the methylene region in CD_2Cl_2 at –90 °C[a]

δ^b	$^1J_{CH}$/Hz	δ^b	$^1J_{CH}$/Hz	δ^b	$^1J_{CH}$/Hz	δ^b	$^1J_{CH}$/Hz
22.3	131	24.2	127	30.0	128	40.0	128
23.7	128	27.9	119	36.2	127	46.6	129

[a] Recorded at 101 MHz. [b] Relative to internal CD_2Cl_2 (δ 53.7).

The ^{13}C NMR spectrum of **1a** at –90 °C (Figure 2.5 and Table 2.2) showed eight resonances in the methylene region. This indicates that each methylene carbon in **1a** differs from the remaining carbons, so that the structure of **1a** has no elements of molecular symmetry, in accord with the results of $^{31}P\{^1H\}$ NMR data. In such occasion, two hydrogens of each methylene group in dppb are inequivalent. The proton-coupled ^{13}C NMR spectrum of **1a**, however, appeared as eight pseudo-triplets, instead of eight doublets of doublets signals, in the methylene region. This is probably

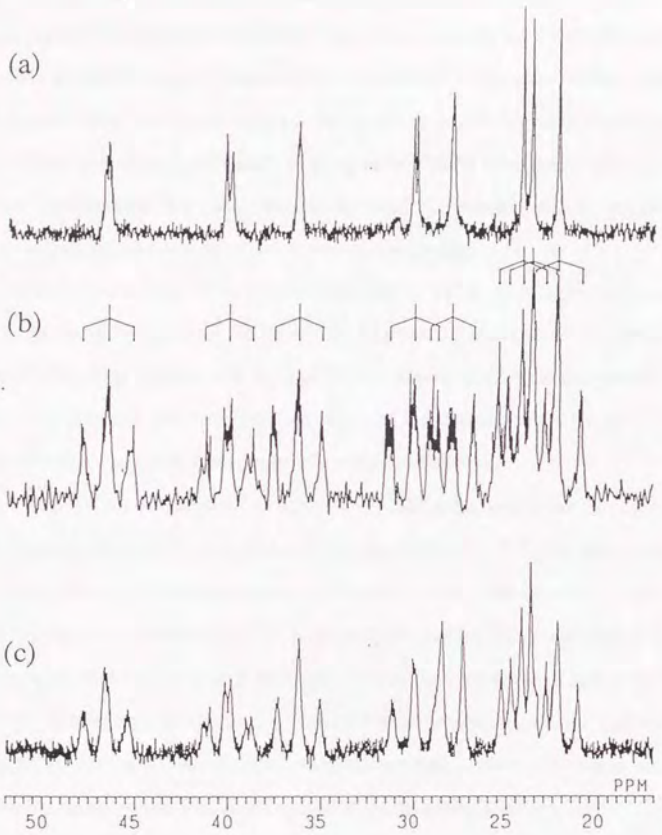

Fig. 2.5 ^{13}C NMR (101 MHz) spectra of $[RuH(dppb)_2]PF_6$ (**1a**) in the methylene region at –90 °C in CD_2Cl_2: (a) proton decoupled; (b) proton coupled; (c) selective decoupled with the agostic hydrogen (δ –7.0).

due to the broadening of the signals resulting from the coupling with ^{31}P nuclei and/or the similarity between the two geminal J_{CH} values. Among the ^{13}C NMR signals of the CH_2 groups of **1a**, the resonance at δ 27.9 showed a J_{CH} value smaller than the others and was assigned to the signal of the agostic carbon.[2a, b] This is consistent with the coordination of the methylene C-H group in **1a**. Under selective decoupling at the agostic hydrogen (δ –7.0), only the resonance at δ 27.9 turned into a simple doublet. This observation confirms the above-mentioned assignment.

As expected, the ^1H-^1H COSY spectrum of **1b** at –90 °C showed two cross peaks between the agostic C-H signal (δ –4.1) and the aliphatic C–H signals of a coordinating diop ligand (ca. δ 3.1 and 3.4, see Figure 2.6). This indicates that the agostic hydrogen of **1b** is also ascribed to one of the α-methylene hydrogens, which couples with the geminal hydrogen and the adjacent β-hydrogen.

Similar agostic interaction could not be detected for analogous five-coordinate complexes of dppp (**1c**), dppe (**1d**), dpbp,[14] and binap.[14b,15] In the case of **1c** and **1d**, the smaller size of the chelate rings prevents a C–H bond in a methylene unit from coordinating to the ruthenium center, whereas dppb and diop ligands provide a flexible seven-membered chelate upon coordination. As to the complexes of dpbp and binap, the ligands have no aliphatic C–H groups in themselves, although these diphosphines form seven-membered chelate rings. As mentioned above, the highest temperature, at which the agostic interaction is recognized in the ^1H NMR spectrum, is –30 °C for **1a** and –60 °C for **1b**. The flexibility of the diop chelate ring should be reduced due to the presence of dioxalane ring, compared to that of the simple four-carbon chain in the dppb chelate. This makes the coordination of an α-methylene hydrogen to the ruthenium center more difficult in **1b** than in **1a**. The difference in the chelate ring

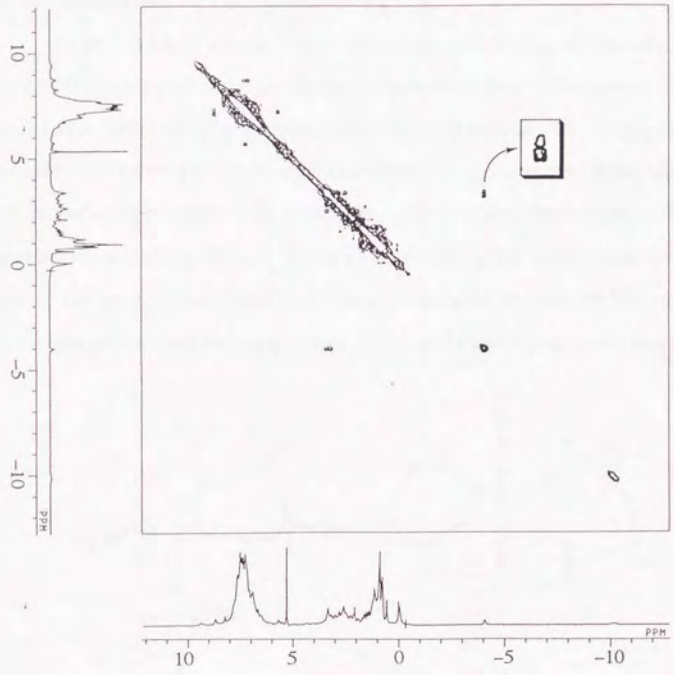

Fig. 2.6 ^{1}H-^{1}H COSY spectrum of $[RuH(diop)_2]PF_6$ (**1a**) at –90 °C in CD_2Cl_2 at 400 MHz.

flexibility between dppb and diop is reflected to the above-mentioned temperature dependence of the agostic interaction.

MM2 Calculation of $[RuH(dppb)_2]PF_6$ (1a).

In the ^1H NMR spectra, the coupling patterns (doublet of quartets) of the terminal hydride signals of **1a** and **1b** at low temperature indicate that the two chelating diphosphine ligands adopt a *cis* arrangement in these complexes. The terminal hydride should be located *trans* to one phosphorus nucleus, and *cis* to the other three. There are two candidates for the way of the coordination of an α-methylene hydrogen of dppb to the ruthenium center in **1a**, both of which fill the other steric requirements described above. The two structures, **I** and **II**, which are possible for the complex **1a** in solution at low temperature, are shown in Figure 2.7. I could not decide on the basis of the

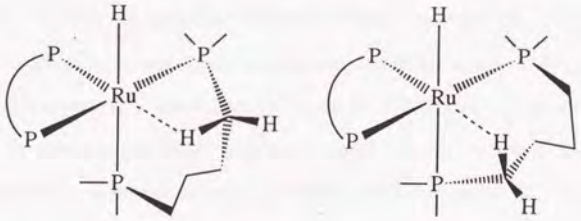

I **II**

Fig. 2.7 Two possible structures for the complex **1a** at –90 °C.

spectroscopic data which of these two structures is probable for **1a**. The molecular mechanics 2 (MM2) calculations using the CAChe System suggest that the structure **I** is more stable than **II**, the energy difference between **I** and **II** being about 8.6 kcal mol^{-1}.

Although electronic effects are completely ignored in the MM2 calculations, it is reasonable to suppose that the difference in the electronic property between **I** and **II** is small. Furthermore, the energy difference obtained above is significantly large to suggest that the structure **I** is a more probable structure of **1a**.

Intramolecular Hydrogen Exchange at Low Temperature.

The signal of the terminal hydride of **1a** shows no clear coupling with phosphorus nuclei above –60 °C in the ^{1}H NMR spectra, and coalesced with the signal of the agostic hydrogen at –20 °C (see Figure 2.1). This suggests a possibility of an exchange between the agostic hydrogen and the terminal hydride in **1a**. Indeed, spin saturation transfer phenomena were observed among the Ru–H, C–H (agostic at ca. δ –7.0), and C-H (methylene at ca. δ 1) groups at –45 °C (Figure 2.8). Saturation of the agostic resonance led to a considerable decrease in the intensity of the terminal hydride resonance. Further, the irradiation of the α-methylene hydrogen (ca. δ 1) resulted in the almost complete disappearance of the signal due to the agostic C–H group and a considerable reduction of signal intensity for the Ru–H resonance. These observations indicate the occurrence of rapid hydrogen exchanges among the Ru–H, agostic C–H and noncoordinating methylene protons of dppb ligands even at –45 °C. The exchange rate, k, between the agostic hydrogen and the terminal hydride was estimated in the temperature range –55 to –90 °C by the spin saturation transfer technique.[16 – 19] The rate constants and the T_1 values of each signal are summarized in Table 2.3. The Eyring plot ($\ln k/T$ vs. $1/T$) is linear (Figure 2.9), and the thermodynamic parameters for the exchange between the agostic hydrogen and the terminal hydride in **1a** are: $\Delta H^{\ddagger}$ = 10.3 ± 0.5 kcal mol^{-1} and $\Delta S^{\ddagger}$ = –3.6 ± 0.6 cal mol^{-1} K^{-1}. These values lie in the range of those reported for the intramolecular hydrogen exchange between the hydride

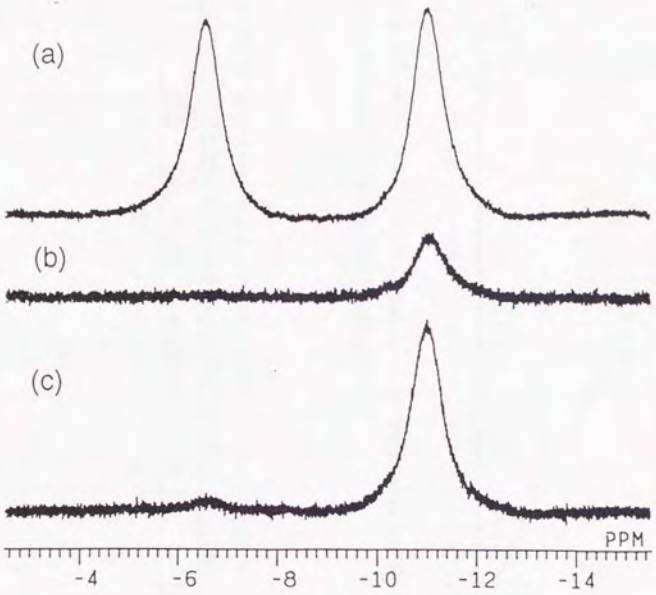

Fig. 2.8 ^{1}H NMR (400 MHz) spectra of **1a** in the high field region at –45 °C in CD_2Cl_2: (a) nonirradiated conditions; (b) irradiated at the agostic hydrogen (ca. δ –7); (c) irradiated at the α-hydrogen in the methylene group (ca. δ 1).

and the dihydrogen ligand in $[RuH(\eta^2\text{-}H_2)(diphosphine)_2]^+$.[14b, 20]

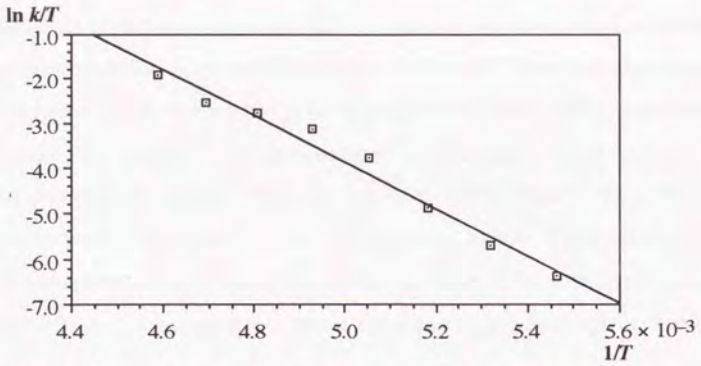

Fig. 2.9 Plot of ln k/T vs. $1/T$ for the exchange between the agostic hydrogen and the terminal hydride in $[RuH(dppb)_2]PF_6$ (**1a**).

Table 2.3 T_1 values and rate constant, k, for hydrogen exchange between the agostic hydrogen and the terminal hydride in $[RuH(dppb)_2]PF_6$ (**1a**)

T/°C	T/K	T_1(agostic)/ms[a]	T_1(hydride)/ms[a]	k/s^{-1}	$\Delta G^{\ddagger}$/kcal mol^{-1} [b]
–55	218	102	120	32.6	11.1
–60	213	141	147	17.1	11.1
–65	208	174	171	12.9	11.0
–70	203	242	182	8.9	10.8
–75	198	284	193	4.5	10.8
–80	193	335	287	1.5	11.0
–85	188	395	389	0.6	11.0
–90	183	483	513	0.3	11.0

[a] The T_1 experiments were performed at 400 MHz with a 180°-τ-90° pulse sequence by the inversion -recovery method. [b] Calculated from the rate constants k.

Two intermediates are possible for the hydrogen exchange as shown in Figure 2.10; i.e., seven-coordinate dihydride (A), and six-coordinate η^2-H_2 complex (B). Albéniz and co-workers recently suggested the formation of the dihydrogen complex as the intermediate for intramolecular hydrogen exchange.[21] They also proposed the direct proton transfer as a key step in the hydrogen exchange of M←H–C system in a transition-metal complex.[21] As mentioned above, the complex **1a**, which involves the agostic interaction between α-CH and ruthenium center, exhibits the hydrogen exchange between the agostic hydrogen and the terminal hydride. The result of ^{1}H-^{1}H COSY measurement demonstrates that this agostic hydrogen has a coupling with the neighboring methylene hydrogens. These observations suggest the possibility that this

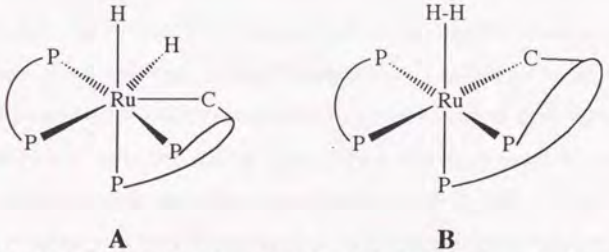

A **B**

Fig. 2.10 Two possible intermediates for the hydrogen exchange in **1a**: (A) seven-coordinate dihydride; (B) six-coordinate η^2-H_2 complex.

hydrogen exchange proceeds via direct proton transfer, rather than the successive process of oxidative addition and reductive elimination.[22 – 25] Recently, Crabtree and co-workers reported either dissociative or nondissociative interaction of a C–H moiety in quinoline derivatives with iridium complexes and suggested the relationship between these hydrogen exchanges and agostic interactions.[26] However, there has been no

direct evidence of the agostic interaction participating in C–H activation. My results are the first example of the observation of the direct intramolecular hydrogen exchange involving the agostic hydrogen.

Intramolecular Hydrogen Exchange at High Temperature.

At higher temperatures, **1a** (above –10 °C) and **1b** (above –40 °C) are highly fluxional in solution, so that it is impossible to decide whether the hydrogen exchange between α-CH and Ru-H is still taking place or not. Judging from the variable temperature ^{1}H NMR spectra, the high temperature behavior of **1a** differs from the low temperature one. With a view to answer this problem, I prepared the partially deuterated dppb; $Ph_2P(CD_2)_4PPh_2$ (dppb-d_8). The ^{1}H NMR spectrum of the complex $[RuH(dppb\text{-}d_8)_2]PF_6$ (**1a-*d*$_{16}$**), obtained by a reaction of dppb-d_8 and $[RuH(cod)(NH_2NMe_2)_3]PF_6$ in ethanol, displays the signals assignable to the methylene protons of coordinating diphosphines. It should be noted that the resonances not only of α-methylene but also of β-methylene of dppb appear with practically equal intensities. The ^{2}D NMR spectrum of **1a-*d*$_{16}$** revealed the resonance assignable to deuteriums incorporated into phenyl group (δ 7.1) and the Ru-D part (δ –14.7), in addition to the C-D signals of methylene groups (δ 0.7 and 2.4, Figure 2.11). Further, a detailed examination of the aromatic region in the ^{1}H NMR spectrum showed that the intensity of the *ortho*-hydrogen resonance of **1a-*d*$_{16}$** is distinctly smaller than that of the *meta*-hydrogens, and that the latter signal broadens considerably as a result of H–D coupling with *ortho*-deuterium (Figure 2.12). It is demonstrated, therefore, that the protium source introduced into the methylene parts of dppb-d_8 is the *ortho* C–H groups on the phenyl moieties.[1c, 22, 23] It is certain that the protiums incorporated into the methylene groups do not originate from ethanol employed as a

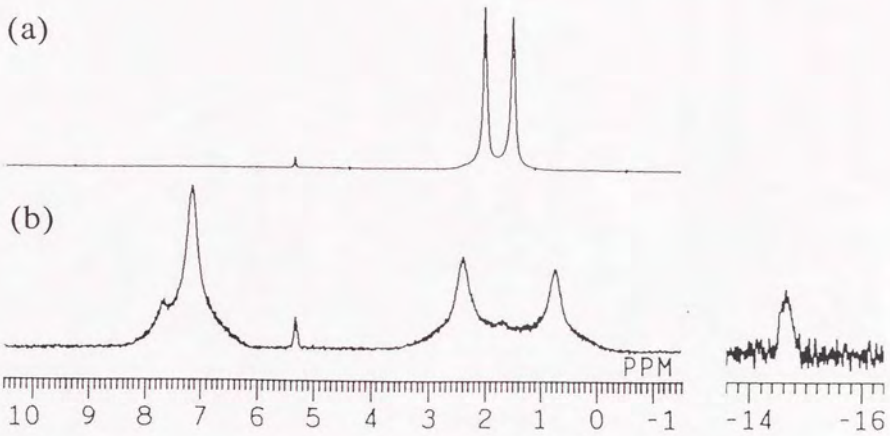

Fig. 2.11 ^{2}D NMR (61 MHz) spectra at 30 °C in CH_2Cl_2; (a) $Ph_2P(CD_2)_4PPh_2$ (dppb-d_8); (b) [RuH(dppb-d_8)$_2$]PF_6 (**1a**-d_{16}).

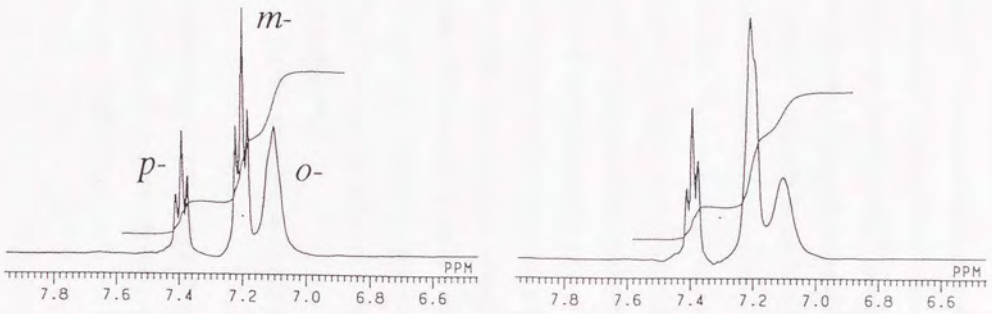

Fig. 2.12 ^{1}H NMR spectra of **1a** (left) and **1a-*d*$_{16}$** (right) in the phenyl region at 30 °C in CD_2Cl_2 at 400 MHz.

solvent, because the use of C_2D_5OD in place of C_2H_5OH causes no change in the ^1H NMR spectrum of **1a-*d*$_{16}$**.[27] The total protium amount of *ortho*, α- and β-methylene positions in **1a-*d*$_{16}$** estimated from the ^1H NMR spectrum corresponds well to the hydrogens that initially exist at the *ortho* positions of dppb-*d*$_8$. These results indicate that this hydrogen exchange proceeds via an intramolecular process.

At lower temperatures, only one of the α-methylene hydrogen of dppb exchanges with the terminal hydride via the agostic interaction. In contrast, at higher temperatures, not only the α-CH_2 but also the β-CH_2 and the *ortho* hydrogen on the phenyl groups of coordinating dppb can be sufficiently activated, so that rapid hydrogen scrambling takes place among these hydrogens and the Ru–H in **1a**. The possible pathway of H–D scrambling among α- and β-CH_2 parts and *o*-hydrogens of dppb-*d*$_8$ is illustrated in Scheme 1.1. Thus, according to the reaction sequence i → ii → iii → iv, a deuterium at the methylene groups, not only of α- but also of β-position, is replaced with protium of Ru-H, while the Ru-H is transformed into Ru–D. The deuteration of the *o*-hydrogen on the phenyl group proceed via the sequence iv → v → vi → i. By uniting these sequences, a complete cycle for H/D scrambling among a coordinating dppb-*d*$_8$ was obtained.

I suppose that in the H/D scrambling in **1a-*d*$_{16}$** the β-CH and *o*-CH groups also take part in the agostic interaction (ii, iii or v, vi) in a similar manner as the α-CH group. Although the agostic interactions involving β-CH or *o*-CH group have not been detected in the ^1H NMR spectra of **1a**, the observed H/D scramblings clearly indicate that these C–H bonds are sufficiently activated in a kinetical sense at higher temperatures.

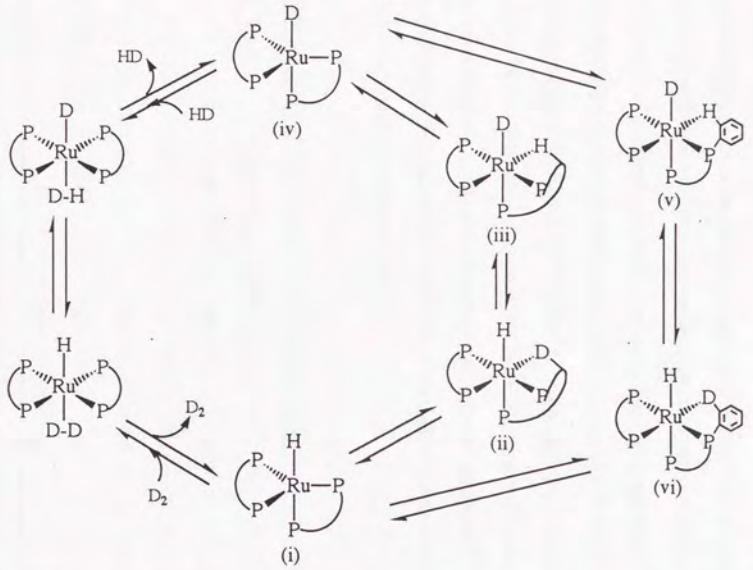

Scheme 1.1 Proposed mechanism of the deuterium incorporation and the hydrogen scrambling in the complex **1**.

Deuterium Introduction into Diphosphine Ligands by Treatments of 1 with D_2 Gas.

It is noteworthy that all steps in the cycle shown in Scheme 1.1 are reversible. If the deuteride species $[RuD(dppb)_2]^+$ were once obtained, the deuterium incorporation into the methylene moieties and *o*-CH parts would be achieved via the sequences (iv → iii → ii → i) and (iv → v → vi → i), respectively. Upon the contact with D_2 gas, **1a** is spontaneously converted into a tautomeric mixture of $[RuH(D_2)(dppb)_2]^+$ and $[RuD(HD)(dppb)_2]^+$, and the latter can afford $[RuD(dppb)_2]^+$ by the dissociation of HD ligand.[8b, 20a] It has been clarified, however, that under H_2 atmosphere, **1a** turned almost completely into $[RuH(H_2)(dppb)_2]^+$ and that the NMR measurements showed no detectable amount of the precursor remained.[8b] Despite that, a trace amount of $[RuD(dppb)_2]^+$ could be generated to promote the deuterium incorporation into the diphosphine ligands.

Table 2.4 Ratio of deuterium incorporation into the diphosphine ligand[a]

Entry	Complex	*o*-CD / %	α-CD / %	β-CD / %
1	**1a**[b]	18	54	92
2	**1a**[c]	0	0	0
3	**1a-*d*$_{16}$**	38	57	55
4	**1b**[b]	61	45	< 5
5	**1c**[b]	52	8	------

[a] Calculated from the signal intensity of ^1H NMR spectra of the diphosphine dioxide obtained by the decomposition of the complexes. [b] Reaction conditions: complex (50 mg), THF (10 mL), under D_2 (1 atm), at 30 °C, 72 h. [c] Reaction conditions: complex (50 mg), THF (10 mL), under Ar, at 30 °C, 72 h.

With a view to examine the above possibility, ^{1}H NMR change of **1a** in tetrahydrofuran was followed under D_2 atmosphere. Indeed, a clear decrease of signal intensities in the methylene region could be observed after keeping a solution of **1a** for several hours under D_2. It was found somewhat difficult to determine the exact intensity ratio of α-CH : β-CH : *o*-CH in the complex itself by the ^{1}H NMR measurements, presumably due to the broadening of the signals resulted from the presence of conformers and isotopomers. Hence, the deuterated complex was decomposed with H_2O_2 and the diphosphine ligands were converted into the diphosphine-dioxide. The dioxide of dppb-d_n was separated from the reaction mixture (dppb-d_n refers to a mixture of partially deuterated dppb) and the ^{1}H NMR spectrum was recorded for this dioxide (dppbO_2). Fortunately, a complete signal separation was obtained between *m*- and *p*-hydrogens and *o*-hydrogens of dppbO_2 in the ^{1}H NMR spectrum. Using the total signal intensity of *m*- and *p*-hydrogens as the internal standard, the intensities of *o*-CH, α-CH_2, and β-CH_2 were evaluated with good accuracy. The results of the deuterium replacement after a 72 h treatment were given in Table 2.4. As shown in entry 1, deuterium substitution occurred at all possible sites of dppb. Interesting is that the D content of each site in dppb is in the order β-CH_2 > α-CH_2 > *o*-CH. The deuterium replacement at β-CH_2 proceeds faster than that at α-CH_2 groups, although β-CH bonds are excluded from the agostic interaction in complex **1a** at lower temperatures.

This strongly suggests that similar H/D exchanges could occur in analogous complexes that exhibit no detectable agostic interaction in the ^{1}H NMR spectra. Thus, **1c** and **1d** were treated with D_2 gas, and the deuterium incorporation into **1c** and **1d** were estimated in the similar manner mentioned above for **1a**. As expected, the deuterium incorporation into the diphosphines were recognized for both **1c** and **1d** (see

Table 2.4). It should be noted that, in **1c** and **1d**, the H/D exchange at *o*-CH proceeded in preference to those at α-CH_2 or β-CH_2.[24, 25] It is supposed that, as the chelate ring of $[RuH(P–P)_2]^+$ becomes smaller, the approach of the methylene parts to the ruthenium center becomes harder, whereas that of *o*-CH is affected by the size of chelate rings to a lesser extent.[24] The experimental results in Table 2.4 are well in accord with this assumption.

Conclusions

I have discovered the agostic interaction between an α-methylene hydrogen of the diphosphine ligand and the ruthenium center in **1a** and **1b** at low temperature. The agostic hydrogen undergoes intramolecular hydrogen exchanges between the terminal hydride and a noncoordinating methylene hydrogen of the diphosphine ligand. In **1c** and **1d**, similar agostic interaction was not recognized. At high temperature, these complexes become highly fluxional and exhibit the hydrogen scrambling between *ortho* hydrogens on the phenyl groups, all the methylene hydrogens, and the terminal hydride. This hydrogen scrambling is detected not only in **1a** but also in **1c** and **1d** by the H/D exchange under D_2 atmosphere. Under D_2, deuterium is introduced into the diphosphine ligands via $[RuD(P\text{–}P)_2]^+$. In **1a**, the H/D exchange proceeds at methylene positions in preference to at *o*-CH, while, in **1c** and **1d**, the deuterium introduction occurs faster at the *ortho* positions than at the methylene parts. The differences between **1a**, **1c**, and **1d** are ascribed to that the smaller size of the chelate rings in **1c** and **1d** make the interaction of methylene hydrogens to the ruthenium hard, whereas dppb in **1a** forms a sufficiently flexible seven membered ring.

Experimental Section

General Procedure.

Unless otherwise noted, all manipulations were carried out under a dry argon or dinitrogen atmosphere by standard Schlenk-tube techniques. All the solvents were dried over appropriate reagents and distilled under N_2.[28] C_2D_5OD and $DO(CD_2)_4OD$ were purchased from Aldrich Chemical Company. Dppb, dppp, and dppe were purchased from Kanto Chemical Co. and used as received without further purification. Diop[29] and $[RuH(cod)(NH_2NMe_2)_3]PF_6$[11] were prepared as reported. $[RuH(dppb)_2]PF_6$,[8] $[RuH(diop)_2]PF_6$,[9] $[RuH(dppp)_2]PF_6$,[8] and $[RuH(dppe)_2]PF_6$[8] were prepared by literature methods, except that *tert*-butyl alcohol (for **1a**, **1c**, and **1d**) or acetone (for **1b**) was employed as a solvent instead of ethanol. $[RuH(dppb\text{-}d_8)_2]PF_6$ was prepared by using dppb-d_8.

NMR Studies.

The preparation of sample solutions of the complexes for NMR measurements was carried out under an argon (not dinitrogen) atmosphere using air free CD_2Cl_2 as a solvent. ^1H NMR (400 MHz), ^2D NMR (61 MHz), ^{13}C NMR (101 MHz), and ^{31}P NMR (162 MHz) spectra were recorded on a JEOL JNM-GX 400 spectrometer. ^1H and ^{13}C NMR chemical shifts are reported in ppm downfield of tetramethylsilane. ^2D NMR chemical shifts are relative to the solvent resonance, $CHDCl_2$ (δ 5.3), as an internal standard. ^{31}P NMR chemical shifts are reported in ppm downfield of external 85 % D_3PO_4. ^1H NMR T_1 determinations were performed with a standard 180°-τ-90° pulse sequence by the inversion-recovery method.

Measurements of the Exchange Rates between the Agostic Hydrogen and the Terminal Hydride in 1a.

Determination of the exchange rates between the two resonances was carried out according to the Forsén-Hoffman method.[17,18] Spin saturation transfer experiments were performed by irradiating the ^{1}H resonance of the agostic hydrogen. The exchange rates, k, were calculated from the following equation;

$$I'/I = \tau / (\tau + T_1)$$

where I and I' are the signal intensities of the terminal hydride without and with saturation of the agostic signal, respectively. T_1 is the spin-lattice relaxation time of the hydride resonance and τ (= $1/k$) is the pre-exchange lifetime of this exchange system. The ratio I'/I were calculated from the difference spectrum recorded by subtracting the spectrum irradiated at the agostic resonance from the reference (nonirradiated) spectrum. The activation parameters, $\Delta H^{\ddagger}$, $\Delta S^{\ddagger}$, and $\Delta G^{\ddagger}$ were obtained from a linear least-squares fit of the Eyring plot (ln k/T versus $1/T$) utilizing the Eyring equation.[18]

1,4-Bis(diphenylphosphino)butane-*1,1,2,2,3,3,4,4-d*$_8$ (dppb-*d*$_8$).

To a pyridine (20 mL) solution of $DO(CD_2)_4OD$ (1.12 g, 11.4 mmol) was added *p*-toluenesulfonyl chloride (4.70 g, 24.6 mmol) at –10 °C. After stirring the mixture at room temperature for 3 h, the mixture was concentrated to about 5 mL and poured into ice-water. The ditosylate deposited as a white solid was filtered, washed with water, and then dried under reduced pressure. This crude ditosylate ($TsO(CD_2)_4OTs$, 2.95 g) was used in the following reaction without further purification. ^{1}H NMR [$CDCl_3$, TMS]: δ 2.46 (s, 6H), 7.35 (d, J = 8 Hz, 4H), 7.76 (d, J = 8 Hz, 4H).

A tetrahydrofuran (5 mL) solution of the crude ditosylate (2.90 g) was added to a solution of $LiPPh_2$ (prepared from PPh_3 (4.53g, 17.3 mmol) and Li (0.26 g, 37.5 mmol) in THF (15 mL), followed by *tert*-BuCl treatment) at 0 °C. After the addition, the mixture was refluxed for 1 h. After the mixture had cooled, THF was removed and degassed water (25 mL) was added. The diphosphine was extracted with hot benzene (25 mL × 4), and the benzene extracts were dried with $MgSO_4$. After the removal of the solvent, the title compound was recrystallized from absolute ethanol to give a colorless needle: 2.33 g (47 %, as a total yield). ^1H NMR [$CDCl_3$, TMS]: δ 7.27 – 7.32 (m, *meta*- and *para*-H), 7.34 – 7.40 (m, *ortho*-H). $^2D\{^1H\}$ NMR [CH_2Cl_2, $CDHCl_2$ (δ 5.3) as internal standard]: δ 1.49 (br, β-CD_2), 1.98 (br, α-CD_2). $^{13}C\{^1H\}$ NMR [$CDCl_3$, TMS]: δ 26.5 (m, α- and β-CH_2), 128.3 (d, $^3J_{PC}$ = 7 Hz, *meta*-C), 128.4 (s, *para*-C), 132.6 (d, $^2J_{PC}$ = 18 Hz, *ortho*-C), 138.8 (d, $^1J_{PC}$ = 13 Hz, *ipso*-C). $^{31}P\{^1H\}$ NMR [$CDCl_3$, D_3PO_4 (85 %) as external standard]: δ –11.8 (s). Anal. Calcd for $C_{28}H_{20}D_8P_2$: C, 77.40 %; H+D, 8.35 %. Found: C, 77.89 %; H+D, 8.01 %.

Reaction of the Complexes (1a, 1c, and 1d) with D_2 Gas.

The complex (50 mg) was dissolved in 10 mL of THF, and the solution was stirred under D_2 atmosphere at 30 °C for 72 h. After the removal of the solvent, 30% H_2O_2 (about 5 mL) was added to the residue. The produced diphosphine-dioxide was extracted with $CHCl_3$ from the mixture, and the chloroform solution was dried with $MgSO_4$. After the removal of the solvent, residual diphosphine-dioxide was purified by appropriate methods. The dioxide of dppb and dppe were recrystallized from acetone. Dppp-dioxide was purified with a HPLC equipped with a silica gel column (Merck RT 250-10) using isopropyl alcohol – *n*-hexane (3 : 7) as an eluent. The ratio

of deuterium incorporation into the diphosphine was determined by the ^1H NMR measurements of these diphosphine-dioxides. ^1H NMR [$CDCl_3$, TMS]: **dppb-dioxide**, δ 1.65 – 1.78 (m, β-CH_2), 2.16 – 2.29 (m, α-CH_2), 7.40 – 7.51 (m, *m*- and *p*-H), 7.63-7.73 (m, *o*-H); **dppp-dioxide**, δ 1.93-2.10 (m, β-CH_2), 2.46-2.59 (m, α-CH_2), 7.39 – 7.53 (m, *m*- and *p*-H), 7.64 – 7.74 (m, *o*-H); **dppe-dioxide**, δ 2.53 (s, α-CH_2), 7.41 – 7.55 (m, *m*- and *p*-H), 7.66 – 7.77 (m, *o*-H).

References and Notes

(1) General reviews of C–H activation in transition metal complex: (a) Parshall, G. W. *Acc. Chem. Res.* **1975**, *8*, 113. (b) Webster, D. E. *Adv. Organomet. Chem.* **1977**, *15*, 147. (c) Bruce, M. I. *Angew. Chem. Int. Ed. Engl.* **1977**, *16*, 73. (d) Crabtree, R. H. *Chem. Rev.* **1985**, *85*, 245. (e) Halpern, J. *Inorg. Chim. Acta* **1985**, *100*, 41. (f) Ryabov, A. D. *Chem. Rev.* **1990**, *90*, 403.

(2) (a) Brookhart, M.; Green, M. L. H. *J. Organomet. Chem.* **1983**, *250*, 395. (b) Brookhart, M.; Green, M. L. H.; Wong, L.-L. *Prog. Inorg. Chem.* **1988**, *36*, 1. (c) Crabtree, R. H.; Hamilton, D. G. *Adv. Organomet. Chem.* **1988**, *28*, 299.

(3) (a) Kubas, G. J.; Ryan, R. R.; Wrobleski, D. A. *J. Am. Chem. Soc.* **1986**, *108*, 1339. (b) Sato, M.; Tatsumi, T.; Kodama, T.; Hidai, M.; Uchida, T.; Uchida, Y. *J. Am. Chem. Soc.* **1978**, *100*, 4447.

(4) Wasserman, H. J.; Kubas, G. J.; Ryan, R. R. *J. Am. Chem. Soc.* **1986**, *108*, 2294.

(5) (a) Fendrick, C. M.; Marks, T. J. *J. Am. Chem. Soc.* **1984**, *106*, 2214. (b) Zeiher, E. H. K.; DeWit, D. G.; Caulton, K. G. *J. Am. Chem. Soc.* **1984**, *106*, 7006. (c) Buchanan, J. M.; Stryker, J. M.; Bergman, R. G. *J. Am. Chem. Soc.* **1986**, *108*, 1537. (d) Desrosiers, P. J.; Shinomoto, R. S.; Flood, T. C. *J. Am. Chem. Soc.* **1986**, *108*, 7964.

(6) (a) Janowicz, A. H.; Bergman, R. G. *J. Am. Chem. Soc.* **1983**, *105*, 3929. (b) Wenzel, T. T.; Bergman, R. G. *J. Am. chem. Soc.* **1986**, *108*, 4856. (c) Field, L. D.; George, A. V.; Messerle, B. A. *J. Chem. Soc., Chem. Commun.* **1991**, 1339.

(7) (a) Calvert, R. B.; Shapley, J. R. *J. Am. Chem. Soc.* **1978**, *100*, 7726. (b) Cree-Uchiyama, M.; Shapley, J. R.; St. George, G. M. *J. Am. Chem. Soc.* **1986**, *108*, 1316.

(8) (a) Ashworth, T. V.; Singleton, E. *J. Chem. Soc., Chem. Commun.* **1976**, 705. (b) Saburi, M.; Aoyagi, K.; Takahashi, T.; Uchida, Y. *Chem. Lett.* **1990**, 601.

(9) (a) Saburi, M.; Aoyagi, K.; Takeuchi, H.; Takahashi, T.; Uchida, Y. *Chem. Lett.* **1990**, 991. (b) Saburi, M.; Takeuchi, H.; Ogasawara, M.; Tsukahara, T.; Ishii, Y.; Ikariya, T.; Takahashi, T.; Uchida, Y. *J. Organomet. Chem.* **1992**, *428*, 155.

(10) Ogasawara, M.; Aoyagi, K.; Saburi, M. *Organometallics* **1993**, *12*, 3393.

(11) Ashworth, T. V.; Singleton, E.; Hough, J. J. *J. Chem. Soc., Dalton Trans.* **1977**, 1809.

(12) Meakin, P.; Muetterties, E. L.; Jesson, J. P. *J. Am. Chem. Soc.* **1973**, *95*, 75.

(13) Ashworth, T. V.; Chalmers, A. A.; Singleton, E. *Inorg. Chem.* **1985**, *24*, 2126. In this paper, they reported the ^{31}P NMR spectrum of **1a** in acetone-d_6 at –80 °C as an A_2MX pattern.

(14) (a) dpbp = 2,2'-bis(diphenylphosphino)-1,1'-biphenyl. (b) Ogasawara, M.; Saburi, M. *J. Organomet. Chem.* submitted.

(15) (a) binap = 2,2'-bis(diphenylphosphino)-1,1'-binaphthyl (b) Tsukahara, T.; Kawano, H.; Ishii, Y.; Takahashi, T.; Saburi, M.; Uchida, Y.; Akutagawa, S. *Chem. Lett.* **1988**, 2055.

(16) Campbell, I. D.; Dobson, C. M.; Ratcliffe, R. G.; Williams, R. J. P. *J. Mag. Res.* **1978**, *29*, 397.

(17) (a) Forsén, S.; Hoffman, R. A. *J. Chem. Phys.* **1963**, *39*, 2892. (b) Forsén, S.; Hoffman, R. A. *J. Chem. Phys.* **1963**, *40*, 1189.

(18) Sandström, J. *Dynamic NMR Spectroscopy;* Academic: New York, 1982.

(19) In the preliminary account,[10] we reported the values for the rate constants, *k*, different from those described here. In the course of further investigations, we found a technical mistake to obtain the difference between the irradiated and the nonirradiated spectra.

(20) (a) Bautista, M. T.; Cappellani, E. P.; Drouin, S. D.; Morris, R. H.; Schweitzer, C. T.; Sella, A.; Zubkowski, J. *J. Am. Chem. Soc.* **1991**, *113*, 4876. (b) Bianchini, C.; Perea, P. J.; Peruzzini, M.; Zanobini, F.; Vacca, A. *Inorg. Chem.* **1991**, *30*, 279. (c) Jessop, P. G.; Morris, R. H. *Coord. Chem. Rev.* **1992**, *121*, 155.

(21) Albéniz, A. C.; Schulte, G.; Crabtree, R. H. *Organometallics* **1992**, *11*, 242.

(22) (a) Parshall, G. W.; Knoth, W. H.; Schunn, R. A. *J. Am. Chem. Soc.* **1969**, *91*, 4990. (b) Parshall, G. W. *Acc. Chem. Res.* **1970**, *3*, 139. (c) Barefield, E. K.; Parshall, G. W. *Inorg. Chem.* **1972**, *5*, 964.

(23) Chaudret, B. N.; Cole-Hamilton, D. J.; Wilkinson, G. *J. Chem. Soc., Dalton Trans.* **1978**, 1739.

(24) Rosete, R. O.; Cole-Hamilton, D. J.; Wilkinson, G. *J. Chem. Soc., Dalton Trans.* **1984**, 2067.

(25) Cheney, A. J.; Mann, B. E.; Shaw, B. L.; Slade, R. M. *J. Chem. Soc. (A)* **1971**, 3833.

(26) (a) Crabtree, R. H.; Holt, E. M.; Lavin, M.; Morehouse, S. M. *Inorg. Chem.* **1985**, *24*, 1986. (b) Lavin, M.; Holt, E. M.; Crabtree, R. H. *Organometallics* **1989**, *8*, 99.

(27) Kiffen, A. A.; Masters, C.; Raynand, L. *J. Chem. Soc., Dalton Trans.* **1975**, 853.

(28) Perrin D. D.; Armarego, W. L. F. *Purification of Laboratory Chemicals;* Pergamon: Oxford, 1988.

(29) Dang, T. P.; Kagan, H. B. *J. Am. Chem. Soc.* **1972**, *94*, 6429.

Chapter 3

Effects of Chelate Ring Rigidity on the Intramolecular Hydrogen Exchange in Hydrido(dihydrogen)bis(diphosphine)ruthenium(II) Ions $[RuH(\eta^2\text{-}H_2)(diphosphine)_2]^+$ (diphosphine = 2,2'-bis(diphenylphosphino)-1,1'-binaphthyl (binap) and 2,2'-bis(diphenylphosphino)-1,1'-biphenyl (dpbp)).

Abstract

The molecular hydrogen complex $[RuH(\eta^2\text{-}H_2)(dpbp)_2]^+$ (**2f**) was prepared *in situ* by a reaction of H_2 gas with five-coordinate complex $[RuH(dpbp)_2]PF_6$ (**1f**) (dpbp = 2,2'-bis(diphenylphosphino)-1,1'-biphenyl). ^1H and $^{31}P\{^1H\}$ NMR behaviors of **2f** were measured in the temperature range –90 to 30 °C, and compared with those of $[RuH(\eta^2\text{-}H_2)(binap)_2]^+$ (**2e**; binap = 2,2'-bis(diphenylphosphino)-1,1'-binaphthyl). In the ^1H NMR spectrum, **2f** showed single broad signal in the hydride region due to a rapid hydrogen exchange between molecular hydrogen and terminal hydride at 30 °C. The signal decoalesced into two peaks at lower temperatures and the characteristic resonances of Ru–(H_2) and Ru-H were detected below –60 °C. In contrast, **2e** showed two signals of Ru–(H_2) and Ru-H even at 30 °C. The differences in the NMR features between dpbp complexes and binap complexes were discussed on the basis of the flexibility or rigidity of diphosphine chelate rings.

Introduction

Since the first confirmation of the coordination of a dihydrogen molecule, without breaking the H–H σ-bond, to a transition metal center in $W(H_2)(CO)_3(PR_3)_2$ (R = cyclohexyl or isopropyl),[1, 2] the investigations on the molecular hydrogen complexes have made great progress not only from experimental but also from theoretical aspects.[3] Among a variety of dihydrogen complexes, complexes of the type $[MH(H_2)(P_4)]^+$ ($M = Fe^{II}$, Ru^{II}, Os^{II}; P_4 = two diphosphines or a tetradentate phosphine),[4] constitute one of the most representative and well documented families.[5–7]

Saburi and collaborators have reported in previous communications that the introduction of H_2 gas into solutions of five-coordinate complexes $[RuH(P–P)_2]PF_6$ (**1**) resulted in the spontaneous formation of $[RuH(H_2)(P–P)_2]^+$ (P–P = diphosphine) (**2**)[8 – 10] and that, for homologous complexes (P–P = dppe, dppp, dppb), the intramolecular hydrogen exchange between the terminal hydride (Ru–H) and coordinating dihydrogen (Ru–(H_2)) in **2** depends considerably on the size and flexibility of the diphosphine chelate rings.[9] Thus, the hydrogen exchange for $[RuH(H_2)(dppe)_2]^+$ (**2d**), in which the diphosphine forms a five-membered chelate, is so slow as to make the ^1H NMR resonances of Ru–H and Ru–(H_2) observable separately at room temperature with distinct spin couplings between Ru–H and phosphorus atoms.[5] In the case of $[RuH(H_2)(dppp)_2]^+$ (**2c**) having six-membered chelate rings, the resonances of Ru–H and –(H_2) are observed still separately, but the hydride-phosphorus couplings were no longer detected at the same temperature.[9] Under the same conditions the signals of dihydrogen and of terminal hydride coalesce into a single broad peak for $[RuH(H_2)(dppb)_2]^+$ (**2a**), where dppb forms a seven-

membered chelate ring.[9] This indicates that a fast intramolecular hydrogen exchange undergoes between Ru–(H_2) and Ru-H in **2a**.[9d] These results suggest that the hydrogen exchange in **2a**, **2c**, and **2d** occurs faster as the diphosphine chelate ring becomes larger and more flexible, due to the easier conformational changes for the larger chelate.

The variable temperature ^{1}H NMR spectra, similar to but clearer than those of **2a**, were obtained for the diop analogue $[RuH(H_2)(diop)_2]^+$ (**2b**).[10] In contrast, the binap complex $[RuH(H_2)(binap)_2]^+$ (**2e**) shows the ^{1}H NMR characteristics similar to those of **2d**, which is typical one for the slow exchange region.[8] Although the chelate rings of diop and binap are chiral and have the same size (seven-membered ring), their conformational rigidities differ significantly with each other. Conformational change of binap chelate should be impossible because of the nature of binaphthyl backbone, while that for diop chelate is probable to some extent due to the presence of methylene units. With a view to examine further the effects of conformational flexibility of diphosphine chelates on the intramolecular hydrogen exchange in **2**, I prepared the dpbp complex $[RuH(H_2)(dpbp)_2]^+$ (**2f**). Although dpbp itself has an apparent structural resemblance to binap, the dpbp chelate ring, also seven-membered, is flexible enough to undergo conformational changes, in contrast to the case of binap. It is expected, therefore, that the complex **2f** exhibits the ^{1}H NMR features similar to those of **2c** or **2d** and different from those of **2e**. In this chapter, I will focus my attention on the differences in the dynamic behaviors between **2e** and **2f** and also in their parent complexes, $[RuH(binap)_2]^+$ (**1e**) and $[RuH(dpbp)_2]^+$ (**1f**).

Results and discussion

It has been clarified by the crystallographic analyses that (*R*)- and (*S*)-binap adopt, respectively, a λ-skew and δ-skew conformation in the transition metal complexes.[11, 12] A simplified structure of (*R*)-binap chelate is illustrated in Figure 3.1, where the phenyl rings bonded to phosphorus atoms are shown by Ph. Figure 3.1 also shows possible structures of dpbp chelate, the λ-skew conformation of which is apparently similar to that of (*R*)-binap. It should be noted that the δ-skew form, the antipode of the λ-skew one, is possible for a dpbp chelate, because the biphenyl

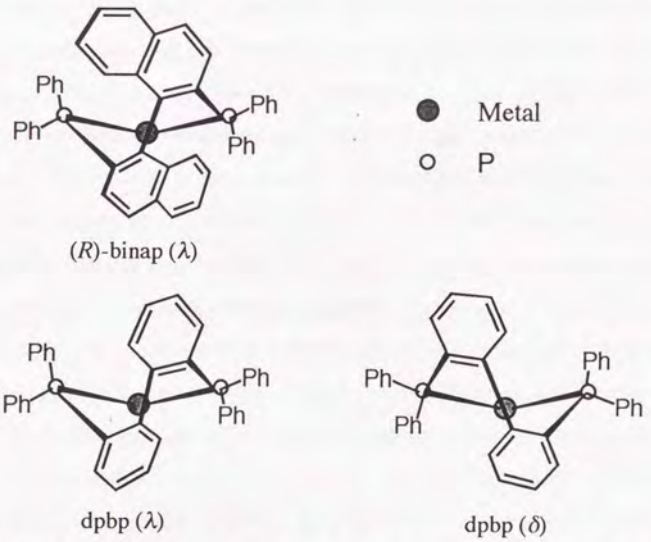

Fig. 3.1 Chelate ring conformations of (R)-binap and dpbp in the complexes.

backbone of dpbp is flexible to allow the rotation around the C–C bond. Conversely, it is impossible for (*R*)-binap chelate to adopt the antipodal conformation, as mentioned above. These differences in flexibility between binap and dpbp chelate are expected to result in the differences in the dynamic behaviors of complexes with these diphosphines.

Five-Coordinate Complexes.

The deep orange-red complexes $[RuH(binap)_2]PF_6$ (**1e**) and $[RuH(dpbp)_2]PF_6$ (**1f**) were prepared readily by reactions of $[RuH(NH_2NMe_2)_3(cod)]PF_6$[13] with two equivalents of respective diphosphines according to the reported method with slight modifications.[14] As described previously,[8] the ^1H NMR spectrum (at 400 MHz in CD_2Cl_2) of the binap complex **1e** shows two hydride signals in the high field region at 30 °C (see Figure 3.2 and Table 3.1). Although the higher field peak broadens gradually as the temperature lowered, no intrinsic change was noticed to occur in the spectra at –30 to 30 °C. In the spectra of the dpbp complex **1f,** we similarly observed two hydride resonances in the temperature range –30 to 30 °C (Figure 3.3). These findings indicate that there are two isomers for **1e** and **1f** in solutions and that they are distinguishable to each other at these temperatures. In other words, the interconversion of two isomers is considerably slow compared with the NMR time scale. When H_2 gas was introduced into a solution of either **1e** or **1f**, a spontaneous color change from deep orange-red to pale yellow took place. The hydride signals for both isomers of **1e** or **1f** disappeared completely, and those for the molecular hydrogen complex, $[RuH(H_2)(binap)_2]^+$ (**2e**) or $[RuH(H_2)(dpbp)_2]^+$ (**2f**), emerged in the ^1H NMR spectra (*vide infra*). This strongly supports that the two hydride signals of the five-coordinate complexes, **1e** and **1f**, are assigned to their stereoisomers.

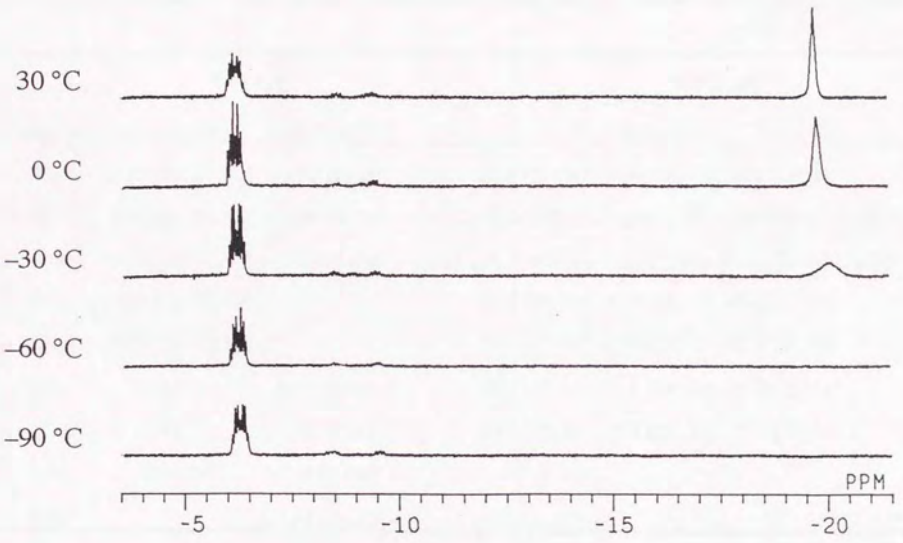

Fig. 3.2 Variable temperature ^1H NMR spectra (400 MHz) of $[RuH(binap)_2]^+$ (**1e**) in the high field region in CD_2Cl_2.

Table 3.1 ^{1}H (at 400 MHz) and ^{31}P (at 162 MHz) NMR data of $[RuH(binap)_2]^+$ (**1e**) and $[RuH(dpbp)_2]^+$ (**1f**) in CD_2Cl_2.

		^{1}H NMR		^{31}P NMR	
Complex	Temp./K	*cis* (J_{PH}/Hz)	*trans* (J_{PH}/Hz)	*cis* (J_{PP}/Hz)	*trans*
1e	303	-6.25 (dq; 27, 73)	-19.75 (br)	29.8 (1P, br), 42.4 (2P, br), 81.9 (1P, br)	44.6 (br)
	273	-6.25 (dq; 21, 68)	-19.80 (br)	29.3 (1P, d; 12), 42.3 (2P, t; 27), 82.8 (1P, dt; 12, 27)	45.7 (br)
	243	-6.26 (dq; 21, 68)	-20.08 (br)	29.6 (1P, d; 12), 42.4 (2P, t; 27), 82.3 (1P, dt; 12, 27)	47.0 (br)
	213	-6.28 (dq; 26, 74)		29.0 (1P, br), 42.3 (2P, br), 83.4 (1P, m)	
	183	-6.29 (dq; 24, 68)		28.4 (1P, br), 42.2 (2P, br), 83.9 (1P, br)	
1f	303	-2.34 (br)	-8.07 (quint; 4)	30.7 (1P, br), 37.1 (2P, br), 49.4 (1P, br)	45.9 (br)
	273	-2.45 (br)	-8.08 (br)	30.3 (1P, br), 37.4 (2P, br), 49.3 (1P, br)	45.9 (br)
	243	-2.61 (br)	-8.06 (br)		ca. 46 (br)
	213		-8.14 (br)		very broad

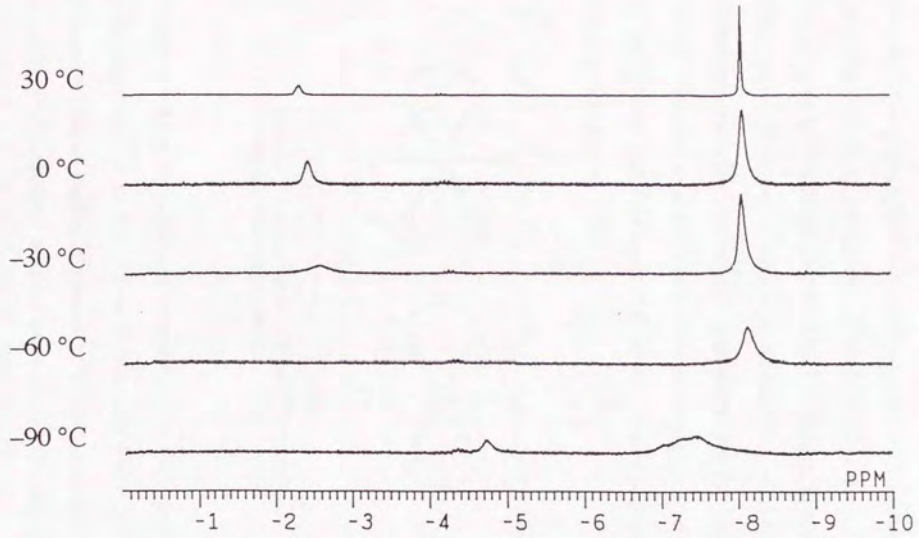

Fig. 3.3 Variable temperature ^1H NMR spectra (400 MHz) of $[RuH(dpbp)_2]^+$ (**1f**) in the high field region in CD_2Cl_2.

The doublet of quartets at δ –6.25 in the spectra of **1e**, which showed no appreciable temperature dependence, exhibited the clear spin couplings with phosphorus atoms. The coupling features suggest that one of four phosphorus atoms is located in a considerably different environment from those of the other three. This signal can be assigned to the hydride (Ru–H) of the "*cis*" isomer, in which the vacant site and the hydride ligand occupy the adjacent coordination sites as illustrated in Figure 3.4. In this structure, one of the P atoms is situated *trans* to the hydride ligand, while the others are *cis*. However, in accord with the true molecular symmetry for the "*cis*" isomer (C_1), the $^{31}P\{^1H\}$ NMR spectrum of **1e** showed four resonances assingnable to this stereoisomer (Table 3.1).

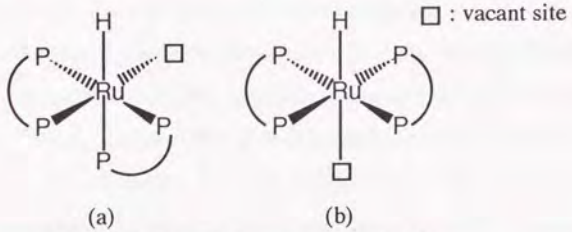

Fig. 3.4 Two possible structures for **1e** and **1f**:
(a) *trans* isomer; (b) *cis* isomer.

It is natural that the other isomer of **1e** is assigned to the "*trans*" form, where the hydride and the vacant site are located *trans* to each other (Figure 3.4). The "*trans*" form of **1e** possesses the C_2 molecular symmetry. It was found that typical *trans*-$[RuHX(binap)_2]^{n+}$ complexes, such as *trans*-$RuHCl(binap)_2$ and *trans*-$[RuH(CO)(binap)_2]^+$, gave a triplet of triplets as the Ru-H resonance, and a pair of

triplets as the phosphorus resonances.[8, 15] These NMR features support that, in the *trans* isomers, the phosphorus atoms belonging to the same chelate are magnetically unequal to each other due to the rigid conformation of binap. However, the second ^{1}H NMR signal of **1e**, observed at δ ca. –20 as a broad peak, had no obvious spin couplings with P atoms and was not a typical hydride signal for the *trans*-$[RuHX(binap)_2]^{n+}$ complexes. Further, the $^{31}P\{^1H\}$ NMR signal assingnable to the second isomer of **1e** was noted as a single broad peak (δ 44.6) at 30 °C (Table 3.1). These NMR characteristics does not suggest clearly that the second isomer of **1e** adopts the "*trans*" configuration. However, a strong evidence that supports the assignment of this isomer to the "*trans*" geometry was given by the ^{1}H NMR measurements of dpbp complex **1f** (*vide infra*).

The ^{1}H and $^{31}P\{^1H\}$ NMR signals for the "*trans*" isomer of **1e** broadened gradually at lower temperatures and could no longer be detected below –60 °C (Figure 3.2). In contrast, the signals for the "*cis*" isomer of the same complex remained almost unchanged even at this temperature. These facts suggest that a fast exchange process occurs only for the "*trans*" isomer. It seems, further, that the rate of exchange decreased as the temperature lowered and became comparable to the NMR time scale at –60 °C. I suppose that the exchange of solvent molecules, interacting weekly at the vacant site, is a candidate for the fast exchange process, which may affect the shape and its temperature dependence of the Ru–H signal of the "*trans*" isomer.

I have noticed a couple of facts suggesting the weak coordination of solvent molecule at the vacant coordination site of **1e**. It is anticipated that the coordination of different solvents should result in the change in the chemical shift of some key NMR resonances. In fact, the Ru–H signal of the "*trans*" isomer of **1e** in acetone-d_6 at –30 °C shifted up field by 1.37 ppm compared to that in CD_2Cl_2, while the corresponding

signal for the "*cis*" isomer showed no significant solvent dependence. In addition, **1e** in $CDCl_3$ solution turned gradually into $RuHCl(binap)_2$ after standing it for several days.[8] This strongly supports that the solvent molecule interacts with **1e** at the vacant site.

The dpbp complex **1f** shows two hydride signals (δ ca –2.4 and –8.1) in the temperature range –30 to 30 °C, in similar manners to those of **1e** (Figure 3.3 and Table 3.1). It is noteworthy that the higher field signal for one of the isomers of **1f** appears as a quintet at 30 °C. It was revealed, further, that the present isomer gives a slightly broad singlet in the $^{31}P\{^1H\}$ NMR spectrum. The spectral features are rationalized by taking the couplings among the terminal hydride and four equivalent phosphorus atoms into consideration. The observation that the phosphorus atoms of two dpbp ligands are practically equivalent indicates that the conformation changes of dpbp chelates are very fast in the "*trans*" form. If the interconversion between δ- and λ-conformation is enough rapid for two chelate rings, all the P atoms in the "*trans*" isomer of **1f** will be regarded as equivalent. On such occasion, the Ru-H signal can appear as a quintet, even if the geometry of the isomer is restricted in the "*trans*" form.

Alternatively, it is expected that the Ru–H signal is observed as a quintet and that the phosphorus signal appears as a singlet, when **1f** is highly fluxional as a whole molecule. In such case, however, only one peak will be found as the Ru–H signal in the hydride region. Since we detected the other hydride signal at δ ca –2.4, the higher field signal at δ ca –8.1 is unambiguously assigned to the terminal hydride of the "*trans*" isomer of **1f**. In fact, the dppb complex **1a** and diop complex **1b** are fluxional at room temperature, so that a broad single peak is found as the hydride resonance.[16] For these systems, however, no coupling between Ru–H and P atoms was observed.

It is noteworthy that the hydride signal assigned to the "*trans*" isomer of **1f** turns into a broad peak (no spin coupling with ^{31}P) below 0 °C. In addition, the spectral changes of this signal at –60 – 0 °C is obviously similar to those of the hydride signal at δ ca –20 of **1e** in the range –30 to 30 °C. The similarities in the temperature dependence of these signals strongly suggest, as described previously, that the higher field hydride signal of **1e** can be assigned to the "*trans*" isomer. The temperature dependence also implies that the rate of conformation change of the diphosphine in **1f** is decreased at lower temperatures, although the other exchange process, possibly the exchange of coordinating solvent at the vacant site, should becomes concomitantly slower.

The other hydride signal of **1f**, which should be ascribed to the "*cis*" isomer, is a broad peak (δ ca –4.2) in the range –30 to 30 °C. No clear coupling with phosphorus atoms was detected even at 30 °C, in sharp contrast to the case of the "*cis*" isomer of the binap complex **1e**. The reason for these differences in the ^{1}H NMR features of "*cis*" isomers is uncertain. The $^{31}P\{^{1}H\}$ NMR data supports that the isomer of **1f** other than the "*trans*" form has no molecular symmetry.

Molecular Hydrogen Complexes.

a. Binap Complex

As described in the preliminary report from our laboratry,[8] the contact of five-coordinate complex **1e** with hydrogen gas in a THF solution afforded white crystals of molecular hydrogen complex $[RuH(H_2)(binap)_2]PF_6$ **2e**. The ^{1}H NMR spectrum of **2e** at 30 °C revealed two high field resonances assignable to Ru–(H_2) and Ru–H groups with the intensities of 2:1 (Figure 3.5 and Table 3.2). Thus, the broad singlet appeared at δ –1.17 was ascribed to the dihydrogen ligand, and the triplet of triplets at δ

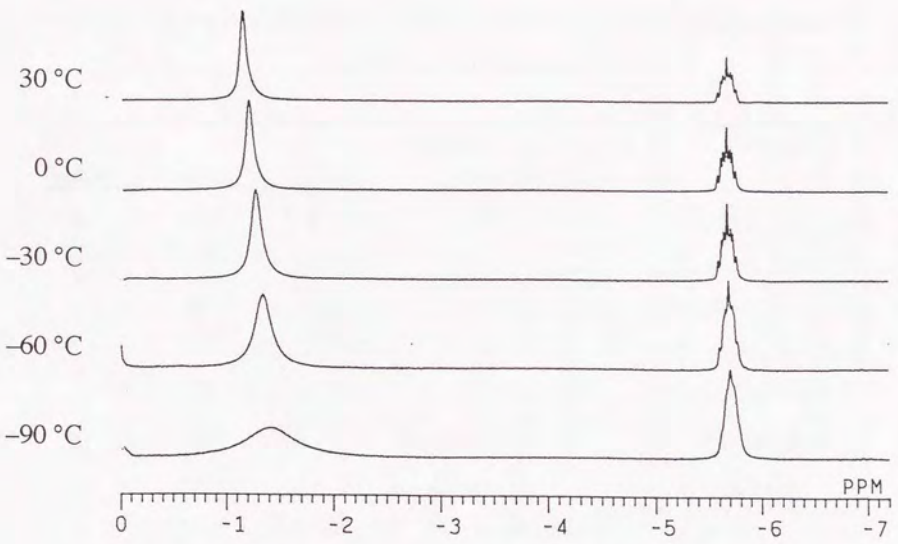

Fig. 3.5 Variable temperature ^1H NMR spectra (400 MHz) of $[RuH(H_2)(binap)_2]^+$ (**2e**) in the high field region in CD_2Cl_2.

Table 3.2 ^{1}H (at 400 MHz) and ^{31}P (at 162 MHz) NMR data of $[RuH(H_2)(binap)_2]^+$ (**2e**) and $[RuH(H_2)(binap)_2]^+$ (**2f**) in CD_2Cl_2.

		^{1}H NMR		^{31}P NMR
Complex	Temp./K	Ru–H_2	Ru–H (J_{PH}/Hz)	
2e	303	–1.17 (br)	–5.68 (tt; 13, 21)	49.0 (t; 30), 50.5 (t; 30)
	273	–1.23 (br)	–5.68 (tt; 13, 21)	49.1 (t; 30), 50.8 (t; 30)
	243	–1.28 (br)	–5.68 (tt; 13, 21)	49.1 (t; 30), 51.0 (t; 30)
	213	–1.35 (br)	–5.69 (m)	49.1 (t; 30), 51.4 (t; 30)
	183	–1.41 (br)	–5.70 (br)	49.1 (t; 30), 51.8 (t; 30)
2f	303	–4.32 (br)		34.2 (br)
	273	ca. –4.2 (br)		ca. 34 (br)
	243	ca. –2.9 (br)	ca. –6.1 (br)	ca. 30 (br), ca. 37 (br)
	213	–2.90 (br)	–6.38 (m)	30.1 (t; 31), 38.2 (t; 31)
	183	–2.91 (br)	–6.53 (tt; 15,27)	30.0 (t; 31), 38.2 (t; 31)

–5.68 (J_{PH} = 13, 21 Hz) was assigned to the terminal hydride in **2e**. The coupling features of the Ru–H signal, which is the same as those of *trans*-RuHCl(binap)$_2$,[12] indicates that **2e** takes the *trans* configuration with regard to the dihydrogen and terminal hydride ligands. These signals showed no significant temperature dependence in the range –90 to 30 °C, except a gradual broadening of the former at lower temperatures (Figure 3.5).

The partially deuterated species [RuD(HD)(binap)$_2$]$^+$ was readily prepared by introducing D_2 gas into a solution of complex **1e** and subsequent intramolecular hydrogen-deuterium exchange. The ^{1}H NMR measurement of the deuterated complex showed a triplet of 1:1:1 intensities (J_{HD} = 30 Hz) at δ –1.1.[8] The coupling features and the chemical shift of this signal are diagnostic of the presence of coordinating HD molecule and, consequently, provide a strong evidence for the formation of η^2-H_2 complex.[2, 3]

It has been recognized that the observation of short T_1 values (< 100 ms at 400 MHz) for metal hydride species are also useful in diagnosing the presence of H_2 ligand,[3] although a limitation for this simple judgment was proposed recently.[17] In fact, the T_1 criteria for the dihydrogen and hydride ligands, proposed initially by Crabtree and co-workers,[3b] could be satisfactorily applied for the case of complex **2e**, where the T_1 values of the signals at δ –1.17 and –5.68 were found to be, respectively, 21 and 185 ms at 30 °C.

The ^{1}H NMR characteristics of **2e** are, as a whole, similar to those of the dppe analogue [RuH(H_2)(dppe)$_2$]$^+$ (**2d**).[5a, 5f, 18] In both instances, the intramolecular exchange between dihydrogen and terminal hydride ligands is sufficiently slow compared with the NMR time scale. In each case, the Ru–H signal exhibits the definite couplings with ^{31}P nuclei of diphosphine ligands (Table 3.2 and ref. 5f), whereas the

Ru–(H_2) signal appears as a broad singlet as in most molecular hydrogen complexes. These NMR features are, however, in sharp contrast to those of the molecular hydrogen complexes of dppb and of diop, $[RuH(H_2)(dppb)_2]^+$ (**2a**) and $[RuH(H_2)(diop)_2]^+$ (**2b**). These complexes are found to be highly fluxional at higher temperature, and the signals of Ru–(H_2) and Ru-H coalesce into a single broad peak at 30 °C.[9, 10]

b. Dpbp Complex

I consider that the clear difference in the hydrogen exchange between **2e** and **2a** or **2b** should be due to the difference in the conformational rigidity between binap and dppb or diop, as described in Introduction, because these diphosphines form equally seven-membered chelate rings. With a view to examine the effects of flexibility or rigidity of diphosphine chelates on the hydrogen exchange in more detail, the NMR properties of the molecular hydrogen complex $[RuH(H_2)(dpbp)_2]^+$ (**2f**) were measured. As mentioned previously, a dpbp chelate also gives rise to a seven-membered ring quite similar to that of binap, but the freedom of inversion of conformation for the former ligand is in sharp contrast to the rigidity of the latter. The variable temperature ^1H NMR spectra of **2f** are shown in Figure 3.6, and the detailed data are collected in Table 3.2.

The ^1H NMR spectra of **2f** exhibited a remarkable temperature dependence as shown in Figure 3.6. The observed spectral changes for **2f** are, as a whole, partly similar to those of $[FeH(H_2)(dppe)_2]^+$ reported by Morris and collaborators.[5f] At and below –60 °C, two dominant resonances, a broad singlet (δ ca –2.9) assigned to Ru–(H_2) and a triplet of triplets (δ ca –6.5, J_{PH} = 15, 27 Hz at –90 °C) due to Ru–H, were detected. The T_1 values of these resonances obtained at –70 °C are as follows: 12 ms

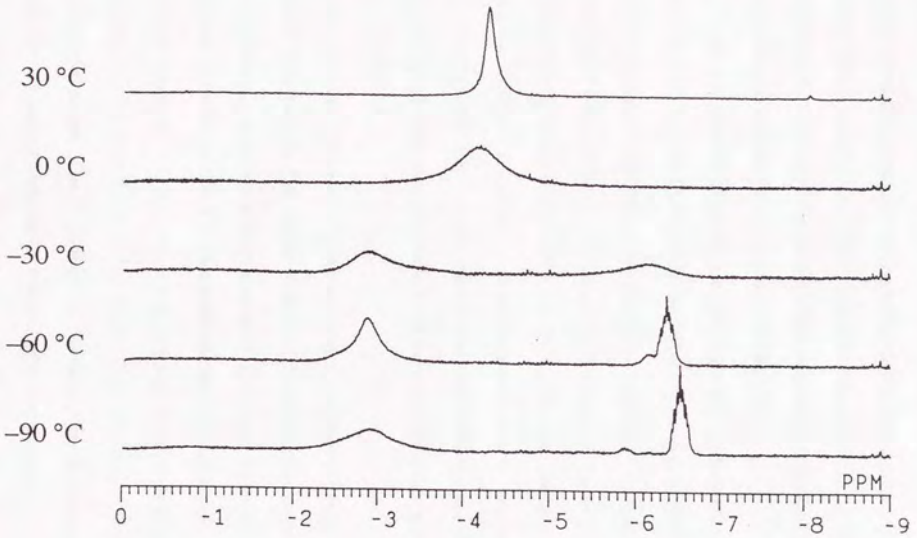

Fig. 3.6 . Variable temperature ^1H NMR spectra (400 MHz) of $[RuH(H_2)(dpbp)_2]^+$ (**2f**) in the high field region in CD_2Cl_2.

for Ru–(H_2) and 240 ms for Ru–H. The values are the indication of slow hydrogen exchange between the dihydrogen and terminal hydride under these conditions. In such slow exchange region, the complex **2f** should hold the *trans* configuration in the same way as the binap complex **2e**. In accord with this assumption, ^{31}P NMR spectra showed a couple of triplets in the same temperature range, reflecting the inequivalence of two phosphorus atoms of a dpbp chelate (Table 3.2).

As the temperature is raised, the intramolecular hydrogen exchange becomes faster, so that the signals for Ru–(H_2) and Ru–H broaden significantly at –30 °C (Figure 3.6). Around this temperature, the spin couplings between Ru–H and P atoms could no longer be detected. In addition, the T_1 values of Ru–(H_2) and Ru–H were found to be 12 and 14 ms, respectively, at –40 °C. The fact that the T_1 times for Ru–(H_2) and Ru–H signals are averaged (relaxation coalescence) suggests the increased rate of exchange between the dihydrogen and terminal hydride. We noticed that $[RuH(H_2)(dppp)_2]^+$ (**2c**) showed similar tendencies in T_1 of the hydride signals in the range 0 – 30 °C.[9]

It is apparent that the two resonances coalesce completely between –30 and 0 °C (line-shape coalescence). The chemical shift of the broad peak (δ ca –4.2 at 273 K), which must have the intensity of three hydrogens, is close to the weighted average (2:1) of δ(H_2) and δ(Ru–H) at –30 °C. This indicates that a fast hydrogen exchange takes place for **2f** above ca. 250 K. The coalesced signal becomes narrower at higher temperatures (see the spectrum at 30 °C, Figure 3.6), but does not show any couplings with phosphorus atoms. The T_1 time of this resonance was as short as 24 ms (30 °C), indicating the influence of (H_2) ligand even at higher temperatures.

I estimated the rate of H atom exchange (k^{H2}) from dihydrogen to hydride for complex **2f** at the line-shape coalescence temperature ($k^{H2} = \pi\nu_0\{\delta(H_2) - \delta(H)\} / \sqrt{2}$;

ν_0 is the spectrometer frequency). Using the chemical shifts $\delta(H_2)$ and $\delta(H)$ at –90 °C, $k^{H2} = 3{,}200\ s^{-1}$ was obtained. Although the exact coalescence temperature was not determined, the activation free energy, $\Delta G^{\ddagger}$, for the rate of H atom exchange in **2f**, was calculated on the basis of the rate constant. Assuming the coalescence temperature of 250 K, $\Delta G^{\ddagger}$ value of 10.5 kcal/mol was approximated.[19] Similar values were reported by Jessop and Morris.[3b] The $\Delta G^{\ddagger}$ for **2f** is comparable to those for **2a** and **2b**, but significantly smaller than those for **2d** and **2e**.[3d]

Two independent mechanisms have been proposed for the hydrogen exchange process in $[MH(H_2)(P\text{-}P)_2]^+$ complexes. Morris and collaborators assumed a *dissociative* mechanism for H atom exchange that involves homolysis of H–H bond to produce a fluxional trihydride intermediate (see Figure 3.7).[3d, 5f] It is supposed that the dissociative mechanism is more reasonable for $[MH(H_2)(P\text{–}P)_2]^+$ having strictly *trans* configuration as **2d** and **2e**. Alternatively, an *associative* mechanism, involving an intermediate with a H_3 unit, was proposed on the basis of *ab initio* calculations on *cis*-$[FeH(H_2)(PH_3)_4]^+$ system (Figure 3.7).[20] This mechanism could be applied for molecular hydrogen complexes that adopt, at least in part, *cis* configuration as **2a** and **2b**. It was reasonably understood that the $\Delta G^{\ddagger}$ values for **2d** and **2e** (> 15 kcal/mol) are remarkably larger than those for **2a** and **2b** (< 12 kcal/mol), taking these hypothetical differences in H atom exchange mechanisms into consideration.[3f]

The occurrence of the *cis* isomer was suggested for **2b** because of that a broad resonance other than those of *trans* isomer is found downfield the Ru–H signal in the variable temperature ^1H NMR spectra.[9] However, detailed examination of ^1H NMR charts (Figure 3.6) revealed no sign for the formation of the *cis* isomer of **2f**. I can recognize, in fact, a broad peak downfield the Ru-H resonance of the *trans* form at –60

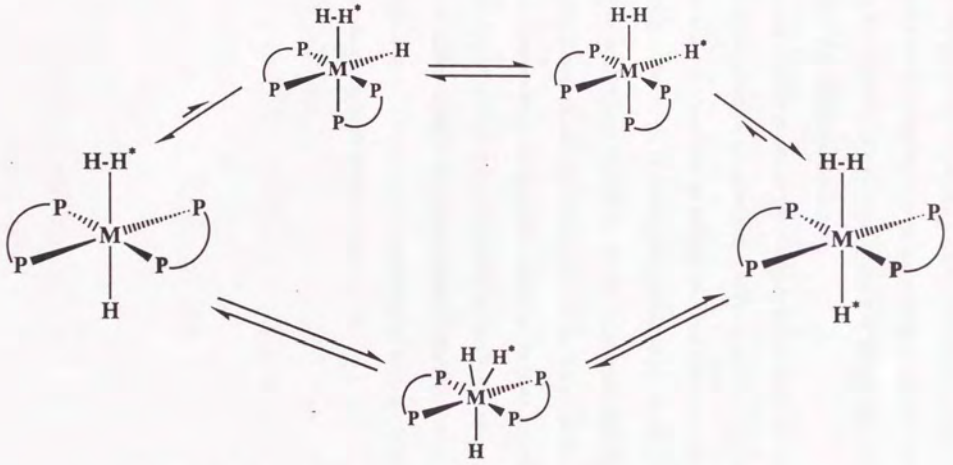

Fig. 3.7 Two proposed mechanisms for intramolecular hydrogen exchange in $[MH(\eta^2\text{-}H_2)(\text{diphosphine})_2]^+$: (above) non-dissociative; (below) dissociative.

and –90 °C, in a similar manner to the case of **2b**. An intrinsic difference between **2b** and **2f** is that the broad Ru–H_2 signal is unsymmetrical and a smaller broad peak seems to overlap at the lower frequency side in the latter case. These findings are rationalized by assuming the presence of two trans isomers of **2f**, which arise from the different combinations of the conformation of dpbp.

Thus, the dominant isomer should have a racemic structure, where both dpbp chelates adopt the same conformation as (δ, δ) or (λ, λ). I consider that the minor isomer takes a *meso* structure, in which the conformations of dpbp chelates are antipodal to each other as (δ, λ). Steric congestion in the racemic form is expected to be similar to or smaller than that of **2e**. In the *meso* form, however, steric repulsions between diphosphines should be severer than in the racemic form. Other examples suggesting the presence of stereoisomers have never been clarified for a variety of *trans*-$[MH(H_2)(P–P)_2]^+$ complexes reported so far.[3] The *meso* form is, of course, regarded as an intermediate in the interconversion between (δ, δ) and (λ, λ) form at elevated temperatures. This strongly supports that a dpbp chelate undergoes facile conformation changes at high temperatures.

Conclusions

The reason for small $\Delta G^{\ddagger}$ value of H atom exchange for **2f** is still uncertain. Whichever the mechanism of H atom exchange actually works for **2f**, it is noteworthy that the temperature dependence in ^{1}H NMR spectra of **2f** obviously differs from that of the binap analogue **2e**. The differences in the hydrogen exchange properties in these complexes should be ascribed to the differences in the flexibility of the respective chelate of diphosphines, as mentioned above. I conclude that the NMR behaviors of the binap complex **2e** is rather exceptional among the analogues with seven-membered diphosphine chelates.

Remarkable differences between diop complex **2b** and binap complex **2e** have been noticed in the asymmetric induction for hydrogenation catalyzed by these complexes.[21] For hydrogenation of several unsaturated carboxylic acids, **2e** revealed sufficiently high selectivities, while **2b** showed only moderate selectivities. This could also be attributed to the differences in the flexibility or rigidity of diphosphines.

Experimental Section

General Procedure.

Unless otherwise noted, all manipulations were carried out under a dry nitrogen atmosphere by standard schlenk-tube techniques. All the solvents were dried over appropriate reagents and distilled under nitrogen. Binap was presented by Takasago International Corporation. Dpbp,[22] $[RuH(NH_2NMe_2)_3(cod)]PF_6$,[13] and $[RuH(binap)_2]PF_6$[21] were prepared by the reported methods. ^1H NMR (400 MHz) and ^{31}P NMR (162 MHz) spectra were measured with a JEOL JNM-GX 400 spectrometer. ^1H NMR T_1 measurements were carried out by the inversion recovery method using a standard 180°-τ-90° pulse sequence.

Hydridobis[2,2'-bis(diphenylphosphino)-1,1'-biphenyl]ruthenium(II) hexafluorophosphate $[RuH(dpbp)_2]PF_6$ (1f).

A solution of $[RuH(NH_2NMe_2)_3(cod)]PF_6$ (199 mg, 0.37 mmol) and dpbp (402 mg, 0.77 mmol) in acetone was stirred at room temperature for 12 h. During this period the color of the solution was changed to deep red. The solution was filtered and the filtrate was concentrated to about 2 ml under reduced pressure. Diethyl ether was added to this solution to afford an oily product, which solidified on standing for several days at room temperature. Anal. Calcd for $C_{72}H_{57}F_6P_5Ru$: C, 66.9; H, 4.5. Found: C, 66.1; H, 4.5 %.

Hydrido(dihydrogen)bis[2,2'-bis(diphenylphosphino)-1,1'-binaphthyl] ruthenium(II) hexafluorophosphate $[RuH(\eta^2\text{-}H_2)(binap)_2]PF_6$ (2e).

$[RuH(binap)_2]PF_6$ (**1e**; 30 mg) was dissolved in CD_2Cl_2 (0.5 mL) in a 5-mm NMR tube. The introduction of dry H_2 gas to this solution resulted in a spontaneous

color change from deep red to pale yellow.. $[RuH(binap)_2]PF_6$ was converted to $[RuH(\eta^2\text{-}H_2)(binap)_2]PF_6$ quantitatively within 3 minutes. The obtained sample was used for NMR measurements without further purification.

Hydrido(dihydrogen)bis[2,2'-bis(diphenylphosphino)-1,1'-biphenyl] ruthenium(II) hexafluorophosphate $[RuH(\eta^2\text{-}H_2)(dpbp)_2]PF_6$ (2f).

The title complex was prepared from $[RuH(dpbp)_2]PF_6$ (**1f**) as described above for **2e**.

References and Notes

(1) Kubas, G. J.; Ryan, R. R.; Swanson, B. I.; Vergamini, P. J.; Wasserman, H. J. *J. Am. Chem. Soc.*, **1985**, *106*, 451.

(2) Kubas, G. J. *Acc. Chem. Res.*, **1988**, *21*, 120.

(3) Recent reviews: (a) Crabtree, R. H.; Hamilton, D. G. *Adv. Organomet. Chem.* **1988,** *28*, 299. (b) Crabtree, R. H. *Acc. Chem. Res.*, **1990**, *23*, 95. (c) Crabtree, R. H.; Luo, X.-L.; Michos, D. *Chemtracts-Inorg. Chem.*, **1991**, *3*, 245. (d) Jessop, P. G.; Morris, R. H. *Coord. Chem. Rev.*, **1992**, *121*, 155. (e) Heinekey, D. M.; Oldham, W. J. *Chem. Rev.*, **1993**, *93*, 913.

(4) The dihydrogen ligand is refereed to (H_2) for simplicity.

(5) (a) Morris, R. H.; Sawyer, J. F.; Zubkowski, J. D. *J. Am. Chem. Soc.*, **1985**, *107*, 5581. (b) Bautista, M. T.; Earl, K. A.; Morris, R. H.; Sella, A. *J. Am. Chem. Soc.*, **1987**, *109*, 3780. (c) Ricci, J. S.; Koetzle, T. F.; Bautista, M. T.; Mofstede, T. M.; Morris, R. H.; Sawyer, J. F. *J. Am. Chem. Soc.*, **1989**, *111*, 8823. (d) Bautista, M. T.; Earl, K. A.; Morris, R. H. *Inorg. Chem.*, **1988**, *27*, 1124. (e) Earl, K. A.; Morris, R. H.; Sawyer J. F. *Acta Crystallogr.*, **1989**, *C45*, 1137. (f) Earl, K. A.; Jia, G.; Maltby, P. A.; Morris, R. H. *J. Am. Chem. Soc.*, **1991**, *113*, 3027. (g) Jia, G.; Lough, A. J.; Morris, R. H. *Organometallics*, **1992**, *11*, 161.

(6) (a) Baker, M. V.; Field, L. D.; Young, D. J. *J. Chem. Soc., Chem. Commun.*, **1988**, 546. (b) Baker, M. V.; Field, L. D. *J. Organomet. Chem.*, **1988**, *354*, 351.

(7) (a) Bautista, M. T.; Earl, K. A.; Maltby, P. A.; Morris, R. H. *J. Am. Chem. Soc.*, **1988**, *110*, 4056. (b) Bianchini, C.; Peruzzini, M.; Zanobini, F. *J. Organomet. Chem.*, **1988**, *354*, C19. (c) Bianchini, C.; Perez, P. J.; Peruzzini, M.; Zanobini, F.; Vacca, A. *Inorg. Chem.*, **1991**, *30*, 279. (d) Bampos, N.; Field, L. D. *Inorg. Chem.*, **1990**, *29*, 587.

(8) Tsukahara, T.; Kawano, H.; Ishii, Y.; Takahashi, T.; Saburi, M.; Uchida, Y.; Akutagawa, S. *Chem. Lett.*, **1988**, 2055.

(9) (a) dppe = 1,2-bis(diphenylphosphino)ethane. (b) dppp = 1,3-bis(diphenylphosphino)propane. (c) dppb = 1,4-bis(diphenylphosphino)butane. (d) Saburi, M.; Aoyagi, K.; Takahashi, T.; Uchida, Y. *Chem. Lett.*, **1990**, 601.

(10) (a) diop = 2,3-*O*-isopropylidene-2,3-dihydroxy-1,4-bis(diphenylphosphino)butane. (b) Saburi, M.; Aoyagi, K.; Takeuchi, H.; Takahashi, T.; Uchida, Y. *Chem. Lett.*, **1990**, 991.

(11) (a) Toriumi, K.; Ito, T.; Takaya, H.; Souchi, T.; Noyori, R. *Acta Crystallogr.*, **1982**, *38B* , 807; (b) Ohta, T.; Takaya, H.; Noyori, R. *Inorg. Chem.*, **1988**, *27*, 566.

(12) Kawano, H.; Ishii, Y.; Kodama, T.; Saburi, M.; Uchida, Y. *Chem. Lett.*, **1987**, 1311.

(13) Ashworth, T. V.; Norte, M. J.; Singleton, E. *J. Chem. Soc., Dalton Trans.*, **1978**, 1040.

(14) Ashworth, T. V.; Singleton, E. *J. Chem. Soc., Chem. Commun.*, **1976**, 705.

(15) Kawano, H.; Ikariya, T.; Ishii, Y.; Kodama, T.; Saburi, M.; Yoshikawa, S.; Uchida, Y.; Akutagawa, S. *Bull. Chem. Soc. Jpn.*, **1992**, *65*, 1595.

(16) Ogasawara, M.; Aoyagi, K.; Saburi, M. *Organometallics*, **1993**, *12* , 3933.

(17) Desrosiers, P. J.; Cai, L.; Lin, Z.; Richards, R.; Halpern, J. *J. Am. Chem. Soc.*, **1991**, *113* , 4173.

(18) Bautista, M.; Earl, K. A.; Maltby, P. A.; Morris, R. H.; Schweitzer, C. T.; Sella, A. J. *J. Am. Chem. Soc.*, **1988**, *110* , 7031.

(19) $\Delta G^{\ddagger}$ = 11.0 kcal/mol was obtained, assuming the coalescence temperature of 260 K.

(20) Maseras, F.; Duran, M.; Lledos, A.; Bertran, J. *J. Am. Chem. Soc.*, **1992**, *114*, 2922.

(21) Saburi, M.; Takeuchi, H.; Ogasawara, M.; Tsukahara, T.; Ishii, Y.; Ikariya, T.; Takahashi, T.; Uchida, Y. *J. Organomet. Chem.*, **1992**, *428* , 155.

(22) Uehara, A.; Bailar, J. C. *J. Organomet. Chem.*, **1982**, *239* , 1.

Chapter 4

Solution Equilibrium between the Two Isomers of

the Hydride-Dihydrogen Ruthenium Complex with Diop

(Diop = 2,3-*O*-isopropylidene-2,3-dihydroxy-1,4-bis(diphenylphosphino)butane).

Abstract

The solution properties of ruthenium hydrido-dihydrogen complexes [RuH(η^2-H_2)(diop)$_2$]PF_6 (**2b**, diop = 2,3-*O*-isopropylidene-2,3-dihydroxy-1,4-bis(diphenylphosphino)butane) were investigated by the various NMR measurements. ^1H and $^{31}P\{^1H\}$ NMR behaviors of **2b**, obtained in the temperature range –90 to 30 °C in a dichloromethane solution, clarified that the complex consists of an equilibrium mixture of the *trans* (**2b-1**) and the second isomer (**2b-2**). The *trans* isomer **2b-1** was found to be thermodynamically more stable than the other **2b-2**, $\Delta G°$ value being 3.6 kcal mol^{-1}. The rate of interconversion of **2b-1** and **2b-2** was evaluated in the temperature range –80 to –55 °C by the spin saturation transfer studies to reveal that $\Delta G^{\ddagger}$ for this interconversion is about 12 kcal mol^{-1}. Unusual acceleration of the intramolecular H-H_2 hydrogen exchange was observed in **2b**. The isomer **2b-2** was considered as a possible intermediate of the H-H_2 hydrogen exchange reaction in the whole system of **2b**. The probable structure of **2b-2** was also discussed.

Introduction

Since the Kubas' initial confirmation of a dihydrogen complex in 1984,[1] a variety of molecular hydrogen complexes has been reported so far.[2] These dihydrogen coordinating complexes have attracted considerable attention as models for key intermediates of H–H bond dissociation at a metal center. Among a large number of dihydrogen complex, some complexes containing both M–(H_2) and M–H groups, such as $[MH(H_2)(R_2PCH_2CH_2PR_2)_2]^+$ (M = Fe, Ru, Os; R = Ph or Et)[3] and related complexes[4, 5], has been revealed to exhibit the intramolecular hydrogen exchange between the terminal hydrides and the dihydrogen ligand. Such intramolecular hydrogen exchange reaction is regarded as the simplest example of the H–H bond activation, and some possible mechanisms and intermediates have been proposed.[3g, 6]

The influence of diphosphine ligand on the kinetics and thermodynamics of the exchange process remains largely unexplored. In preliminary reports, Saburi and co-workers demonstrated that the dihydrogen complex $[RuH(H_2)(P–P)_2]^+$ (P–P = diphosphine) is readily prepared by introducing H_2 gas into a solution of five-coordinate complex $[RuH(P\text{-}P)_2]^+$ [7, 8, 9] and that, for the homologous complexes (P–P = dppe, dppp, dppb)[10], the intramolecular hydrogen exchange between Ru–H and Ru–(H_2) is affected considerably by the size and flexibility of the diphosphine chelate ring.[8]

In this chapter, I describe the unique NMR spectroscopic behaviors of $[RuH(H_2)(diop)_2]PF_6$ (**2b**). In CD_2Cl_2 solution, **2b** was observed to be consist of a tautomeric mixture of *trans* (**2b-1**) and unidentified isomer (**2b-2**) at low temperature. In the preliminary communication ,[9] we temporary proposed the structure of the isomer **2b-2** to be the *cis* form, where the Ru–H and Ru–H_2 occupy the adjacent coordination sites. However, this assignment should be reconsidered and revised, the reason for

which will be described in the following section. Since the equilibrium between **2b-1** and **2b-2** is temperature dependent, the thermodynamic parameters and the exchange rate for the equilibrium between two forms were determined by variable temperature NMR measurements. On these results, we propose a possible structure of the isomer **2b-2**. We also discuss the mechanism of the dihydrogen-hydride exchange in **2b** and analogous complexes.

Results and Discussion

^{1}H and ^{31}P{^{1}H} NMR properties of 2b. The presence of the two tautomeric isomers for 2b in an equilibrium at low temperature.

The introduction of dihydrogen gas to a dichloromethane solution of the formally five-coordinate complex, $[RuH(diop)_2]PF_6$ (**1b**),[11] resulted in a spontaneous color change from deep red to pale yellow. This observation suggests the incorporation of H_2 molecule to the vacant site of **1b** to give the dihydrogen complex, $[RuH(H_2)(diop)_2]PF_6$ (**2b**).[9] However, several attempts to isolate **2b** as the crystalline product were unsuccessful due to the difficulties in crystallization. This complex is soluble and thermally stable in solutions of dichloromethane, acetone, and THF under H_2 gas atmosphere. The ^{1}H NMR spectrum of **2b** shows a very broad signal ($w_{1/2}$ = ca. 280 Hz) at δ –7.4 in the high field region at 30 °C, while the parent five-coordinate complex **1b** exhibits a broad signal at δ –9.1 under argon at the same temperature.[9b] The broad signal of **2b** gives a short T_1 value (31 ms) at 30 °C, and this fact indicates the participation of the nonclassical ligand, "η^2-H_2" in **2b**.[12] As recognized for many dihydrogen complexes, the coordination of the H_2 ligand in **2b** is so weak that it is necessary to store the solution of **2b** under H_2 atmosphere to avoid the dissociation of the H_2 ligand. Furthermore, the dihydrogen ligand can be easily displaced by other strong monodentate ligands such as CH_3CN or CO. When an inert gas, such as argon, was bubbled through a solution of **2b**, the dihydrogen ligand was eliminated from **2b** to regenerate the original five-coordinate complex **1b**.

The high field region of variable temperature ^{1}H NMR spectra of **2b** are shown in Figure 4.1. On decreasing the temperature, the broad signal observed above 0 °C decoalesced into three resonances (δ –3.2, –8.1, and –8.5). The signal at δ –8.5 turns

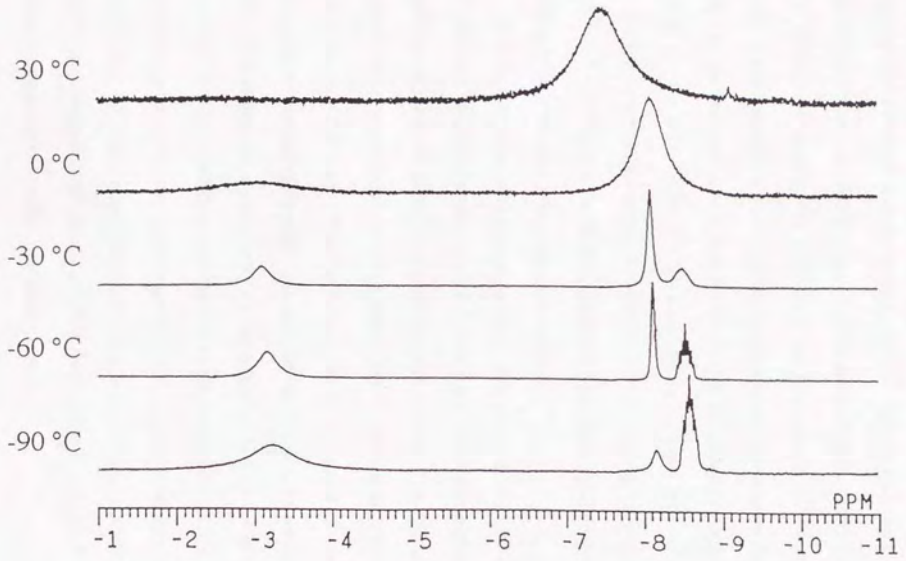

Fig. 4.1 Variable temperature ^1H NMR spectra of $[RuH(\eta^2\text{-}H_2)(diop)_2]PF_6$ (**2b**) in the high field region at 400 MHz in CD_2Cl_2.

into a pseudo-septet due to the spin couplings with phosphorous nuclei ($^2J_{HP}$ = 13 and 26 Hz) below –40 °C, while the other two resonances are found as the broad signals throughout the accessible temperature (> –90 °C). The resonances at δ –3.2 and –8.5 exhibit the intensity ratio of 2:1 at any temperatures, while the intensity of the signal at δ –8.1 changes in comparison with the other two signals as the temperature was lowered. These facts show that the complex **2b** consists of a tautomeric mixture of two isomers in dichloromethane solution. Although a variety of molecular hydrogen complex of the type $[MH(\eta^2\text{-}H_2)(L)_4]^+$ ($(L)_4$ = four monophosphines, two diphosphines, or a tetraphosphine) has been reported for group 8 triad (M = Fe^{II}, Ru^{II}, and Os^{II}),[2-5, 7-9, 13] this is the first example of observing two distinguishable isomers for such type of molecular hydrogen complexes.

Among the three hydride resonances recognized in the low temperature ^1H NMR spectra of **2b**, the signals at δ –3.2 and –8.5 are ascribed respectively to Ru–(η^2-H_2) and Ru–H for *trans*-$[RuH(\eta^2\text{-}H_2)(diop)_2]PF_6$ (**2b-1**). The T_1 value of the broad signal at δ –3.2 is considerably small (8 ms) at –60 °C, while that of the septet at δ –8.5 is much longer (201 ms). The former should be assigned to the signal of the coordinating dihydrogen (Ru–(η^2-H_2)), and the latter to that of the terminal hydride (Ru–H). The isomer **2b-1** also shows a pair of triplets at δ 13.0 and 35.3 ($^2J_{PP}$ = 34 Hz) in the $^{31}P\{^1H\}$ NMR spectra (Figure 4.2) between –90 and –60 °C, which is a characteristic pattern for a six-coordinate bis(diphosphine) complex taking the *trans* configuration. All these NMR features, which are the typical NMR ones of *trans*-$[MH(\eta^2\text{-}H_2)(diphosphine)_2]^+$ (M = Fe^{II}, Ru^{II}, and Os^{II}) complexes,[2-5, 7-9] support the above assignment of **2b-1** as the rigid *trans* isomer.

Introduction of D_2 gas to a deuterated dichloromethane solution of **1b** leads to the formation of partially deuterated isotopomers of **2b**. Among the isotopomers,

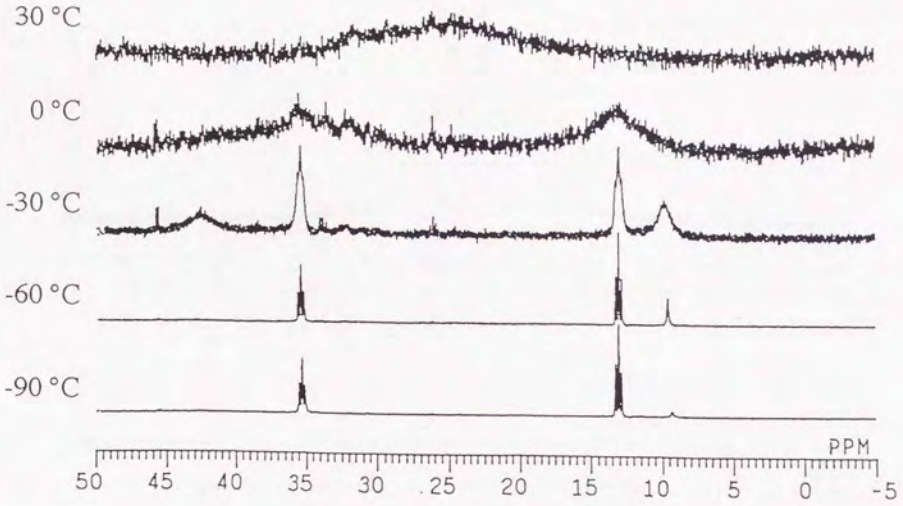

Fig. 4.2 Variable temperature ^{31}P NMR spectra of $[RuH(\eta^2\text{-}H_2)(diop)_2]PF_6$ (**2b**) in the high field region at 400 MHz in CD_2Cl_2.

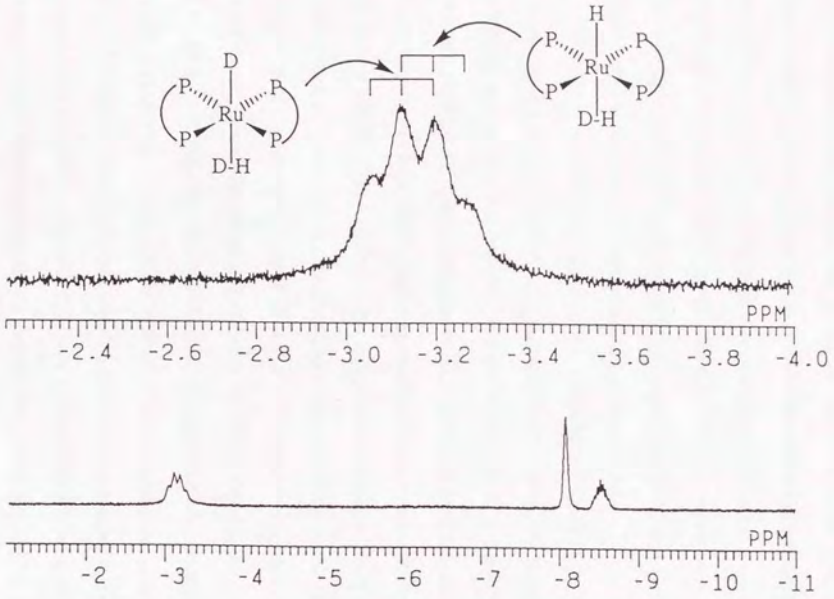

Fig. 4.3 Observation of $^1J_{HD}$ coupling in the partially deuterated complexes $[RuH(\eta^2\text{-}HD)(diop)_2]PF_6$ and $[RuD(\eta^2\text{-}HD)(diop)_2]PF_6$.

trans-[RuD(η^2-HD)(diop)$_2$]PF_6 and *trans*-[RuH(η^2-HD)(diop)$_2$]PF_6 should present the hydride signals due to η^2-HD moiety. As shown in Figure 4.3, the coordinating HD resonances of both isotopomers appear at δ ca. –3.1 as two overlapping 1:1:1 triplets at –60 °C, indicating the coupling between protium and deuterium nucleus. The observed $^1J_{HD}$ values, 30.5 Hz for both isotopomers, are an unequivocal evidence for the non-classical character of HD ligand in **2b**, since the $^1J_{HD}$ values reported so far for molecular hydrogen complexes range from 11 to 34 Hz.[2] This observation also strongly supports the structural assignment of the isomer **2b-1**.

The other isomer, **2b-2**, showed the single broad signal at δ –8.1 at all the accessible temperature below 0° C in the ^{1}H NMR spectra. In accord with this observation, a broad signal is observed at δ 9.4 below –30 °C in the $^{31}P\{^1H\}$ NMR spectra (see Figure 4.2). Interestingly, the relative intensities of this signal and those of **2b-1** are temperature dependent. This suggests that **2b-2** is in an equilibrium with the *trans* isomer **2b-1**. The validity of the equilibrium between **2b-1** and **2b-2** is supported by the spin saturation transfer studies in the ^{1}H NMR at –60 °C. Thus, the irradiation of the η^2-H_2 resonance of **2b-1** at δ –3.1 resulted in marked decreases in the intensity of not only the signal at δ –8.5 (Ru–H of **2b-1**) but also the resonance at δ –8.1 of **2b-2**. Alternatively, the irradiation of the signal at δ –8.1 effected an almost complete disappearance of the signals of **2b-1**. These observations demonstrate that **2b-1** and **2b-2** are in equilibrium and interchanging with each other at a considerable rate under these conditions. At –90 °C, however, it is difficult to observe such a spin saturation transfer phenomenon, due to that the interconversion rate is significantly reduced at this temperature. The determination of the exchange rate between **2b-1** and **2b-2** will be described in the following section.

Based on the results of the spin saturation transfer experiments for the two isomers and the intensity ratio of **2b-1** and **2b-2** in both ^{1}H and ^{31}P NMR spectra, it was concluded that the isomer **2b-2** contains three hydrogen nuclei of hydride character in itself, i.e. the formula of **2b-2** is decided as $[Ru"H_3"(diop)_2]PF_6$.

Thermodynamic and Kinetic Parameters for the Equilibrium between the Two Isomers of 2b.

As described above, the solution equilibrium between the two isomers of **2b** is temperature dependent. At higher temperatures the equilibrium is driven toward **2b-2**. Figure 4.1 shows that **2b-2** is dominant over **2b-1** at –30 °C, while the latter becomes the preferable form at –90 °C. The equilibrium constant, K_{eq}, was obtained from the high field ^{1}H NMR signal intensity ratio of the resonances of the two tautomers in the

Table 4.1 The solution equilibrium between **2b-1** and **2b-2**.

T/°C	T/K	K_{eq} [a]	$\Delta G°$/cal mol^{-1} [b]
-30	243	0.906	47.7
-40	233	0.678	180.0
-50	223	0.507	301.3
-60	213	0.360	433.1
-70	203	0.241	574.4
-80	193	0.141	751.2
-90	183	0.076	939.1

[a] K_{eq} is defined as **[2b-2]**/**[2b-1]** and determined by ^{1}H NMR integration of the hydride resonances of **2b-1** and **2b-2**. [b] Calculated from the equilibrium constants K_{eq}.

temperature range –90 to –30 °C, and listed in Table 4.1. The plot of ln K_{eq} versus $1/T$ (Figure 4.4) is linear and gives the following thermodynamic parameters: $\Delta H° = 3.6$ kcal mol^{-1} and $\Delta S° = 14.8$ cal mol^{-1} K^{-1}, for the isomers **2b-1** and **2b-2**. The small positive enthalpy change explains that **2b-1** is less stable than **2b-2** at rather higher temperature.

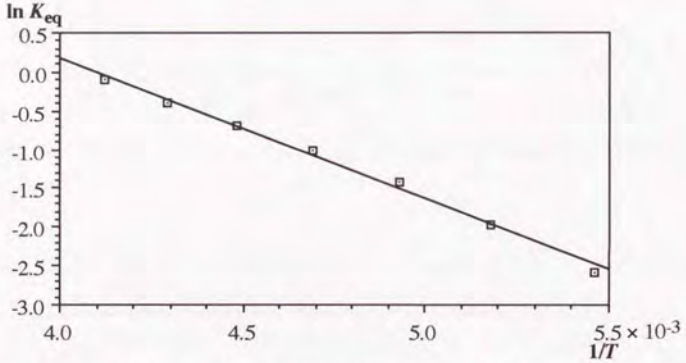

Fig. 4.4 Plot of ln K_{eq} vs. $1/T$ for the equilibrium between the two isomers of **2b**.

The exchange rate between **2b-1** and **2b-2** was estimated in the temperature range –80 to –55 °C by the spin saturation transfer method (see Experimental Section).[14 – 16] The rate constant, k, and the T_1 values of each signal are summarized in Table 4.2. The Eyring plot is linear (see Figure 4.5) and the thermodynamic parameters for the conversion from **2b-1** to **2b-2** are evaluated as follows: $\Delta H^{\ddagger} =$ 10.9 kcal mol^{-1} and $\Delta S^{\ddagger} = -6.0$ cal mol^{-1} K^{-1}. The small negative entropy change indicates that the interconversion undergoes intramolecularity, i.e. the dissociation of the η^2-H_2 ligand during the isomerization is unlikely.

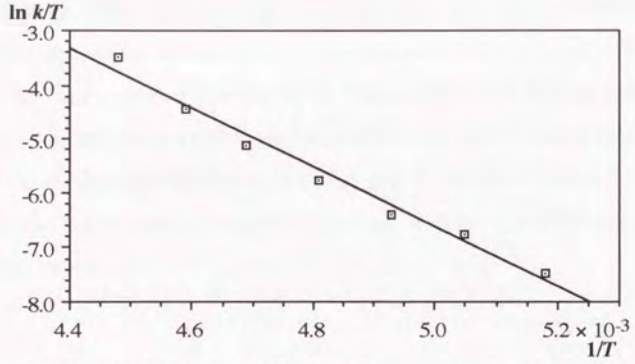

Fig. 4.5 Plot of ln k/T vs. $1/T$ for the interconversion between **2b-1** and **2b-2**.

Table 4.2 T_1 values and rate constant, k, for the interconversion between **2b-1** and **2b-2**.

T/°C	T/K	$T_{1(\text{H of 1a})}$/ms[a]	$T_{1(\text{H}_2 \text{ of 1a})}$/ms[a]	$T_{1(\text{1b})}$/ms[a]	k/s^{-1}	$\Delta G^{\ddagger}$/kcal mol^{-1} [b]
-50	223	124	7	78	6.870	12.1
-55	218	161	7	103	2.612	12.2
-60	213	201	8	139	1.275	12.2
-65	208	211	9	177	0.634	12.2
-70	203	290	10	252	0.341	12.2
-75	198	291	12	260	0.231	12.0
-80	193	382	12	304	0.109	12.0

[a]The T_1 experiments were performed with a 180°-τ-90° pulse sequence by the inversion-recovery method. [b]Calculated from the rate constants k.

The Role of Isomer 2b-2 for the Hydrogen Exchange in Isomer 2b-1.

It is apparent that there are two exchange processes in the diop complex **2b**; (i) one is the interconversion between the two isomers **2b-1** and **2b-2** as described above, and (ii) the other is the hydrogen exchange between the terminal hydride and the dihydrogen ligand in the *trans* isomer **2b-1** (see Figure 4.6). As for the latter phenomena, the intramolecular hydrogen exchange in $[MH(H_2)(P)_4]^+$ was recently reviewed extensively.[2d]

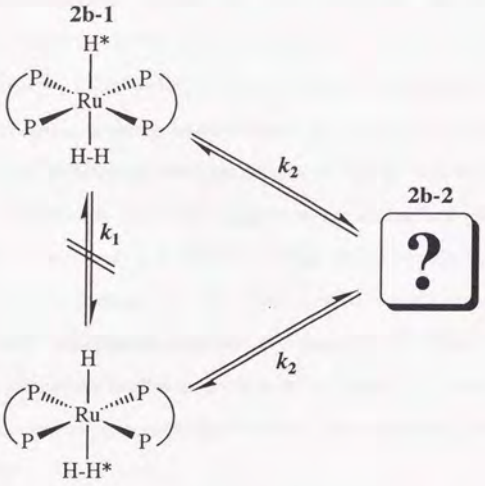

Fig. 4.6 Two exchange process in **2b**.

In the variable temperature ^1H NMR spectra of **2b** (Figure 4.1), two resonances of the isomer **2b-1** seemed to coalesce into one broad signal at a certain temperature

between 10 and 20 °C. Because of the broadness of the resonances, it is difficult to determine the accurate coalesce temperature. The $\Delta G^{\ddagger}$ value of the H-H_2 hydrogen exchange in **2b-1** was, however, estimated from the approximated coalesce temperature as in the range 11.8 to 12.2 kcal mol^{-1}.[17] A similar $\Delta G^{\ddagger}$ value was given for the dppb analogue $[RuH(\eta^2\text{-}H_2)(dppb)_2]PF_6$ (**2a**) as well ($\Delta G^{\ddagger}$ = 10.4 kcal mol^{-1}).[2d] Probably due to the presence of conformational isomers,[8] the low temperature ^1H NMR spectra (Figure 4.7) of **2a** is more complicated than that of **2b**, and shows the presence of unassignable several isomers, one of which is supposed to have a structure analogous to **2b-2**. Although it is difficult to analyze in detail the ^1H NMR spectra of **2a** owing to the existence of isomers, it is expected that the presence of the isomer similar to **2b-2** should accelerate the hydrogen exchange reaction in **2a**.

Two mechanisms involving the independent intermediates or transition state have been proposed for the hydrogen exchange process in $[MH(\eta^2\text{-}H_2)(P\text{–}P)_2]^+$ complexes (Figure 4.8). Morris and co-workers suggested that a fluxional seven coordinate trihydride species, generated by homolytic cleavage of coordinated dihydrogen, could be a probable intermediate for the hydrogen exchange process in *trans*-$[RuH(H_2)(dppe)_2]^+$ and that the calculated $\Delta G^{\ddagger}$ value is larger than 15 kcal mol^{-1}.[3g] An alternative path, which involve the initial isomerization from the *trans* to *cis* isomer and the subsequent hydrogen exchange in the *cis* form, was considered unlikely by these authors.[3g]

It should be noted that the estimated $\Delta G^{\ddagger}$ values for the hydrogen exchange in **2b** and **2a** are considerably smaller than those for the intramolecular H-H_2 exchange in some of other $[RuH(H_2)(diphosphine)_2]^+$ complexes.[2d] For $[RuH(H_2)(dppe)_2]^+$ and $[RuH(H_2)(binap)_2]^+$, both of which are demonstrated to adopt the rigid *trans* configuration even at room temperature,[3g, 7] the $\Delta G^{\ddagger}$ of the hydrogen exchange is

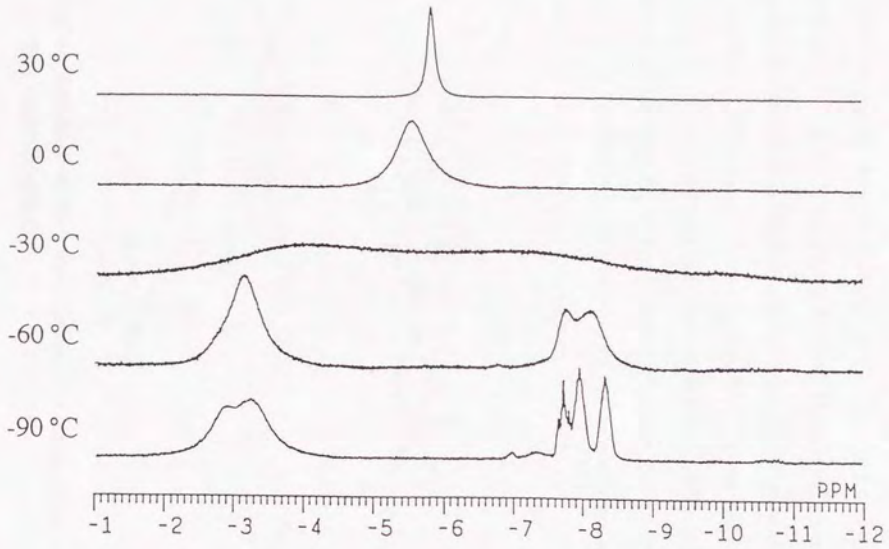

Fig. 4.7 Variable temperature ^1H NMR spectra of $[RuH(\eta^2\text{-}H_2)(dppb)_2]PF_6$ (**2a**) in the high field region at 400 MHz in CD_2Cl_2.

estimated as large as 16 kcal mol^{-1} or more.[2d, 3g] Interestingly, the $\Delta G^{\ddagger}$ value for the hydrogen exchange in **2b-1** (11.8—12.2 kcal mol^{-1}) accords with that for the interconversion process between **2b-1** and **2b-2** (12.0—12.2 kcal mol^{-1}; see Table 4.2) with good accuracy. Judging from these results, it is suggested that the H-H_2 hydrogen exchange in **2b-1** takes place synchronous with the interconversion between **2b-1** and **2b-2**. We suppose, therefore, that **2b-2** can be regarded as the key intermediate for the H-H_2 exchange reaction in the *trans* isomer **2b-1** and, further, that there is a H-H_2 exchange mechanism for *trans*-$[MH(H_2)(P)_4]^+$ complexes, which is facilitated by the transformation from the *trans* into the second isomer such as **2b-2** and does not proceed via the initial homolytic cleavage of H–H bond.

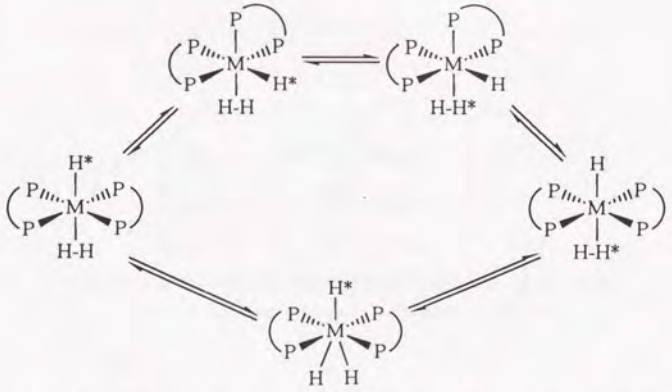

Fig. 4.8 Two proposed mechanisms for intramolecular hydrogen exchange in $[MH(\eta^2\text{-}H_2)(\text{diphosphine})_2]^+$.

Possible Structure of the Isomer 2b-2.

Based on the fact that the isomer **2b-2** can be formulated as $[Ru"H_3"(diop)_2]^+$, three possible structures of **2b-2** are shown in Figure 4.9: i.e., (i) six-coordinate *cis*-H, η^2-H_2 complex under fast hydrogen exchange, (ii) seven-coordinate classical trihydride species, and (iii) five-coordinate non-classical trihydrogen complex. The structure (i) is expected to have two pairs of inequivalent phosphorus nuclei, provided that the fast hydrogen exchange occurs even at low temperature. Therefore, the $^{31}P\{^1H\}$ NMR spectrum of **2b-2** should show two resonances (probably two triplets different from the triplets due to the *trans* isomer), if **2b-2** assumes the *cis* configuration (i). Recently Bianchini and co-workers reported the NMR properties of *cis*-$[RuH(\eta^2\text{-}H_2)\{P(CH_2CH_2PPh_2)_3\}]^+$,[11] in which the dihydrogen and terminal

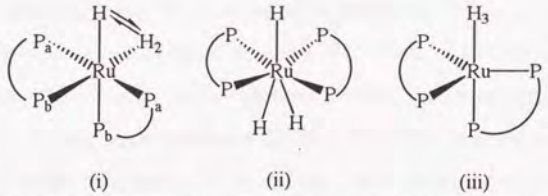

(i) (ii) (iii)

Fig. 4.9 Three possible structures for **2b-2**; (i) *cis*-H, η^2-H_2 under fast exchange, (ii) classical trihidride, (iii) nonclasical trihydrogen.

hydride are forced to adopt the adjacent coordination site (*cis* configuration) by the steric regulation of the tetradentate phosphine. The $\Delta G^{\ddagger}$ value for this complex was shown to be 12 kcal mol^{-1}, apparently equivalent to that of **2b-1**. Importantly, the

four phosphorus nuclei of this complex were observed inequivalent to each other in the $^{31}P\{^{1}H\}$ NMR spectra below –20 °C. In contrast, however, **2b-2** exhibits only one signal in the $^{31}P\{^{1}H\}$ NMR spectra throughout the accessible temperatures. This fact rules out that the *cis* form (i) is improbable as the structure of the isomer **2b-2**.

Seven- or five-coordinate ruthenium complexes are usually highly fluxional. The structures (ii) and (iii) in Figure 4.9 are consistent with the $^{31}P\{^{1}H\}$ NMR characteristics of **2b-2** mentioned above. It is noticed that the T_1 value of the ^{1}H NMR signal of **2b-2** decreased as the temperature rose. Unfortunately, it was difficult to determine the minimum T_1 value of this resonance, because the exchange between **2b-1** and **2b-2** brought about the coalescence of the hydride signals. It is noteworthy that, at 90 °C, the coalesced broad signal shows a considerably short T_1 time (34 ms). If the kinetic parameters $\Delta H°$ and $\Delta S°$ had negligible temperature dependency, the ratio of **2b-2/2b-1** at 90 °C was calculated as about 11.4. Therefore, a great influence from the **2b-2** isomer to the small T_1 value (34 ms) is anticipated at this temperature; i.e. **2b-2** possibly has a non-classical character.[12] It was shown that the complex $ReH_3(dppe)_2$, which is isoelectronic with the structure (ii) and certainly has a long T_1 value for the hydride signal (178 ms at 230 K at 400 MHz), exhibits the clear P–H coupling at higher temperatures.[3f] In contrast, the ^{1}H NMR resonance of **2b** was observed as a broad signal, and exhibited no P–H coupling even at 90 °C. On these reasons, it is hard at this stage to decide that the isomer **2b-2** is a classical trihydride as (ii).

Trihydrogen species, either open-chain or triangular, has been supposed as a probable intermediate for intramolecular hydride-dihydrogen exchange in molecular hydrogen complex, and its existence has been suggested from not only experimental[3f, 5b, 5c] but also theoretical[18] points of view. Although the trihydrogen species has not

been observed directly, Luo and Crabtree pointed out recently that a trihydrogen ligand is not so unstable in their system, and it would be observed as a ground-state species.[6b] A possibility that the isomer **2b-2** adopts the trihydrogen form as (iii) still remains, although no unambiguous evidence has been found yet.

Conclusions

The hydrido-dihydrogen complex of the ruthenium-diop system (**2b**) exist as a tautomeric mixture of the two isomers, **2b-1** and **2b-2**, in dichloromethane solution. This is the first example of observing a solution equilibrium between two distinguishable isomers for the complexes $[RuH(\eta^2\text{-}H_2)(L)_4]^+$. The structure of **2b-1** is the *trans* form, while that of **2b-2** is still uncertain. Interconversion between the two isomers proceeds faster than the intramolecular hydrogen exchange between the terminal hydride and the dihydrogen ligand in **2b-1**. Hence the hydrogen exchange in **2b-1** undergoes synchronously with the interconversion of **2b-1** and **2b-2**. The isomer **2b-2** is considered as an intermediate of the hydrogen exchange process in $[RuH(\eta^2\text{-}H_2)(P\text{–}P)_2]^+$ system. There are two possible structures for the isomer **2b-2**; one is the seven-coordinate classical trihydride, and the other is five-coordinate trihydrogen species. The real structure of **2b-2** is still uncertain.

Experimental Section

General Procedure.

Unless otherwise noted, all manipulations were carried out under a dry argon or dinitrogen atmosphere by standard Schlenk-tube techniques. All the solvents were dried over appropriate reagents and distilled under N_2.[19] CD_2Cl_2 was purchased from Aldrich Chemical Company. Diop[20] and $[RuH(cod)(NH_2NMe_2)_3]PF_6$[21] were prepared as reported. $[RuH(diop)_2]PF_6$ were prepared by the literature methods,[11a] except that acetone was employed as a solvent instead of ethanol. Experimental details of an improved synthesis of $[RuH(diop)_2]PF_6$ are described below.

NMR Studies.

The preparation of sample solutions of the complexes for NMR measurements was carried out under an argon or a dihydrogen atmosphere, using air free CD_2Cl_2 as a solvent. ^1H NMR (400 MHz) and $^{31}P\{^1H\}$ NMR (162 MHz) spectra were recorded on a JEOL JNM-GX 400 spectrometer. ^1H NMR chemical shifts are reported in ppm downfield of tetramethylsilane. $^{31}P\{^1H\}$ NMR chemical shifts are reported in ppm downfield of external 85 % D_3PO_4. ^1H NMR T_1 determinations were performed with a standard 180°-τ-90° pulse sequence by the inversion-recovery method.

Measurements of the Exchange Rates between the Two Isomers (2b-1 and 2b-2) of $[Ru"H_3"(diop)_2]PF_6$.

Determination of the exchange rates between the two isomers was carried out according to the Forsén-Hoffman method.[14,15] Spin saturation transfer experiments were performed by irradiating the ^1H resonance of the isomer **2b-2** (δ ca. –8.1). The exchange rates, *k*, were calculated from the following equation;

$$I'/I = \tau / (\tau + T_1)$$

where I and I' are the signal intensities of the terminal hydride of the *trans* isomer **2b-1** without and with saturation of the signal of isomer **2b-2**, respectively. T_1 is the spin-lattice relaxation time of the hydride resonance of **2b-1** and τ (= $1/k$) is the pre-exchange lifetime of this exchange system. The ratio I'/I were calculated from the difference spectrum recorded by subtracting the spectrum irradiated at the resonance of **2b-2** from the reference (nonirradiated) spectrum. The activation parameters, $\Delta H^{\ddagger}$, $\Delta S^{\ddagger}$, and $\Delta G^{\ddagger}$ were obtained from a linear least-squares fit of the Eyring plot (ln k/T versus $1/T$) utilizing the Eyring equation.[16]

Hydridobis[2,3-*O*-isopropylidene-2,3-dihydroxy-1,4-bis(diphenyl-phosphino)butane]ruthenium(II) hexafluorophosphate [RuH(diop)$_2$]PF$_6$ (1b).

A solution of [RuH(NH_2NMe_2)$_3$(cod)]PF_6 (199 mg, 0.37 mmol) and diop (384 mg, 0.77 mmol) in acetone was stirred at room temperature for 12 h. During this period the color of the solution was turned into deep red. After the removal of the solvent under reduced pressure, the residual solid was dissolved in absolute ethanol (3 mL). The solution was filtered, and to this solution hexane (10 mL) was added. The precipitated deep red powder was washed twice with hexane (15 mL), and then dried under reduced pressure at 60 °C to give the title complex in 78 % yield. Anal. Calcd for $C_{62}H_{65}F_6O_4P_5Ru$: C, 59.9; H, 5.4. Found: C, 59.5; H, 5.5 %.

Hydrido(dihydrogen)bis[2,3-*O*-isopropylidene-2,3-dihydroxy-1,4-bis-(diphenyl-phosphino)butane]ruthenium(II) hexafluorophosphate [RuH(η^2-H$_2$)(diop)$_2$]PF$_6$ (2b).

$[RuH(diop)_2]PF_6$ (**1b**; 30 mg) was dissolved in CD_2Cl_2 (0.6 mL) in a 5-mm NMR tube. The introduction of dry H_2 gas to this solution resulted in a spontaneous color change from deep red to pale yellow. $[RuH(diop)_2]PF_6$ is converted to $[RuH(\eta^2\text{-}H_2)(diop)_2]PF_6$ quantitatively within 3 min. The obtained sample solution was used for NMR measurements without further purification.

References and Notes

(1) (a) Kubas, G. J.; Ryan, R. R.; Swanson, B. I.; Vergamini, P. J.; Wasserman, H. J. *J. Am. Chem. Soc.*, **1984**, *106*, 451. (b) Kubas, G. J.; Ryan, R. R.; Swanson, B. I.; Vergamini, P. J.; Wasserman, H. J. *J. Am. Chem. Soc.*, **1985**, *106*, 451.

(2) Recent Reviews: (a) Kubas, G. J. *Acc. Chem. Res.*, **1988**, *21*, 120. (b) Crabtree, R. H. *Acc. Chem. Res.*, **1990**, *23*, 95. (c) Crabtree, R. H.; Luo, X.-L.; Michos, D. *Chemtracts-Inorg. Chem.*, **1991**, *3*, 245. (d) Jessop, P. G.; Morris, R. H. *Coord. Chem. Rev.*, **1992**, *121*, 155. (e) Heinekey, D. M.; Oldham, Jr., W. J. *Chem. Rev.*, **1993**, *93*, 913.

(3) (a) Morris, R. H.; Sawyer, J. F.; Shiralian, M.; Zubkowski, J. D. *J. Am. Chem. Soc.*, **1985**, *107*, 5581. (b) Bautista, M. T.; Earl, K. A.; Morris, R. H.; Sella, A. *J. Am. Chem. Soc.*, **1987**, *109*, 3780. (c) Ricci, J. S.; Koetzle, T. F.; Bautista, M. T.; Hofstede, T. M.; Morris, R. H.; Sawyer, J. F. *J. Am. Chem. Soc.*, **1989**, *111*, 8823. (d) Bautista, M. T.; Earl, K. A.; Morris, R. H. *Inorg. Chem.*, **1988**, *27*, 1124. (e) Earl, K. A.; Morriis, R. H.; Sawyer, J. F. *Acta Crystallogr.*, **1989**, *C45*, 1137. (f) Earl, K. A.; Jia, G.; Maltby, P. A.; Morris, R. H. *J. Am. Chem. Soc.*, **1991**, *113*, 3027. (g) Bautista, M. T.; Cappellani, E. P.; Drouin, S. D.; Morris, R. H.; Schweitzer C. T.; Sella, A.; Zubkowski, J. *J. Am. Chem. Soc.*, **1991**, *113*, 4876. (h) Jia, G.; Lough, A. J.; Morris, R. H. *Organomataliics*, **1992**, *11*, 161.

(4) (a) Baker, M. V.; Field, L. D.; Young, D. J. *J. Chem. Soc., Chem. Commun.*, **1988**, 546. (b) Baker, M. V.; Field, L. D. *J. Organomet. Chem.*, **1988**, *354*, 351.

(5) (a) Bautista, M. T.; Earl, K. A.; Maltby, P. A.; Morris, R. H. *J. Am. Chem. Soc.*, **1988**, *110*, 4056. (b) Bianchini, C.; Peruzzini, M.; Zanobini, F. *J. Organomet. Chem.* **1988**, *354*, C19. (c) Bianchini, C.; Perez, P. J.; Peruzzini, M.; Zanobini, F.; Vacca, A. *Inorg. Chem.*, **1991**, *30*, 279. (d) Bianchini, C.; Linn, K.;

Masi, D.; Peruzzini, M.; Polo, A.; Vacca, A.; Zanobini, F. *Inorg. Chem.*, **1993**, *32*, 2366.

(6) (a) Luo, X.-L.; Crabtree, R. H. *J. Chem. Soc., Chem. Commun.*, **1990**, 189.

(b) Luo, X.-L.; Crabtree, R. H. *J. Am. Chem. Soc.*, **1990**, *112*, 6912.

(7) Tsukahara, T.; Kawano, H.; Ishii, Y.; Takahashi, T.; Saburi, M., Uchida, Y.; Akutagawa, S. *Chem. Lett.*, **1988**, 2055.

(8) Saburi, M.; Aoyagi, K.; Takahashi, T.; Uchida, Y. *Chem. Lett.*, **1990**, 601.

(9) Saburi, M.; Aoyagi, K.; Takeuchi, H.; Takahashi, T.; Uchida, Y. *Chem. Lett.*, **1990**, 991.

(10) The abbreviations of diphosphines: dppe = 1,2-bis(diphenylphosphino)ethane, dppp = 1,3-bis(diphenylphosphino)propane, dppb = 1,4-bis(diphenylphosphino)-butane.

(11) (a) Saburi, M.; Takeuchi, H.; Ogasawara, M.; Tsukahara, T.; Ishii, Y.; Ikariya, T.; Takahashi, T.; Uchida, Y. *J. Organomet. Chem.*, **1992**, *428*, 155. (b) Ogasawara, M.; Saburi, M. *Organometallics*, submitted for publication.

(12) (a) Hamiltion, D. G.; Crabtree, R. H. *J. Am. Chem. Soc.*, **1988**, *110*, 4126.

(b) Luo, X.-L.; Crabtree, R. H. *Inorg. Chem.*, **1990**, *29*, 2788.

(13) Albertin, G.; Antoniutti, S.; Bordignon, E. *J. Am. Chem. Soc.*, **1989**, *111*, 2072.

(14) Campbell, I. D.; Dobson, C. M.; Ratcliffe, R. G.; Williams, R. J. P. *J. Mag. Res.* **1978**, *29*, 397.

(15) (a) Forsén, S.; Hoffman, R. A. *J. Chem. Phys.* **1963**, *39*, 2892. (b) Forsén, S.; Hoffman, R. A. *J. Chem. Phys.* **1963**, *40*, 1189.

(16) Sandström, J. *Dynamic NMR Spectroscopy;* Academic Press: New York, 1982.

(17) A similar value (12.0 kcal mol^{-1}) was proposed by Morris and Jessop (ref. 2(d)) on the basis of the same assumption, using ^1H NMR spectra in ref. 9.

(18) (a) Burdett, J. K.; Pourian, M. R. *Organometallics*, **1987**, *6*, 1684. (b) Burdett, J. K.; Pourian, M. *Inorg. Chem.*, **1988**, *27*, 4445. (c) Maseras, F.; Duran, M.; Lledós, A.; Bertrán, J. *J. Am. Chem. Soc.*, **1991**, *113*, 2879. (d) Maseras, F.; Duran, M.; Lledós, A.; Bertrán, J. *J. Am. Chem. Soc.*, **1992**, *114*, 2922.

(19) Perrin D. D.; Armarego, W. L. F. *Purification of Laboratory Chemicals;* Pergamon: Oxford, 1988.

(20) Dang, T. P.; Kagan, H. B. *J. Am. Chem. Soc.* **1972**, *94*, 6429.

(21) Ashworth, T. V.; Singleton, E.; Hough, J. J. *J. Chem. Soc., Dalton Trans.* **1977**, 1809.

Chapter 5

Asymmetric Hydrogenation of Prochiral Carboxylic Acids Catalyzed by Five-Coordinate Ruthenium(II)-Hydride Complex $[RuH(binap)_2]PF_6$ (binap = (*R*)- or (*S*)-2,2'-bis(diphenylphosphino)-1,1'-binaphthyl).

Abstract

The five-coordinate complex $[RuH(binap)_2]PF_6$ (**I**, binap = (*R*)- or (*S*)-2,2'-bis(diphenylphosphino)-1,1'-binaphthyl) has been found to have sufficient catalytic activity for asymmetric hydrogenation of itaconic acid and other prochiral carboxylic acids under mild conditions. The catalytic hydrogenation of itaconic acid by **I** was examined under a variety of conditions, and the addition of triethylamine was found to effect high enantioselectivities (> 90 % e.e.). ^{1}H and ^{31}P NMR examinations of reaction mixtures of **I** and itaconic acid under conditions similar to the hydrogenation suggested the formation of ruthenium species containing one binap chelate.

Introduction

In a previous communication,[1] the preparation and some reactions have been reported of a five-coordinate ruthenium(II) complex $[RuH(binap)_2]PF_6$ (**I**, binap = (*R*)- or (*S*)-2,2'-bis(diphenylphosphino)-1,1'-binaphthyl[2]). It was found that **I** forms a mixture of two isomers in solution, and both stereoisomers of the $[RuH(binap)_2]^+$ cation assume square-pyramidal geometry (*trans* and *cis* form, Figure 5.1 (a) and (b)).[1] I observed, further, that complex **I** is readily converted into a molecular hydrogen complex $[RuH(\eta^2\text{-}H_2)(binap)_2]PF_6$ upon contact with H_2 gas (Figure 5.1 (c)).[1]

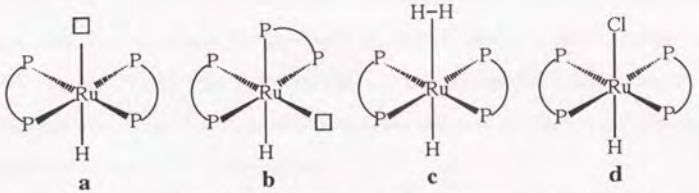

Fig. 5.1 Structures of Ru-binap complexes; (**a**) "*trans*" form of $[RuH(binap)_2]^+$; (**b**) "*cis*" form of $[RuH(binap)_2]^+$; (**c**) *trans*-$[RuH(\eta^2\text{-}H_2)(binap)_2]^+$; (**d**) *trans*-$RuHCl(binap)_2$; a small square represents a vacant coordination site in **a** and **b**.

The excellent catalytic activity of Ru-binap systems for asymmetric hydrogenation of a variety of substrates has attracted considerable attentions in recent years.[3, 4, 5] Among the Ru^{II}-binap complexes investigated in this context such as $Ru_2Cl_4(binap)_2(NEt_3)$[4] and $Ru(RCOO)_2(binap)$ (R = CH_3-, CF_3-, etc.),[5] *trans*-$RuHCl(binap)_2$ (**II**)[6] provides a unique example that contains two binap ligands per Ru atom. In the course of my studies on the asymmetric hydrogenation using Ru-binap

catalysts, I have proposed[4] that the five-coordinate $[RuH(binap)_2]^+$ cation could be a possible activated form of the coordinatively saturated complex **II**. Thus, the dissociation of a Cl^- from **II** should lead to the formation of the *trans* isomer of the five-coordinate species (see Figure 5.1(a) and (d)). In this chapter, asymmetric hydrogenations of several prochiral carboxylic acids employing **I** and **II** as the catalysts were carried out to look into the similarities or differences in catalytic behaviors of these complexes.

With the aim of establishing appropriate conditions to give sufficient enantioselectivities in complex **I**-catalyzed hydrogenation, the effects of reaction temperature, hydrogen pressure, and the addition of triethylamine (NEt_3) on the enantiomeric purities of the products were examined with regard to the hydrogenation of itaconic acid. The observation that the hydrogenation of this dicarboxylic acid in the presence of NEt_3 proceeds more selectively than that in its absence prompted us to investigate the reactions of complex **I** with itaconic acid in the presence or absence of NEt_3 under conditions similar to the hydrogenation.

The ^1H and ^{31}P NMR measurements of a mixture involving complex **I**, itaconic acid, and NEt_3 indicated the liberation of a binap from **I**, which resulted in the formation of new ruthenium species containing only one binap chelate. Another type of binap dissociation was also detected in the absence of NEt_3, although most part of **I** remained unchanged. I will discuss the differences in NMR behaviors among Ru-binap species in reaction mixtures, which should be responsible not only to the features of truly catalytically active species, but to the asymmetric inductions effected under the corresponding conditions.

Results and Discussion

Asymmetric hydrogenation of itaconic acid catalyzed by [RuH((*R*)-binap)$_2$]PF$_6$ (*R*-I).

Saburi and co-workers previously reported that RuHCl((*S*)-binap)$_2$ (*S*-**II**) effects the asymmetric hydrogenation of itaconic acid, one of extensively investigated substrates in asymmetric hydrogenations catalyzed by transition metal complexes, to afford (*R*)-methylsuccinic acid with high optical purity.[4b] In order to compare the catalytic activity and selectivity of the the five-coordinate complex [RuH(binap)$_2$]PF$_6$ **I** with **II**, we first tested the hydrogenation of itaconic acid (**1**) using **I** as the catalyst. The complexes **I** and **II** containing (*R*)- and (*S*)-binap as the ligands will be refered hereafter as *R* -**I** and -**II**, and *S* -**I** and -**II**, respectively.

As expected, the complex *R* -**I** displayed a sufficient catalytic activity for the hydrogenation of **1** under mild conditions. Thus, under initial H_2 pressure of 3 atm at 50° C (substrate / catalyst (S / C) = 100, no NEt_3 was added), **1** was hydrogenated completely within 24 h to give the product (*S*)-methylsuccinic acid (*S* -**2**) with a selectivity (76 % e.e.) comparable to that obtained using *R* -**II** under the same conditions[7] (see Table 5.1, Entries 1 and 16). As will be described later, **I** and **II** displayed comparable enantioselectivities in the asymmetric hydrogenation of other prochiral carboxylic acids.

With a view to attain sufficient selectivity for the complex **I**-catalyzed asymmetric hydrogenation of **1**, the effects of temperature, H_2 pressure, and addition of NEt_3 on the enantiomeric purities of the products were investigated, and the results are listed in Table 5.1. Under low H_2 pressure (1—3 atm), the hydrogenation products showed moderate to high enantiomeric excesses without exception, while the selectivity

Table 5.1 Asymmetric hydrogenation of itaconic acid catalyzed by [RuH((*R*)-binap)$_2$]PF_6 and related complexes

Entry	Catalyst[a]	H_2 / atm	Temp / °C	N / C[b]	N / S[c]	Conv./ %	e.e. / %[d]
1	*R* -**I**	3	50	0	0	100	76
2		3	25	0	0	100	57
3		1	50	0	0	100	81
4		1	25	0	0	75	83
5		50	25	0	0	100	1
6		3	25	200	2	100	91
7		3	50	200	2	100	90
8		1	25	200	2	83	94
9		1	50	200	2	100	89
10		50	25	200	2	100	19
11		3	25	50	0.5	100	71
12		3	25	100	1	100	90
13		3	25	400	4	100	93
14		3	25	200	1	100	93
15		3	25	50	2	100	94
16	*R* -**II**	3	50	0	0	100	82
17		3	25	200	2	100	93
18	**III**	3	50	0	0	100	31
19		3	50	50	0.5	100	32

a) Catalysts. *R* -**I**, [RuH((*R*)-binap)$_2$]PF_6; *R* -**II**, RuHCl((*R*)-binap)$_2$; **III**, [RuH(diop)$_2$]PF_6. b) The molar ratio of triethylamine vs catalyst. c) The molar ratio of triethylamine vs itaconic acid. d) The (*S*) enantiomer was preferentially formed.

was markedly reduced under higher initial H_2 pressure (50 atm, Entries 5 and 10). It has been described that the degree of enantioselection in the hydrogenation catalyzed by $Ru(CH_3COO)_2$(binap) is significantly affected by H_2 pressure and that the effect depends on the substrates.[5b] The pressure dependence of e.e.in the hydrogenation of **1** with complex **I** is similar to that in the hydrogenation of *E* -2-methyl-2-butenoic acid with the acetato complex.

The addition of NEt_3 exhibited a striking effect on the asymmetric induction. When the molar ratio of amine vs. substrate (N / S) equals or exceeds unity, the selectivities higher than 90 % e.e. were achieved under low H_2 pressure in the temperature range 25—50° C (Entries 6—9 and 12—15). Under these conditions, no significant temperature effect on the selectivity was observed (see Entries 6—9).

Under NEt_3-free conditions, the asymmetric induction of complex **I**-catalyzed hydrogenation of **1** showed an unusual temperature dependency. As Entries 1 and 2 in Table 1 show, the product obtained at 50° C has a higher e.e. value (76 %) than that obtained at 25° C (57 %) under initial H_2 pressure of 3 atm. The fact that the e.e of the product at an elevated temperature is higher than that obtained at a lower temperature is opposite to the general tendency of asymmetric induction encountered in most asymmetric reactions. Under H_2 pressure of 1 atm, the selectivities at 25° C and at 50° C were almost equal to each other.

I supposed that there are at least two reaction paths for the complex **I**-catalyzed hydrogenation under amine-free conditions, and that the dominant active species which generated from **I** at 50° C should be different from that formed at 25° C. It was also anticipated that these active species formed in the absence of NEt_3 are considerably distinct from those in the presence of amine. The probable evidences suggesting the

formation of different active species or their precursors from complex **I** under respective conditions will be described later.

Asymmetric hydrogenation of prochiral carboxylic acids.

Complex **I**-catalyzed asymmetric hydrogenations of several prochiral carboxylic acids **3**—**7** were carried out under two representative conditions employed for the hydrogenation of itaconic acid; i.e., (i) at 50° C without NEt_3, and (ii) at 25° C in the presence of NEt_3. The results of hydrogenation are summarized in Table 5.2.

Benzylidenesuccinic acid (**3**), which is a phenyl-substituted derivatives of **1**, was hydrogenated under above-mentioned conditions to give (*S*)-benzylsuccinic acid of 72—82 % e.e. Under the conditions (i), the asymmetric induction for **3** is almost equal to that for **1**, suggesting that there is no significant difference at the stereocenter determining stage in the catalytic cycle for the hydrogenation of these substrates. Under the conditions (ii), the selectivity for **3** is considerably lower than that for **1**. This may be attributed to the substituent effects of the phenyl group in **3**.

The hydrogenation of 3-phenyl-3-butenoic acid (**4**) and 3-ethyl-3-butenoic acid (**5**), both of which contain a vinylidene group and a carboxyl function at its β-position in a similar manner as **1**, proceeded smoothly under the same conditions. The enantiomeric purities of the products were somewhat lowered compared to those for **1**, especially in the case of **5**. It was observed, further, that the hydrogenation product of **4** in the presence of NEt_3 was contaminated with 3-phenyl-2-butenoic acid (**6**), which should be formed through the isomerization of **4** promoted by some ruthenium species (see Scheme 5.1).

As the hydrogenation product of **6** is same as that of **4**, the asymmetric hydrogenation of **6** was also carried out. It turned out that 3-phenylbutanoic acid

Table 5.2 Asymmetric hydrogenation of prochiral carboxylic acids[a]

Substrate	Catalyst[b]	N / S	Temp / °C	Conv./ %	e.e. / %	Configu.
3	(*R*)-**I**	0	50	100	82	(*S*)
	(*R*)-**I**	1	25	100	72	(*S*)
	(*R*)-**I**	2	25	100	75	(*S*)
	(*R*)-**II**	0	50	100	80	(*S*)
4	(*R*)-**I**	0	50	100	71	(*R*)
	(*R*)-**I**	1	25	100[c]	82	(*R*)
	(*S*)-**II**	0	50	100	71	(*S*)
	III	0	50	100	32	(*R*)
5	(*R*)-**I**	0	50	100	69	(*S*)
	(*R*)-**I**	1	25	100	60	(*S*)
	(*S*)-**II**	0	50	100	73	(*R*)
	III	0	50	100	23	(*S*)
6	(*R*)-**I**	0	50	100	39	(*R*)
	(*R*)-**I**	1	50	100	43	(*R*)
	(*S*)-**II**	0	50	93	46	(*S*)
7	(*R*)-**I**	0	50	100	77	(*R*)
	(*R*)-**I**	1	25	100	88	(*R*)
	(*R*)-**II**	0	50	100	79	(*R*)

a) Reaction conditions: H_2, 3 atm; Substrate / catalyst = 100; Time, 24 h; Solvent, THF-EtOH (1:1). b) Catalysts: **I**, $[RuH(binap)_2]PF_6$; **II**, $RuHCl(binap)_2$; **III**, $[RuH((R,R)\text{-diop})_2]PF_6$. c) 3-phenylbutanoic acid (84 %) + 3-phenyl-2-butenoic acid (14 %)

obtained by the hydrogenation of **6** has only moderate enantiomeric purities (39—43 % e.e.), in spite of the fact that it assumes the identical configuration (*R*) with that from **4**. This suggests that the hydrogenation products of **4** should partly contain those arising from the preceding isomerization into **6** and successive hydrogenation (Scheme 5.1), and that the by-path route is responsible, at least in part, to the lower selectivity for **4** in comparison with **1**. Although no corresponding unsaturated acid, 3-methyl-2-pentenoic acid, which can be formed by a double bond migration, was detected in crude hydrogenation products of **5**, the insufficient enantioselectivity for this substrate would be ascribed to the influence of similar two step process concomitantly taking place with the ordinary hydrogenation.

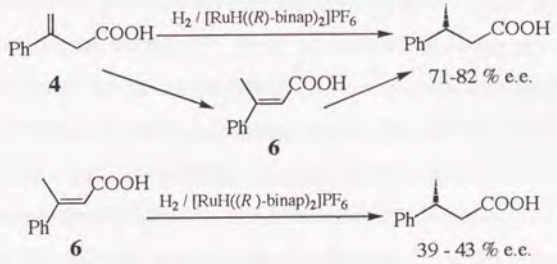

Scheme 5.1 Hydrogenation of **4** and **6** catalyzed by complex **I**.

The asymmetric hydrogenation of (*E*)-2-methyl-2-butenoic acid (tiglic acid; **7**) was performed under the same conditions. The selectivities, ranging 77—88 % e.e., are considerably high compared to those for **6**. While both **6** and **7** belong to

substituted acrylic acids, the mode and sort of substitutions are different: the phenyl and methyl groups at C_3 for **6** and the methyl groups at C_2 and C_3 for **7**, respectively. The results observed here suggest that the differences of substitutions in analogous substrates lead to significant selectivity differences in the asymmetric hydrogenation.

Catalyst effects

As described in Introduction, I have postulated that complex **I** could be an activated form of complex **II**. The five-coordinate species generated by the dissociation of Cl^- from **II** is identical with the complex cation of **I**. Indeed, **II** was found to be effective for the asymmetric hydrogenation of itaconic acid under the same conditions employed for **I**-catalyzed reactions (see Table 5.1). Further, the **II**-catalyzed hydrogenation of other unsaturated carboxylic acids in the absence of NEt_3 proceeded to give the expected products having the enantiomeric purities almost equal to those obtained with complex **I** (Table 5.2). These facts strongly suggest that the change of **II** into the five-coordinate species $[RuH(binap)_2]^+$ should be the initial process for the generation of catalytically active species from **II** under NEt_3-free conditions.

Another chiral five-coordinate complex $[RuH(diop)_2]PF_6$ (**III**, diop = (*R,R*)-4,5-bis(diphenylphosphinomethyl)-2,2-dimethyl-1,3-dioxolane[7]) was recently prepared by the essentially same procedure for obtaining **I**.[8] With a view to examine the effects of chiral diphosphines between **I** and **III** on the activity and selectivity, the asymmetric hydrogenations of typical unsaturated carboxylic acids catalyzed by **III** were carried out under the same conditions, and the results are listed in Tables 5.1 and 5.2.

Although the hydrogenations with complex **III** underwent completely for three substrates examined (**1**, **4**, and **5**), the products showed distinctly lower enantiomeric

purities (< 40 % e.e.) compared with those from the corresponding **I**-catalyzed reactions. This demonstrates evidently that the effectiveness of binap as the ligand for Ru(II) complex catalysts is much superior to that of diop.

Deuterium distribution in hydrogenation products using D_2 or CH_3OD as deuterium sources.

In recent mechanistic investigations on the asymmetric hydrogenation of unsaturated acids employing $Ru(CH_3COO)_2$(binap) as a catalyst,[9,10] it was pointed out that one of two hydrogens incorporated into the products originates from a solvent methanol, while the other from gaseous hydrogen molecule. The deuterium incorporation study[9] using D_2 or CH_3OD as deuterium sources indicated that the proton from hydrogen gas and that from methanol are introduced, respectively, to the β and α positions of α,β-unsaturated acids, while these protons to the γ and β positions for a β,γ-unsaturated acid.

Itaconic acid **1** has two carboxyl groups and possesses partial structures of both α,β- and β,γ-unsaturated acid in a molecule. In order to clarify which partial structure actually works in the catalytic cycle, the pattern and extent of deuterium incorporation were examined by ^1H NMR analysis of methylsuccinic acid obtained under D_2 atmosphere or in CH_3OD solvent. The results of hydrogen isotope incorporation are shown in Scheme 5.2, along with reaction conditions.

It is evident that the hydrogen from gaseous H_2 is dominantly introduced to the methyl group and the proton from a methanol OH group to the methine part. This indicates that itaconic acid interacts as a β,γ-unsaturated acid with Ru-binap species in the course of hydrogenation. In addition, solvent methanol commonly participates into the catalytic cycle promoted by Ru-binap catalysts, even if the truly active Ru-binap

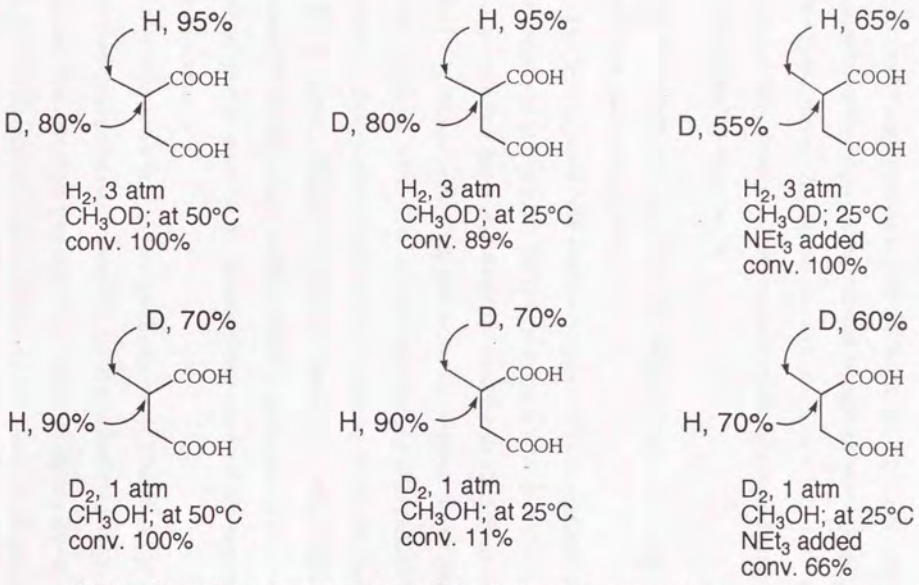

Scheme 5.2 Hydrogen incorporation to methyl and methylene positions of methylsuccinic acid formed by hydrogenation of itaconic acid catalyzed by complex **I**.

species, generated from such independent precursors as complex **I** and $Ru(CH_3COO)_2$(binap), may be fairly different from each other. Further, the addition of NEt_3 causes a more significant disorder for the deuterium incorporation, presumably due to an enhanced hydrogen isotope exchange between gaseous hydrogen and solvent promoted by Ru species. We consider that such difference in deuterium incorporation is in accord with the observation that the enantioselectivity obtained in the presence of NEt_3 is better than that in its absence.

^{1}H and ^{31}P NMR examinations of interactions of complex I with itaconic acid and triethylamine.

It has been expected that a coordinatively saturated six-coordinate ruthenium(II) complex employed as a *catalyst* for hydrogenation or other reactions is ineffective unless it is converted into a *coordinatively unsaturated* (or solvent coordinated) species.[11] For instance, a Ru-binap species having a hydride ligand (Figure 5.2(a)) was postulated as the active form derived from $Ru(CH_3COO)_2$(binap).[9] We have proposed the transformation of six-coordinate complex **II** into a Ru species with a binap and a hydride (Figure 5.2(b)) in the presence of NEt_3 under hydrogen atmosphere.[4b] In these cases, however, NMR examinations of reaction mixtures provided no direct evidence for the presence of such coordinatively unsaturated mono-hydride complexes.

It is noteworthy that the five-coordinate cation $[RuH(binap)_2]^+$ is by itself coordinatively unsaturated (see Scheme 5.3, (**i**)). It is probable that a solvent molecule occupies the vacant site of the five-coordinate cation (**i**) to afford a solvent coordinated species (**ii**; L^1 = solvent) in a solution (Scheme 5.3). Under a hydrogen atmosphere, however, it readily converted into the molecular hydrogen complex $[RuH(\eta^2\text{-}H_2)$-

$(binap)_2]^+$ (**iii**) as shown in Scheme 5.3.[1] We consider it very interesting to examine the conversion of (**i**) into other coordinatively unsaturated or solvent coordinated species under conditions similar to hydrogenation. Thus, ^1H and ^{31}P NMR spectral changes of a mixture of complex **I** and itaconic acid **1** were followed under various conditions.

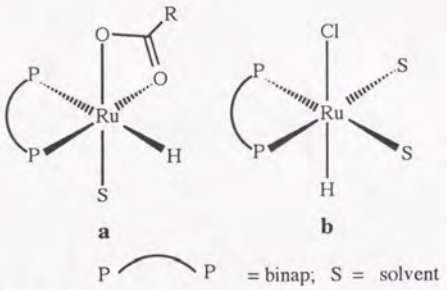

Fig. 5.2 Proposed structures of catalytically active species derived from (**a**) $Ru(CH_3COO)_2(binap)$,[9] and from (**b**) trans-$RuHCl(binap)_2$.[4b]

The ^{31}P NMR spectra of complex **I** alone in a mixture of THF and methanol (1 : 1) and of a mixture of **I** and **1** (molar ratio, 1 : 50) in the same mixed solvent are shown in Figure 5.3 (a) and (b). Importantly, we observed the singlet at δ -15.5 in (b) assignable to the non-coordinating binap. Further, two small signals at δ 29.5 and 63.8 appeared in (b),in addition to the original signals due to the five-coordinate (**i**). This indicates that a small portion of (**i**) loses one of two binap ligands to give rise to a coordinatively unsaturated mono-binap Ru species, although it is uncertain which of these signals should be ascribed to the mono-binap species. The mono-binap Ru(II) species derived from (**i**) upon contact with **1** is given as (**iv**) in Scheme 5.3 (the ligands

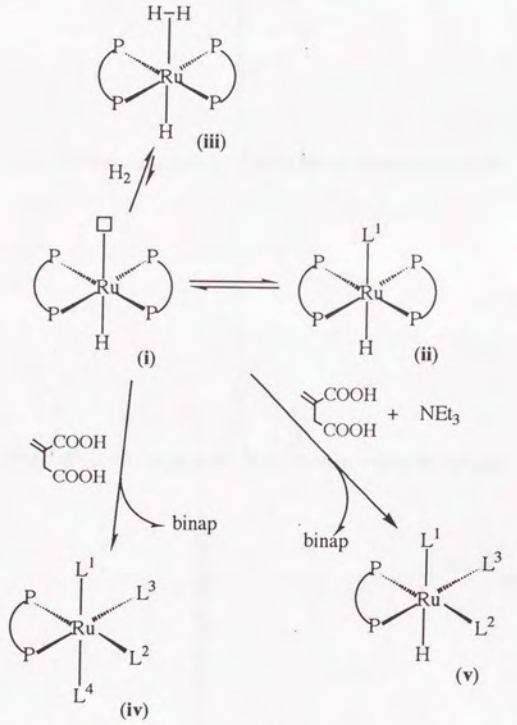

Scheme 5.3 Transformation of complex I under various conditions (see Text).

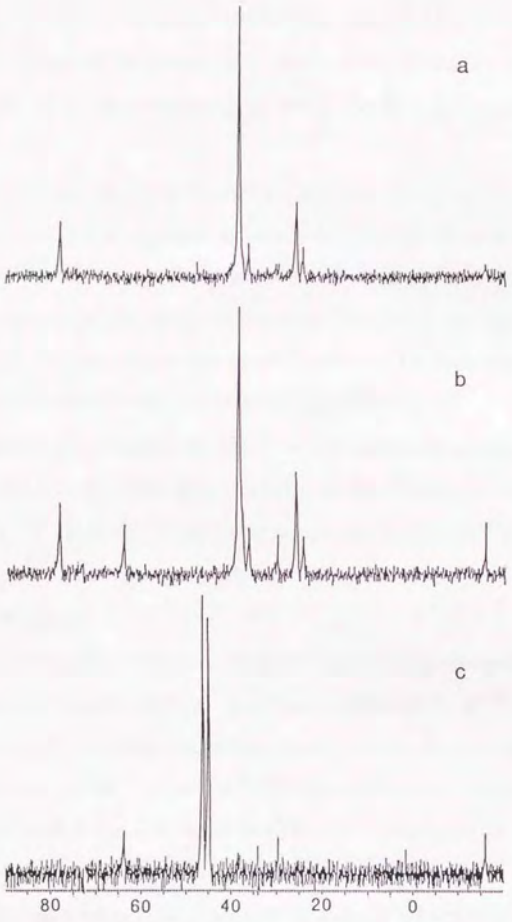

Fig. 5.3 ^{31}P NMR spectra in THF-CH_3OH (1 : 1): (**a**) an isomeric mixture of complex **I**; (**b**) a mixture of complex **I** and itaconic acid (1 : 50); (**c**) a mixture of **I** and itaconic acid (1 : 50) after introducing H_2 gas.

L^1—L^4 not specified). However, the ^1H NMR spectra of **I** revealed no apparent change before and after the addition of **1**. We consider it reasonable not to detect the hydride signal of such mono-binap species, because its intensity is expected to be very weak.

When H_2 gas was introduced into the solution containing **I** and **1** (1 : 50), the ^{31}P NMR signals of **I** disappeared completely and those of the molecular hydrogen complex $[RuH(\eta^2\text{-}H_2)(binap)_2]^+$ emerged (Figure 5.3 (c)). It should be noted that the signals of non-coordinating binap and of new species (**iv**) were observed unchanged. This suggests that some highly unsaturated species as (**iv**) exist in a small amount under the hydrogenation conditions (without NEt_3, at 25—30° C).

With a view to elucidate the previously mentioned unusual temperature effects of the enantioselectivity in the absence of NEt_3, the above sample solution was heated to 50° C for 1 h. However, no remarkable change took place in the ^{31}P NMR spectra. Both the signals of the H_2 complex (**iii**) and of the mono-binap species (**iv**) remained practically unchanged.

Then, we directed our efforts toward elucidating the significant effects of NEt_3 on the selectivity. We observed that the successive additions of 1 and NEt_3 to **I** (1 : 50 : 100 molar ratio) at ambient temperature resulted in a remarkable change of NMR spectra in a short period. Thus, in the ^{31}PNMR spectrum, two doublets (δ 48.0 and 68.3, J(P,P) = 42.3 Hz) and the singlet (δ -15.9) assignable to the free binap appeared by the above treatments, while the signals of complex **I** concomitantly disappeared (Figure 5.4 (a)). In accord with the changes in ^{31}P NMR, the signals due to the Ru-H resonances of **I** were no longer observed, but a doublet of doublets (δ -15.9, J(H,P) = 23.2 and 35.4 Hz) emerged alternatively in the hydride region of ^1H

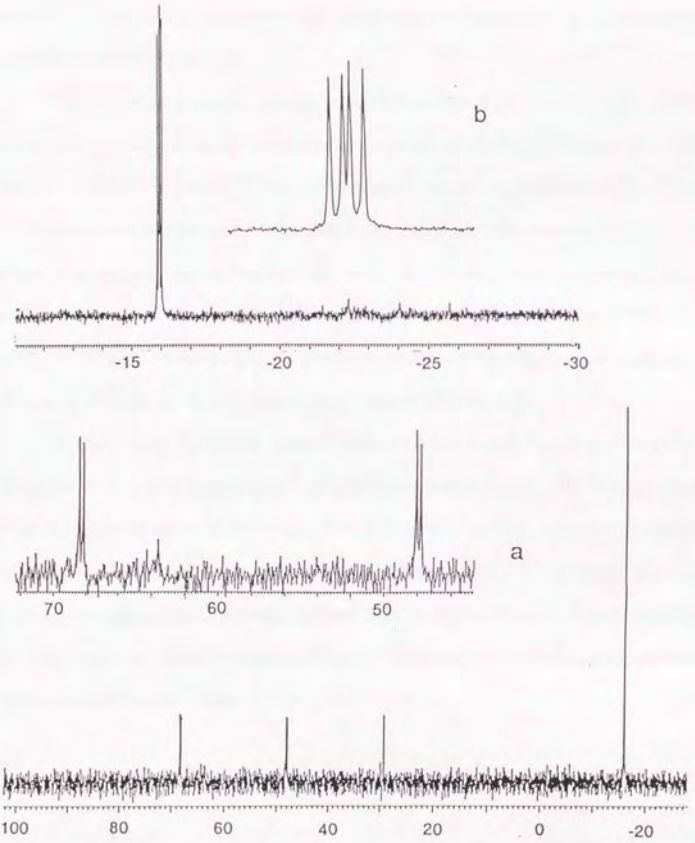

Fig. 5.4 NMR spectra of a mixture of complex **I**, itaconic acid, and NEt_3 (1 : 50 : 100): (**a**) ^{31}P NMR spectrum in THF-CH_3OH; (**b**) ^{1}H NMR spectrum in THF-d_8-CD_3OD.

NMR spectrum (Figure 5.4 (b)). These NMR features coincide with the assumption that a new ruthenium(II) species coordinating both a binap and a hydride, in such a manner as (**v**) in Scheme 3, is produced almost quantitatively from (**i**) (or (**ii**)) without heating or introducing H_2 gas.

It is noteworthy that the structural characteristics of (**v**), having only one binap chelate and a hydride, is the same as those of the proposed activated form of the diacetate complex (Figure 5.2 (b)),[9] although the remaining ligands in (**v**), L^1—L^3, have not been determined yet. We consider that the mono-binap complex as (**v**) should be the catalytically active species by itself or a catalytic precursor under the hydrogenation conditions in the presence of NEt_3. It is reasonable, therefore, that the results of complex **I**-catalyzed hydrogenation under these conditions are considerably different from those in the absence of NEt_3 (Tables 5.1 and 5.2).

In conclusion, by NMR measurements we have detected two novel Ru(II) species with only one binap ligand, (**iv**) and (**v**), derived from the five-coordinate cation (**i**) under different conditions. The species (**iv**) is formed by a reaction of (**i**) with itaconic acid in the absence of NEt_3. The other (**v**) readily generates by simultaneous additions of itaconic acid and NEt_3 to a solution of **I**. These species are expected to act as or to be converted into the principal active species under the respective reaction conditions.

Experimantal Section

General Procedure.

All the solvents used and triethylamine were dried and distilled by conventional methods, and stored under nitrogen. (*R*)- and (*S*)-binap were presented by Takasago Research Institute Inc. 3-Phenyl-2-butenoic acid (**4**)[11] and 3-methylenepentanoic acid (**5**)[12] were prepared by the reported methods.

Gas chromatographic (GC) analysis was performed with a Shimadzu GC-14A instrument equipped with a fused silica capillary column (Shimadzu CBP10, 25 m) and a flame ionization detector. High performance liquid chromatography (HPLC) was carried out with a Jasco VIP-2 apparatus equipped with a Shimadzu SPC-7A UV spectrometric detector and a Shimadzu Chromatopac CR-5A, employing chiral stationary columns Daicel CHIRALCEL-OB or -OD. ^{1}H NMR (400 MHz) and ^{31}P NMR (162 MHz) spectra were measured with a JEOL JNM-GX 400 spectrometer.

Hydridobis[(*R*)- or (*S*)-2,2'-bis(diphenylphosphino)-1,1'-binaphthyl] ruthenium(II) hexafluorophosphate [RuH((*R*)- or (*S*)-binap)$_2$]PF_6 (I).

These complexes were prepared according to the reported method[13] with slight modifications. A mixture of [RuH(cod)(NH_2NMe_2)$_3$]PF_6[14] (**IV**) (0.242 g, 0.45 mmol) and (*R*)- or (*S*)-binap (0.566 g, 0.91 mmol) in ethanol (10 ml) was heated under reflux for 2 h under nitrogen atmosphere. The resultant mixture containing deep red precipitates was evaporated under reduced pressure, and the solid thus obtained was dissolved in THF. The solution was filtered to remove insoluble materials, and diethyl ether was added to the filtrate. The red fine needle crystals were collected, washed three times with diethyl ether, and dried under reduced pressure (0.483 g, 72 %). Found: C, 69.4; H, 4.5 %. Calcd for $C_{88}H_{65}F_6P_5Ru$: C, 69.8; H, 4.4 %.

Hydridobis[(*R*,*R*)-4,5-bis(diphenylphosphinomethyl)-2,2-dimethyl-1,3-dioxolane]-ruthenium(II) hexafluorophosphate [RuH(diop)$_2$]PF$_6$ (III).

A mixture of **IV** (0.100 g, 0.187 mmol) and diop (0.195 g, 0.392 mmol) in ethanol (10 ml) was stirred at room temperature for 3 h. The deep red solution was evaporated under reduced pressure to dryness at room temperature, and the residue was dissolved in dichloromethane. Hexane was added to afford an oily product, which solidified by standing for several days at room temperature. Found: C, 59.5; H, 5.5 %. Calcd for $C_{62}H_{65}F_6O_4P_5Ru$: C, 59.9; H, 5.4 %.

Asymmetric hydrogenation of prochiral carboxylic acids.

A mixture of carboxylic acid (**1**, **3**—**7**) (1.0 mmol), catalyst (**I**, **II**, or **III**) (0.01 mmol) and triethylamine (as required) in a mixture of THF (5 ml) and ethanol (5 ml) was stirred under hydrogen for 24 h. The detailed reaction conditions are given in Tables 1 and 2. The solvent was removed under reduced pressure, and 1 M aqueous NaOH (M = mol / l) (10 ml) was added. After filtration, the aqueous layer was washed with chloroform, and then acidified with 2 M HCl to pH 1. The acidic aqueous solution was extracted three times with chloroform, and the dried chloroform solution was evaporated to give the crude product. An aliquot of the product was dissolved in THF and then treated with diazomethane to determine the conversion of hydrogenation by GC analysis.

Enantiomeric excesses of the products were determined as follows. Another aliquot of the product (ca. 0.1 mmol) was dissolved in THF (2 ml) and aniline (1.1 mol / carboxyl group), N,N'-dicyclohexylcarbodiimide (1.1 mol / carboxyl group), and 4-dimethylaminopyridine (2 mg) were added. The mixture was stirred at room temperature for 20 h, the precipitate was filtered off, and the filtrate was evaporated.

The residue was purified by short column chromatography on silica gel with diethyl ether as an eluent. The enantiomeric purities of the amides thus obtained were determined by chiral HPLC analysis.[15]

References and Notes

(1) Tsukahara, T.; Kawano, H.; Ishii, Y.; Takahashi, T.; Saburi, M.; Uchida, Y.; Akutagawa, S. *Chem. Lett.*, **1988**, 2055.

(2) Miyashita, A.; Takaya, H.; Souchi, T.; Noyori, R. *Tetrahedron*, **1984**, *40*, 1245.

(3) Recent reviews: (a) Noyori, R.; Takaya, H. *Acc. Chem. Res.*, **1990**, *23*, 345. (b) Takaya, H.; Ohta, T.; Mashima, K.; Noyori, R. *Pure Appl. Chem.*, **1990**, *62*, 1135. (c) Noyori, R.; Kitamura, M. *Modern Synthetic Methods 1989*, R. Schefford, ed., Springer-Verlag, **1989**, pp. 115.

(4) (a) Ikariya, T.; Ishii, Y.; Kawano, H.; Arai, T.; Saburi, M.; Yoshikawa, S.; Akutagawa, S. *J. Chem. Soc., Chem. Commun.*, **1985**, 922. (b) Kawano, H.; Ishii, Y.; Ikaraya, T.; Saburi, M.; Yoshikawa, S.; Uchida, Y.; Kumobayashi, H. *Tetrahedron Lett.*, **1987**, *28*, 1905; *J. Chem. Soc., Perkin Trans. 1*, **1989**, 1571. (c) Kawano, H.; Ishii, Y.; Saburi, M.; Uchida, Y. *J. Chem. Soc., Chem. Commun.*, **1988**, 87.

(5) (a) Noyori, R.; Ohta, M.; Hsiao, Y.-I.; Kitamura, M.; Ohta, T.; Takaya, H. *J. Am. Chem. Soc.*, **1986**, *108*, 7117. (b) Ohta, T.; Takaya, H.; Kitamura, M.; Nagai, K.; Noyori, R. *J. Org. Chem.*, **1987**, *52*, 3176. (c) Noyori, R.; Ohta, T.; Kitamura, M.; Takaya, H.; Sayo, N.; Kumobayashi, H.; Akutagawa, S. *J. Am. Chem. Soc.*, **1987**, *109*, 5856. (d) Kitamura, M.; Ohkuma, T.; Inoue, S.; Sayo, N.; Kumobayashi, H.; Akutagawa, S.; Ohta, T.; Takaya, H.; Noyori, R. *J. Am., Chem. Soc.*, **1988**, *110*, 629.

(6) Kawano, H.; Ishii, Y.; Kodama, T.; Saburi, M.; Uchida, Y. *Chem. Lett.*, **1987**, 1311.

(7) The enantiomeric excesses of the products obtained by complex II-catalyzed reactions were reexamined in this study, using HPLC with a chiral stationary phase column (see Experimental).

(8) Saburi, M.; Aoyagi, K.; Takeuchi, H.; Takahashi, T.; Uchida, Y. Chem. Lett., **1990**, 991.

(9) Ohta, T.; Takaya, H.; Noyori, R. *Tetrahedron Lett.*, **1990**, *31*, 7189.

(10) Ashby, M. T.; Halpern, J. *J. Am. Chem. Soc.*, **1991**, *113*, 589.

(11) Yamamoto, K.; Ikeda, K.; Yin, L. K. *J. Organometal. Chem.*, **1989**, *370*, 319.

(12) Abe, Y.; Sato, M.; Goto, H.; Sugawara, R.; Takahashi, E.; Kato, T. *Chem. Pharm. Bull.*, **1981**, *31*, 4346.

(13) Ashworth, T. V.; Singleton, E. *J. Chem. Soc., Chem. Commun.*, **1976**, 705.

(14) Ashworth, T. V.; Singleton, E.; Hough, J. J. *J. Chem. Soc., Dalton Trans.*, **1977**, 1809.

(15) Shao, L.; Miyata, S.; Muramatsu, H.; Kawano, H.; Ishii, Y.; Saburi, M.; Uchida, Y. *J. Chem. Soc., Perkin Trans. 1*, **1990**, 1441.

Acknowledgment

The studies described in this thesis was carried out under the direction of Associate Professor Masahiko Saburi from 1989 to 1993. I wish to express my deep gratitude to Professor Masahiko Saburi for his patient guidance and earnest encouragement throughout the course of this work. I would like to express my sincere thanks to Professor Yasuzo Uchida, the President of Nagaoka Institute of Science and Technology, for his invaluable suggestions and constant encouragement.

I am grateful to Mr. Teruyuki Kodama for his technical support. I also would like to acknowledge Dr. Hiromichi Noguchi and Professor Tamotsu Takahashi for their valuable discussions and kind help. I wish to thank Mr. Hitoshi Muramatsu and Dr. Shao Liming, as well as the past and present member of Saburi Laboratory and Uchida Laboratory for their valuable discussions and friendship-assistance.

I am grateful to Professor Masanobu Hidai, Dr. Yasushi Mizobe, Dr. Youichi Ishii, and Dr. Hiroyuki Matsuzaka for their kind help. I am deeply grateful to Dr. Makoto Koike for his advice, mainly concerning NMR.

Finally, I especially express my heartfelt thank to my parents Shoji and Kazuko Ogasawara for their kind encouragement.

Masamichi OGASAWARA

M. Ogasawara

Department of Industrial Chemistry
Faculty of Engineering
The University of Tokyo
February, 1994.

List of Publications

Chapter 2

1. Agostic Interaction and Hydrogen Exchange in Coordinatively Unsaturated Ruthenium Complexes.
   Ogasawara, M.; Aoyagi, K.; Saburi, M.
   Organometallics, **1993**, *12*, 3393.

2. Agostic Interaction and Intramolecular Hydrogen Exchange in Coordinatively Unsaturated Ruthenium Complexes: Effects of Chelate Ring Size on Intramolecular Carbon-Hydrogen Bond Activation of Diphosphine Ligands.
   Ogasawara, M.; Saburi, M.
   Organometallics, submitted for publication.

Chapter 3

3. Effects of Chelate Ring Rigidity on the Intramolecular Hydrogen Exchange in Hydrido(dihydrogen)bis(diphosphine)ruthenium(II) Ions $[RuH(\eta^2\text{-}H_2)(diphosphine)_2]^+$ (diphosphine = binap and dpbp).
   Ogasawara, M.; Saburi, M.
   J. Organomet. Chem., submitted for publication.

Chapter 4

4. Solution Equilibrium between the Two Isomers of the Hydride-Dihydrogen Ruthenium Complex with Diop (Diop = 2,3-*O*-isopropylidene-2,3-dihydroxy-1,4-bis(diphenylphosphino)butane).
   Ogasawara, M.; Saburi, M. (in preparation)

Chapter 5

5. Asymmetric Hydrogenation of Prochiral Carboxylic Acids Catalyzed by Five-Coordinate Ruthenium(II)-Hydride Complex $[RuH(binap)_2]PF_6$ (binap = (*R*)- or (*S*)-2,2'-bis(diphenylphosphino)-1,1'-binaphthyl)
Saburi, M.; Takeuchi, H.; Ogasawara, M.; Tsukahara, T.; Ishii, Y.; Ikariya, T.; Takahashi, T.; Uchida, Y.
J. Organomet. Chem., **1992**, *428*, 155.

Others

6. Asymmetric Transfer Hydrogenation of Prochiral Carboxylic Acids Catlyzed by a Five-Coordinate Ru(II)-binap Complex.
Saburi, M.; Ohnuki, M.; Ogasawara, M.; Takahashi, T.; Uchida, Y.
Tetrahedron Lett., **1992**, *33*, 5783.

7. Application of NMR Techniques to Organometallic Compounds.
Ogasawara, M.; Koike, M.; Saburi, M.
J. Synth. Org. Chem., Jpn., **1993**, *51*, 48.

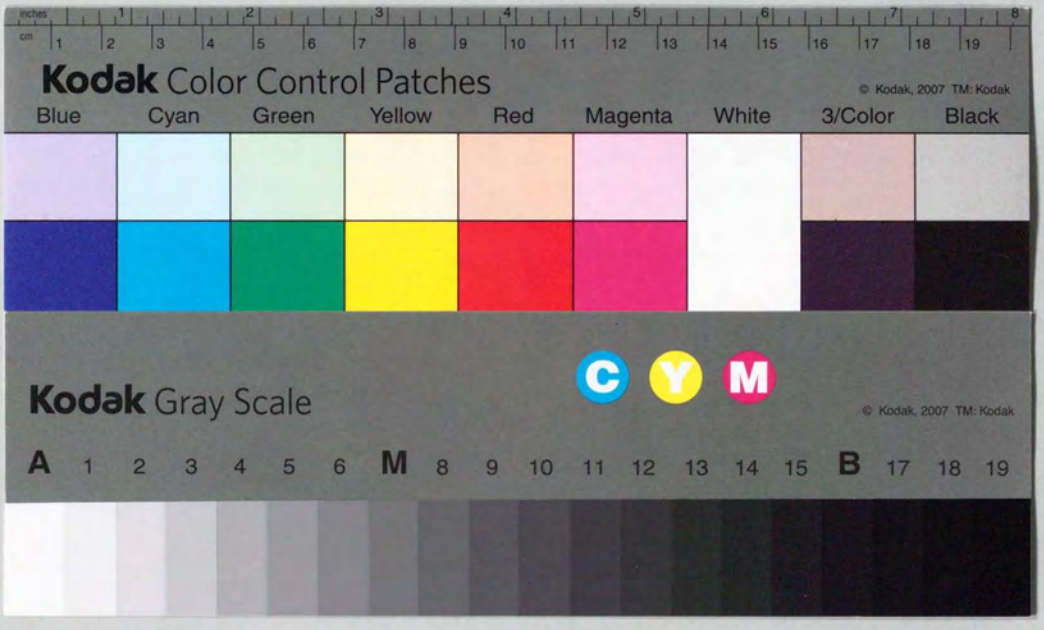
inches
cm
Kodak Color Control Patches
© Kodak, 2007 TM: Kodak
Blue
Cyan
Green
Yellow
Red
Magenta
White
3/Color
Black
Kodak Gray Scale
C
Y
M
© Kodak, 2007 TM: Kodak
A 1 2 3 4 5 6 M 8 9 10 11 12 13 14 15 B 17 18 19